Identification of FKBP25 as a pre-ribosome associated prolyl isomerase

by

Geoffrey Gudavicius
BSc, University of Victoria, 2010

A Dissertation Submitted in Partial Fulfillment
of the Requirements for the Degree of

DOCTOR OF PHILOSOPHY

in the Department of Biochemistry and Microbiology

Supervisory Committee

Identification of FKBP25 as a pre-ribosome associated prolyl isomerase

by

Geoffrey Gudavicius
BSc, University of Victoria, 2010

Supervisory Committee

Dr. Christopher J. Nelson, Department of Biochemistry and Microbiology
Supervisor

Dr. Perry L. Howard, Department of Biochemistry and Microbiology
Departmental Member

Dr. Juan Ausio, Department of Biochemistry and Microbiology
Departmental Member

Dr. Leigh Anne Swayne, Division of Medical Sciences
Outside Member

Abstract

The FK506-binding proteins (FKBPs) are a class of peptidyl-prolyl isomerase enzyme (PPIs) that catalyze the *cis-trans* inter-conversion of peptidyl-prolyl bonds in proteins. This non-covalent post-translational modification is a reversible mechanism to modulate protein structure and function. PPIs have been implicated in a wide variety of processes from protein folding to signal transduction. Despite these enzymes being ubiquitous, the substrates and functions of most PPIs have yet to be described.

FKBP25 is a nuclear FKBP that has been shown to associate with transcription factors and chromatin modifying enzymes, however its functions and substrates remain largely unresolved. FKBP25 is the human ortholog of *S. cerevisiae* Fpr4, which has been shown to regulate the chromatin landscape by two distinct mechanisms: 1. Acting as a histone chaperone at ribosomal DNA, and 2. Isomerizing histone prolines. Based on these observations, I hypothesized FKBP25 regulates chromatin and/or ribosome biogenesis through isomerization of histone prolines and a discrete collection of substrate proteins.

While small molecule inhibitors exist for FKBPs, applying them to dissect the specific function(s) of any given FKBP is confounded by the fact that multiple FKBPs are found in each organism, and several are inhibited by these molecules. In Chapter 2, I biochemically and structurally characterize a set of FKBP25 loss-of-function mutants, yielding a toolset capable of distinguishing between catalytic and non-catalytic functions. These reagents provide the tools necessary to analyze potential substrates of FKBP25 identified in my research going forward. In Chapter 3, I present the first unbiased proteomic screen of FKBP25 associated proteins and show that it interacts with a large number of ribosomal proteins, ribosomal processing factors and a smaller subset of chromatin proteins. I focus on the interaction between FKBP25 and nucleolin, a multi-functional nucleolar protein, and show that FKBP25 interacts with nucleolin and the pre-60s ribosomal subunit in an RNA dependent fashion. In Chapter 4, I gain insight into the role of FKBP25 in ribosome biology, and demonstratex that FKBP25 regulates RNA binding activity of nucleolin, however this does not appear to involve *cis-trans* prolyl isomerization.

Collectively, my work establishes FKBP25 as the first human FKBP to be implicated in the maturation of the pre-60S ribosomal subunit in the nucleus. My data supports a model whereby FKBP25 associates with the assembling large ribosomal subunit, where it is likely to chaperone protein-RNA interactions.

Table of Contents

List of Tables

List of Figures

List of Abbreviations

ACF	ATP-dependent chromatin assembly factor
ATM	Ataxia telangiectasia mutated
BioID	Biotin identification
BirA	Bifunctional ligase/repressor A
BGS	Bovine growth serum
BSA	Bovine serum albumin
BTHB	Basic-tilted helical bundle
CDK	Cyclin dependent kinase
ChIP	Chromatin immunoprecipitation
CNTRL	Control
Cryo-EM	Cryogenic electron microscopy
CsA	Cyclosporine A
CSK	Cytoskeleton
Cyp	Cyclophilin
Cyto	Cytoplasm
DAPI	4’,6-diamidino-2-phenylindole
DDX	DEAD-box helicase
DFC	Dense fibrillar component
DMEM	Dulbecco’s modified eagles’ medium
DMSO	Dimethyl sulfoxide
DNA	Deoxyribonucleic acid
dsRNA	Double stranded RNA
DTT	Dithiothreitol
E. coli	*Escherichia coli*
ECM	Evolutionary conserved motif
EDTA	Ethylenediaminetetraacetic acid
EF1B	Translation elongation factor 1B
EMSA	Electrophoretic mobility shift assay
Endog.	Endogenous
EtBr	Ethidium bromide
EtOH	Ethanol
ETS	Externally transcribed spacer
FACT	Facilitates chromatin transcription
FBS	Fetal bovine serum
FC	Fibrillar component
FKBP	FK506-binding protein
Fpr	FK506-binding protein proline rotamase
GC	Granular component
GR	Glucocorticoid receptor
GST	Glutathione S transferase
HDAC	Histone deacetylase

HDX	Hydrogen deuterium exchange
HP1	Heterochromatin protein 1
HSQC-NMR	Heteronuclear single quantum coherence NMR
IL-2	Interleukin 2
IP	Immunoprecipitation
IRF-4	Interferon regulatory factor 4
Itk	Interleukin-2-inducible T cell kinase
IPTG	Isopropyl β-D-1-thiogalactopyranoside
ITS	Internally transcribed spacer
JNK	c-Jun N-terminal kinase
KAP1	Kruppel-associated box domain associated protein 1
LC/MS	Liquid chromatography mass spectrometry
MALDI-TOF	Matrix-assisted laser desorption/ionization time of flight
MAPK	Mitogen-activated protein kinase
MDM2	Mouse double minute 2
me2	Dimethylation
me3	Trimethylation
MLL1	Mixed-lineage leukemia 1
Mnase	Micrococcal nuclease
mRNA	Messenger RNA
mTOR	Mechanistic target of rapamycin
MW	Molecular weight
Mybbp1a	Myb binding protein 1a
NB	Northern blot
ncRNA	Non-coding RNA
NCL	Nucleolin
NF-kB	Nuclear factor kB
$NHEIII_1$	Nuclease hypersensitivity element III_1
NIMA	Never in mitosis gene A
NL	Nucleophosmin-like
NMR	Nuclear magnetic resonance spectroscopy
Nog2	Nucleolar G-protein 2
Nop	Nucleolar protein
NoRC	Nucleolar remodelling complex
NRE	Nucleolin recognition element
NS5	Nonstructural protein 5
rDNA	Ribosomal DNA
RelA	v-rel avian reticuloendotheliosis viral oncogene homolog A
RIP	RNA immunoprecipitation
RNA	Ribonucleic acid
RNA pol	RNA polymerase
rRNA	Ribosomal RNA
RPA1	Replication protein A1
RyR	Ryanodine receptor
OE	Over-express
Par	Parvulin

PARP1	Poly-ADP-ribose polymerase 1
PBS	Phosphate buffered saline
PCR	Polymerase chain reaction
PHD3	Plant homeodomain 3
Pin1	Peptidylprolyl isomerase NIMA interacting 1
pNA	Para-nitroaniline
PPI	Peptidyl-prolyl isomerase
ppm	Part per million
PPWD1	Peptidylprolyl isomerase domain and WD repeat 1
pS/T-P	Phosphorylated serine/threonine-proline motif
PTM	Post-translational modification
qPCR	Quantitative PCR
RGG	Glycine arginine rich region
RIP	RNA immunoprecipitation
RNase	Ribonuclease
RPL	Ribosomal protein of the large subunit
RPS	Ribosomal protein of the small subunit
RRM	RNA recognition motif
SDS	Sodium dodecyl sulfate
SDS-PAGE	SDS-poly acrylamide gel electrophoresis
shRNA	Short hairpin RNA
siRNA	Small interfering RNA
SL-1	Selectivity factor 1
S. cerevisiae	*Saccharomyces cerevisiae*
snoRNA	Small nucleolar RNA
SRSF3	Serine/arginine rich splicing factor 3
ssRNA	Single stranded RNA
SSU	Small subunit
SWI/SNF	Switch/sucrose non-fermentable
TBE	Tris Borate EDTA buffer
TBS	Tris buffered saline
TBS-T	Tris buffered saline with Triton X100
TCEP	tris(2-carboxyethyl)phosphine
TFA	Trifluoroacetic acid
TFIIF	Transcription factor II F
TRIBE	Targets of RNA-binding proteins by editing
tRNA	Transfer RNA
TPR	Tetratricopeptide repeat
TTF-1	Transcription termination factor 1
UTP	U Three Protein
WB	Western blot
WCE	Whole cell extract
UBF	Upstream binding factor
Xaa	Any amino acid
YY1	Yin yang 1

Acknowledgments

First, I would like to thank Dr. Chris Nelson for his support, advice and guidance throughout my undergraduate and graduate studies. I appreciate the freedom to explore different ideas and the support of my research path as we entered new territory.

I would also like to thank the members of my committee: Dr. Perry Howard, Dr. Juan Ausio and Dr. Leigh Anne Swayne. I truly appreciate the investment of time, advice and willingness to help with all aspects of my project.

The members of the Nelson lab, past and present, deserve much recognition and thanks. David Dilworth, especially, for the many discussions, helpful advice, and reagents. Additionally, Andrew Leung, Neda Savic, and Drew Bowie for the years we have spent together in the lab and out. It has truly been a pleasure to work in such a great group.

I could not have reached this point without the help of many people in the Department and at UVic. Especially, our neighbours in the Petrotchenko lab: Jenya, Jason Serpa, Nicole Sessler, and Nick Brodie for their advice and always having space to run my samples. Our newer neighbours in John Burke's lab: John, Meredith Jenkins and Gill Dornan for sharing reagents, equipment and always having discussions on random topics. Dr. Connor O'Sullivan and Andrew Boyce, for their help with imaging. The Ausio lab and Cameron lab for use of their equipment. Scott Scholz, Stephen Horak and Albert Labossiere for their hard work maintaining the equipment in the Department. Melinda Powell and Deb Penner for always having the answers to my questions. And the many people around the department who made the years as a graduate student a great place to spend the past 6 years.

Finally, I couldn't have made it this far without the support of my family. My wife, Lauren, deserves a special thank you for providing endless encouragement and support throughout this long endeavour. She has been at my side for nearly the entire time I spent as a graduate student and I couldn't imagine doing it without her. And of course, our kitty cat, Mocha, for being no more than two feet away from me at all times during the hours upon hours I spent sitting in front of the computer writing this dissertation.

Dedication

For Lauren

Chapter 1: Introduction

1.1 General introduction.

The organization of eukaryotic DNA into chromatin is essential for processes including replication and transcriptional regulation. Chromatin is comprised of repeating units, referred to as nucleosomes, in which approximately 147 bp of DNA is wrapped around a histone octamer. The octamer is composed of the four core histones (H2A, H2B, H3 and H4), making up the core of the nucleosome [1]. Each histone also contains both N- and C-terminal tails that extend from the nucleosome structure.

While the formation of chromatin solves the issue of storing large amounts of DNA, there is still a requirement for accessibility to the genetic information to permit transcription, replication and repair. Regulation of the chromatin landscape is in part modulated by post-translational modifications (PTMs) of histones and chromatin-associated proteins, such as transcription factors. Additionally, DNA methylation, histone variants, histone chaperones and nucleosome remodellers provide an additional level of chromatin regulation.

Much of the focus on chromatin research lies in understanding the role of post-translational modifications as a method to regulate access to the DNA template. Modification enzymes decorate histones with a variety of PTMs to their core and tails. Some of the most studied modifications include: acetylation, methylation, and phosphorylation (for comprehensive review, refer to [2]).

Histone PTMs can affect chromatin in two ways. Firstly, the presence of the modification itself may directly influence the overall structure of chromatin. Lysine acetylation, for example, neutralizes basic charges, subsequently weakening or disrupting the interaction between histones and DNA [3,4]. Secondly, histone PTMs can also function indirectly on chromatin structure by serving as a platform to recruit additional regulatory enzymes. For example, HP1 recognizes H3K9me2/3 and serves as a scaffold to recruit other chromatin modifying enzymes that reinforce a repressive environment [5,6]. It should also be noted that the same enzymes imparting histone modifications are

not limited to the chromatin template and have targets distal to chromatin and the nucleus. SETD2, for example, has dual functions as a histone methyltransferase, and recently has been shown to target mitotic microtubules [7]. Loss of α-tubulin K40 methylation by SETD2 is associated with mitotic and cytokinetic errors, leading to genomic instability [7].

In addition to the widely studied covalent histone PTMs, prolyl isomerization has emerged as a non-covalent modification to both histones and chromatin-proximal proteins. *Cis/trans* isomerization of peptidyl-proline induces a 180° rotation of the peptide bond preceding the proline, subsequently altering structure and function. As such, prolyl isomerization has been implicated in gene regulation, through isomerization of histone prolines, chromatin-modifying enzymes, and transcription factors [8-10]. As will be discussed, like other chromatin modifications, *cis-trans* proline isomerization also occurs in other cellular locales.

In this Chapter, I will start by introducing the significance of prolyl isomerization and prolyl isomerase enzymes, providing examples of how this modification and class of enzyme regulates biological events. The known functions of nuclear FKBPs will be examined in detail, focusing on the human prolyl isomerase FKBP25. I will then provide an overview of ribosome biogenesis, which represents a major part of my research path and model for FKBP25 going forward. Additionally, nucleolin, an FKBP25-interacting protein with functions in multiple aspects of ribosome biogenesis will be examined. I will also describe the methods, tools, limitations and considerations in studying prolyl isomerase enzymes. Finally, I will outline the central questions of my thesis and my specific research objectives.

1.2 Prolyl isomerization.

Proline is a unique amino acid in that it adopts both *cis* and *trans* peptide bonds in proteins. Statistics from solved protein structures reveal 5-6% of proline bonds to be in the *cis* conformation [11], however this may actually be underrepresented due to ambiguity in low-resolution structures and in proteins with intrinsically disordered regions [12,13]. This is in contrast to the other 19 amino acids, which heavily favour the *trans* conformation due to steric constraints (<0.1% *cis*) [11,12]. The discrepancy in *cis* prevalence between proline and other amino acids can be explained by proline's unique

imide peptide bond, which has a reduced energy barrier between the *cis* and *trans* states in comparison to the amide peptide bond [14,15].

Isomerization of proline between the *cis* and *trans* isomers has major structural consequences resulting in a 180-degree rotation of the peptide bond preceding the proline (Ω=0° *cis* to Ω=180° *trans*) (Figure 1). This interconversion occurs spontaneously, albeit slowly, on the order of seconds-minutes [16,17]. Isomerization and the formation of ordered protein structure are interrelated processes as proteins with incorrect prolyl bond isoforms can only partially fold [18]. Therefore, prolyl isomerization and the adoption of the correct isoform can be a rate-limiting step in protein folding. Indeed, this was the basis for the prolyl isomerization hypothesis put forth by Brandts et al. in 1975 where they proposed the difference between fast and slow folding molecules differed in the *cis-trans* isomeric state of one or more prolyl bonds [18]. A number of proteins, including RNase A, thioredoxin and RNase T1, have been extensively studied in light of this hypothesis, and it has been determined that prolyl isomerization is required in the unfolding and refolding of these proteins [19-21].

The first demonstration of enzymatic prolyl isomerase activity was from porcine kidney extract [22]. Fischer et al. observed *cis/trans* interconversion of proline-containing peptides and accelerated proline isomer dependent refolding of RNase A *in vitro* [23]. Subsequently, this enzyme was named peptidyl-prolyl *cis-trans* isomerase.

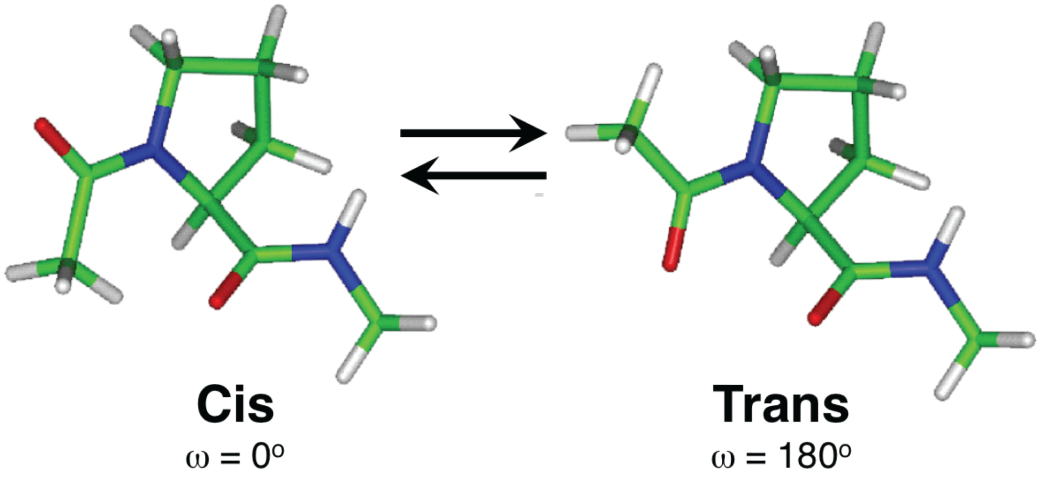

Figure 1. *Cis* and *trans* proline isomers impart distinct geometries on proline containing peptides.

The *cis*-proline peptide induces a sharp bend in the backbone, whereas the *trans*-proline peptide has a relatively straight backbone. Molecule is acetyl-propyl-N-methamide.

1.3 Peptidyl-prolyl isomerases.

Peptidyl-prolyl isomerases (PPIs) are a ubiquitous class of enzymes that are responsible for catalyzing the *cis-trans* isomerization of peptidyl-proline bonds. Three structurally distinct families make up this class of enzyme: cyclophilins, parvulins, and FK506-binding proteins (FKBPs) (Figure 2). PPIs significantly enhance *cis-trans* isomerization by several orders of magnitude [24] and thus have been classically regarded as *de novo* protein folding chaperones. In support of PPIs aiding protein folding, the prokaryotic prolyl isomerase, Trigger Factor, interacts with translating ribosomes and contributes to the folding of emerging polypeptide chains [25-27]. While eukaryotes do not have a ribosome-associated homolog of Trigger Factor, there are examples of eukaryotic PPIs functioning as chaperone-like proteins [28,29].

The precise mechanism of prolyl isomerization by FKBP enzymes has yet to be determined. Isomerization does not require proton donors or nucleophilic residues [30], and a number of factors likely contribute. These include substrate desolvation, substrate auto-catalysis and preferential transition state binding, where each contributes to lowering the energy barrier between the *cis* and *trans* states [31,32].

Although most eukaryotic PPIs are restricted to the cytoplasm, which is consistent with a function in protein folding, there is a growing body of evidence that this is not the only place these enzymes function within the cell. Some PPIs are also found in the mitochondria, nucleus and nucleolus [33]. The obvious interpretation is that they do not function solely as folding chaperones; instead some PPIs isomerize prolines to regulate the activity of substrates. This will be described in more detail below in the respective sections for the PPI families, focusing on the FKBPs.

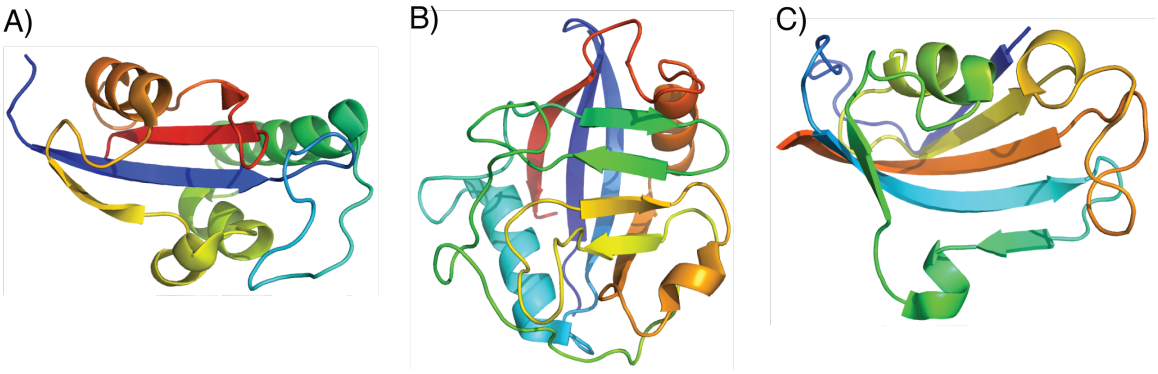

Figure 2. Isomerase domain structure of parvulins, cyclophilins and FKBPs. Comparison of PPI domain structures of A) Pin1 (PDB: 1NMW), B) CypA (PDB: 3K0N) and C) FKBP12 (PDB: 2PPN). Images were rendered in PyMOL.

1.3.1 Cyclophilins.

The cyclophilin family of isomerases is named for their ability to bind the immunosuppressive drug cyclosporine A (CsA). CsA is a non-ribosomal synthesized peptide that was identified as an immunosuppressant in the 1970s [34] inhibiting T cell proliferation [35]. Cyclophilin A, the first CsA binding proteins to be identified [36], is actually the same protein as peptidyl-prolyl *cis-trans* isomerase identified by Fischer et al. [22] in porcine kidney extract. It was originally proposed that the prolyl isomerase activity of CypA regulated the signal transduction events of T cell activation. Instead, it was later discovered that CypA-CsA forms a ternary complex with the phosphatase calcineurin, inhibiting its activity and preventing the transcription of IL-2 and cytokines [37,38]. In the absence of drug, CypA itself does not have a role in the immune response through calcineurin. CypA does however regulate T cell signalling through the Itk kinase [39], revealing it may have roles in the immune response independent of CsA.

CypA is the founder of the cyclophilin family whose members share the namesake peptidyl-prolyl isomerase cyclophilin domain. In general, the number of Cyps increases with organism complexity; eight are found in yeast, compared to sixteen in humans. Cyclophilins differ greatly in size and structure with some containing just a single PPI domain, and others possessing a variety of accessory domains (Figure 3). Refer to [33] for comprehensive review of human cyclophilin domain architectures.

Cyclophilins are involved in a multitude of processes, including: viral replication [40,41], splicing [42], and transcriptional regulation [9,43]. The involvement of

cylophilins in these processes was inferred through a loss of function that is dependent on the expression or activity of these enzymes. Therefore, the assumption has been that isomerization targets must exist in these pathways. The identification of proline substrates for cyclophilins however, has proven to be a significant challenge. Cyp33 regulating the activity of the histone methyltransferase MLL1 through prolyl isomerization [9,44] represents one notable exception (described in more detail below), supporting the underlying assumption that proline targets exist for these processes. This level of mechanistic detail is unique for Cyp33-MLL1, and the molecular mechanisms of cyclophilin function remains largely unknown.

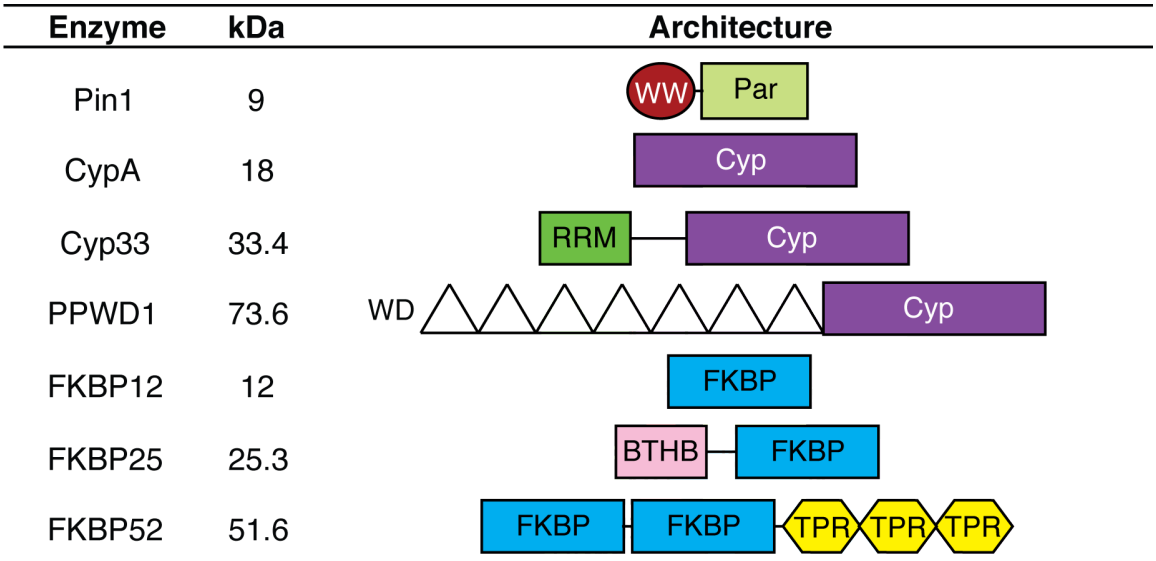

Figure 3. Variation in the domain composition of human PPIs.
Examples of domain composition of selected human parvulins, cyclophilins and FKBPs. Abbreviations: Par, parvulin; Cyp, cyclophilin; RRM, RNA-recognition motif; WD, WD40 repeat; FKBP, FK506-binding protein; BTHB, basic-tilted helical bundle; TPR, tetratricopeptide.

1.3.2 Parvulins.

Unlike cyclophilins, parvulins are not named by their binding of immunosuppressant drugs; instead they receive their distinction based on homology to an *E. coli* PPI [45]. The human genome consists of three parvulins: Pin1, Par14, and Par17. The latter two are isoforms transcribed from the same gene.

Pin1 is the only PPI that possesses a substrate recognition sequence, selectively isomerizing phosphorylated serine-proline (pS-P) and threonine-proline (pT-P) motifs [46]. Two phospho-specific domains facilitate this: an N-terminal WW domain recruits Pin1 to pS/T-P motifs, while the PPI domain selectively isomerizes phospho-epitopes. Par14 and Par17 however, do not exhibit the same substrate specificity for phospho-motifs and they exhibit relatively limited prolyl isomerase activity *in vitro [47]*.

Pin1 has received the most attention of all prolyl isomerases. The initial discovery of Pin1 came as a result of a yeast two-hybrid screen to identify proteins that interact with the mitotic kinase, Never-In-Mitosis gene A (NIMA) in *Aspergillus Nidulans [48]*. Deletion of Pin1 results in mitotic arrest, whereas over-expression (in HeLa cells) arrests cells in the G2 phase of the cell cycle [48]. Pin1 promotes progression through G1/S as well [49].

Together, the link of Pin1 selectively isomerizing pS/T-P motifs and its regulation of cell cycle progression, suggests it acts downstream of proline-directed kinases, such as cyclin-dependent (CDK) and mitogen-activated (MAPK) kinases. One mechanism of cell cycle regulation by Pin1 is through the modulation of Cyclin D1 levels. Pin1 promotes *cyclin D1* transcription by stabilizing the transcription factor c-Jun. Upon stimulation, c-Jun N-terminal kinase (JNK) directly phosphorylates c-Jun at S63/73-P motifs, leading to *cyclin D1* transcription [10]. Pin1 can then interact with the S63/73-P motifs, preventing ubiquitination and degradation of c-Jun [50]. Additionally, Pin1 interacts with a second motif (pT286-P) of c-Jun, increasing its stability and nuclear localization [51]. Therefore, through these two mechanisms, Pin1 is able to promote passage through the G1 phase of the cell cycle.

Out of all prolyl isomerases, Pin1 has by far the most reported interactions with transcription factors and signalling proteins [52], and its importance in phosphorylation-dependent signalling pathways is well documented [53]. The breadth and quantity of Pin1 substrates is beyond the scope of this thesis, and more information can be found in these comprehensive Pin1 review articles [32,54-56].

1.3.3 FK506-binding proteins (FKBPs).

Identification of the FKBP family came as a result of screening for FK506 binding proteins. FK506 is a non-ribosomal synthesized peptide that was originally

isolated from the soil bacterium *Steptomyces tsukubaensis,* and was subsequently identified as an immunosuppressant [57]. While both FK506 and CsA are immunosuppressants [58], they are unrelated molecules. FKBP12 was the first protein identified as an intracellular receptor for FK506 [59,60]. The immune suppression observed with FK506 occurs via a similar mechanism to CsA: that is, the formation of a ternary complex of FKBP12, FK506 and calcineurin [37,38] inhibits calcineurin's phosphatase activity and the activation of signalling. The presence of an a-keto (homo)proline amide linkage in FK506 led to the speculation and confirmation that FKBP12 is a distinct class of prolyl isomerase enzyme. The fact that both CsA and FK506 are unrelated molecules, yet confer a similar gain of function phenotype was unexpected. Further, the intracellular receptors for both of these molecules have PPI activity, which is also surprising.

FKBPs are the target of another immunosuppressive drug, rapamycin, which acts in a manner distinct from that of FK506 inhibiting calcineurin. Instead, rapamycin bridges an interaction between FKBP12 and the kinase mTOR, inhibiting its activity [61,62]. As mTOR is a major nutrient sensor in the cell [63], inhibiting its kinase activity prevents signalling through these pathways and decreases cellular proliferation [64].

Like cyclophilins, FKBPs also increase in number with organism complexity: four are encoded in budding yeast, whereas eighteen FKBPs are found in humans. Additionally, the architecture and size of FKBPs varies widely; some possess only a single FKBP isomerase domain, while others contain multiple FKBP domains as well as accessory domains (Figure 3). Refer to [33] for comprehensive review of human FKBP domain architectures.

FKBP12 and its modulation of the ryanodine receptor (RyR) represents one of the best-studied examples of regulation by an FKBP. RyRs are calcium-release channels that function as conduits to pass intracellular Ca^{2+} from the sarcoplasmic reticulum to the cytoplasm. FKBP12 tightly associates with the RyR [65] and interacts in a cleft formed by multiple domains [66]. Binding of FKBP12 promotes a closed state, however its modulation of the receptor occurs independently of catalytic activity [67,68]. The binding of FKBP12 alone exerts its function, as catalytically inactive FKBP12 maintains binding and a closed receptor state.

FKBPs are for the most part cytoplasmic [33], however FKBP25, FKBP51 and FKBP52 localize to the nucleus [69,70]. Below I will provide specific examples of the nuclear functions of FKBPs and set the stage for the reasoning and data that led to my hypothesis and research objectives of this dissertation.

1.4 Nuclear FKBPs.

1.4.1 Yeast Fpr4.

The *S. cerevisiae* genome encodes four FKBPs: Fpr1 and Fpr2 are cytoplasmic, while Fpr3 and Fpr4 localize to the nucleus and nucleolus. Fpr4 has unique domain architecture, containing an N-terminal 'nucleophosmin-like' (NL) domain and a C-terminal canonical FKBP domain.

The NL domain of Fpr4 contains acidic stretches characteristic of histone chaperone proteins [71]. Indeed, Fpr4 possesses histone chaperone activity *in vitro* and this occurs independent of prolyl isomerase activity [72,73]. Histone deposition is mediated by the NL domain interacting with H2A-H2B and H3-H4 [73]. Kuzuhara et al. also demonstrated Fpr4 localizes to ribosomal DNA (rDNA) chromatin, where the NL domain promotes silencing [72]. It is likely that Fpr4 mediates silencing through the creation of a repressive nucleosome environment via its histone chaperone activity.

Fpr4's interaction with histones is not restricted to a single function as a chaperone. Nelson et al. showed Fpr4 interacts with the histone H3 and H4 N-terminal tails and isomerizes histone H3 prolines [8]. Unlike Pin1, which interacts with its substrate prolines, Fpr4's interaction with the H3 tail does not include the prolines, implying an alternative mechanism from that of Pin1. Isomerization of H3 P38 consequently reduces the methylation kinetics of nearby H3 K36 by Set2, suggesting a structural change influences methylation. Fpr4's activity *in vivo* does not translate to a genome-wide regulation of H3 K36 methylation however; instead it promotes the rapid induction and transcription of uninduced genes [8]. Although the exact mechanism is unknown, H3P38 isomerization may affect the recognition or deposition of methylation by Set2.

Additionally, Fpr4's function in the nucleolus may extend beyond rDNA transcriptional regulation. Fpr4 associates with structural ribosomal proteins and ribosomal assembly factors [74-76]. Notably, Fpr4 interacts with proteins involved in the

maturation and export of the large ribosomal subunit, suggesting its functions may be limited to the 60S molecule. Whether Fpr4 is truly involved in the processing and assembly of pre-ribosomes in the nucleus/nucleolus has yet to be fully examined.

Together these reports reveal dual chromatin proximal functions for the two domains of Fpr4, regulating the chromatin landscape through its histone chaperone and prolyl isomerization activity.

1.4.2 FKBP25 is the human ortholog of Fpr4.

FKBP25 is regarded as the human ortholog of Fpr4, since the FKBP catalytic domains have a similar charge distribution and basic surface features. Despite this, the N-terminal domains of Fpr4 and FKBP25 are markedly different; FKBP25 possesses a basic-tilted helical bundle (BTHB), which does not contain the same acidic features present in Fpr4. The BTHB contains a unique fold found only in one other protein, HectD1. Although the function of this fold is unknown, it is expected to be an interaction surface for protein and DNA based on structural analysis [77]. Despite lacking the NL domain features of Fpr4, FKBP25 does interact with nucleolin [78], a multi-functional nucleolar protein that contains an acidic histone chaperone domain [79] (Figure 4). Therefore, it is possible that the chaperone functions of Fpr4 are conserved through the FKBP25-nucleolin interaction in higher eukaryotes.

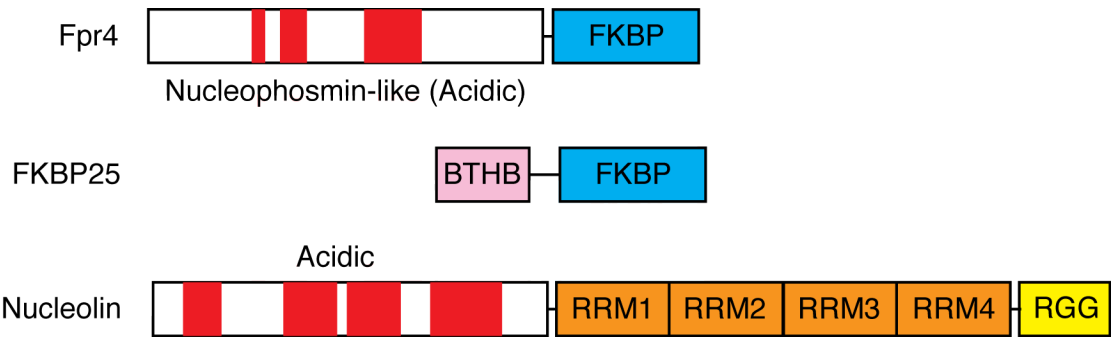

Figure 4. Domain architectures of yeast Fpr4, human FKBP25 and nucleolin.
Fpr4 has an N-terminal nucleophosmin-like (NL) domain and a C-terminal FKBP isomerase domain. FKBP25 lacks the acidic NL domain, instead possessing a basic-tilted helical bundle (BTHB). FKBP25 physically interacts with nucleolin, which contains an acidic domain. Nucleolin also contains four RNA-recognition motifs (RRM) and a glycine-arginine rich (RGG) domain.

1.5 FKBP25.

1.5.1 FKBP25 is associated with chromatin regulators.

FKBP25 was first identified in 1992 by the Schreiber lab [80] and shortly after was revealed to be nuclear localized, bind DNA and interact with nucleolin and casein kinase II [78,81].

The first functional study of FKBP25 linked this PPI to chromatin and transcription [82]. Yang et al. found that FKBP25 immunoprecipitated material contained histone deacetylase activity [82]. FKBP25 interacts with both HDAC1 and HDAC2, as well as the transcription factor YY1. Interestingly, amino acids 1-90 of FKBP25 augments YY1 DNA binding *in vitro* and enhances YY1-mediated repression in reporter assays *in vivo* [82]. This effect appears to occur independently of FKBP25's prolyl isomerase activity. FKBP25 1-90 was sufficient to mediate an effect and impairment of FKBP25's activity with FK506 was shown to have no impact on YY1 regulation. Together, this report provided evidence of FKBP25 functioning to regulate DNA-binding of a transcription factor. Still, the role of FKBP25's PPI domain in proximity to chromatin remains unclear.

More recently, Prakash et al. provided structural insight into the FKBP25-YY1 interaction [83]. A surface in the BTHB of FKBP25 mediates an interaction with the DNA-binding domain of YY1. Additionally, through NMR titration experiments, it was demonstrated surfaces in both domains of FKBP25 mediate interactions with DNA. Assaying DNA binding of mutagenized FKBP25 proteins by gel shift assays subsequently confirmed the key residues mediating DNA interactions. This led to a model being proposed whereby FKBP25 interacts first with YY1, altering its affinity for DNA and the binary complex searches for a DNA substrate to bind.

Additionally, all four core histones (H2A, H2B, H3, and H4), and the linker, histone H1, co-immunoprecipitate with FKBP25 [84]. This, combined with the above, support FKBP25 as a chromatin associated protein. Whether or not FKBP25 regulates gene expression independent of YY1 has yet to be demonstrated.

1.5.2 FKBP25 and the p53-MDM2 axis.

FKBP25 has also been shown to be a regulator of the E3 ubiquitin ligase MDM2 and subsequently, p53 levels. MDM2 and p53 are involved in an auto-regulatory loop,

where p53 positively regulates MDM2 gene expression [85] and MDM2 regulates p53 levels through ubiquitination and proteasome-dependent degradation [86,87]. This balance between p53 and MDM2 is tightly regulated and can be disrupted by various cellular stresses leading to a p53 response. Interestingly, FKBP25's expression is repressed in a p53 dependent manner [88].

Ochocka et al. identified FKBP25 as an MDM2 interacting protein in yeast two-hybrid assays, and confirmed an FKBP25-MDM2 interaction by co-immunoprecipitation and *in vitro* GST-pulldowns [70]. To determine how FKBP25 is involved in the p53-MDM2 pathway, myc-FKBP25 was co-expressed with p53 and MDM2 in H1299 cells. Overexpression of FKBP25 resulted in a significant decrease in MDM2 levels, and an absence of ubiquitinated p53. By using a ubiquitination deficient mutant of MDM2 (C464A), as well as treating cells with the proteasome inhibitor MG132, Ochocka et al. demonstrated that FKBP25 acts upstream of MDM2 self-ubiquitination and proteasome-dependent degradation [70]. FKBP25's interaction with MDM2 occurs through its PPI domain, suggesting the possibility of prolyl isomerization altering MDM2 structure to favour auto-ubiquitination and degradation. However, the use of the potent FKBP inhibitor, rapamycin, had no effect on MDM2 levels. Whether this result is due to the short rapamycin treatment (2-6 hours) or other confounding factors is not known. Performing MDM2-ubiquitination assays in a controlled *in vitro* system may shed light on whether catalytic function of FKBP25 mediates this effect.

1.5.3 FKBP25 and RNA.

There is a growing body of evidence that FKBP25 is not just a DNA binding protein. FKBP25 can be found in neuronal RNA granules which are large bodies consisting of mRNA, ribosomes, RNA binding proteins and motor proteins that function to transport the components for protein synthesis to distant synaptic surfaces [89,90]. Moreover, Galat et al. revealed FKBP25 to be associated with polyribosomes in cellular fractionations [84]. FKBP25 can be dissociated from the ribosomal fraction with the addition of RNA, suggesting its association is through an RNA interaction. Further supporting this is the observation that FKBP25 interacts with both immobilized RNA and heparin *in vitro* [91].

FKBP25 associates with ribosome-associated proteins such as nucleolin, nucleophosmin, EF1B and structural ribosomal proteins RPS4, RPL7, RPL13A and RPLP2 [84,91], suggesting a function in ribosome biology. Additionally, the splicing factor SRSF3 interacts with FKBP25 [84]. Therefore, FKBP25 may have potential roles in ribosome assembly, splicing and translation, although a more thorough analysis of these is needed to decipher its functions.

1.6 Ribosome biogenesis.

Growing cells require continuous ribosome production to meet immediate protein needs and to ensure sufficient ribosomes are available to divert to daughter cells in mitosis. This requires the coordinated action of all three RNA polymerases. RNA polymerase I transcribes the 47S rRNA, making up the bulk of the rRNA content of the ribosomes. RNA polymerase II is required to produce the mRNAs needed for the structural protein content of the ribosome, whereas RNA polymerase III transcribes the 5S rRNA.

The nucleolus is the major site of ribosome synthesis in eukaryotes, containing a tandem array of rDNA repeats, as well as a variety of factors involved in transcription, pre-rRNA processing and ribosome assembly. The nucleolus contains structural compartments for the steps of ribosome biogenesis: the fibrillar center (FC), dense fibrillar component (DFC) and granular component (GC) [92]. rDNA transcription occurs at the interface between the FC and DFC, while early rRNA processing/assembly events occur in the DFC and ribosomal subunit assembly occurs in the GC [93].

Until recently, the understanding of ribosome assembly in mammals has lagged significantly behind that in yeast. This is largely a result of the tools available in yeast (ie. genetic screens and pre-ribosomal purification) that make them amendable to the study of ribosome biogenesis. It is a widely acknowledged assumption that eukaryotic ribosome assembly is largely conserved, mostly based on homology of known ribosomal factors between yeast and humans. While conserved functions may exist for these proteins, recent studies suggest a proportion of human rRNA processing factors possess distinct or additional functions not shared by their yeast counterparts [94]. With the emergence of novel genetic tools and structural techniques, such as CRISPR/Cas and cryo-EM, the

understanding of ribosome biogenesis in humans will undoubtedly be improved in the coming years.

The following sections are meant to provide an overview of the coordinated events required for eukaryotic ribosome assembly. For excellent, detailed reviews on nucleolar function and ribosome biogenesis please refer to [95-97]. A schematic of the general process of ribosome biogenesis is summarized in Figure 5 below.

1.6.1 rDNA organization and transcriptional regulation.

The process of assembling a ribosomal subunit requires the initial transcription of rDNA by RNA polymerase I. In humans, rDNA repeats occur in tandem arrays in nucleolus organizer regions distributed along acrocentric chromosomes 13, 14, 15, 21 and 22. Each 43 kb repeat consists of an intergenic spacer and the transcribed sequence corresponding to the 47S rRNA. The 47S rRNA is transcribed as a single unit, which is then processed into the mature 18S, 5.8S and 28S forms. While there are approximately 400 rDNA repeats in humans, only about half are actively transcribed at any given time [98].

Actively transcribed repeats are marked by the presence of UBF, a member of the pre-initiation complex along with SL1 [99]. Binding of UBF to the rDNA promoter stabilizes SL1, which mediates the recruitment of the RNA pol I transcriptional machinery [100,101]. Similar to protein coding genes, two distinct epigenetic mechanisms regulate rDNA: DNA methylation and histone modifications. Features of active genes are low nucleosome occupancy, DNA hypomethylation, acetylation of H4 and H3K4 dimethylation. Conversely, silent genes are nucleosome rich and exhibit DNA hypermethylation, H4 hypoacetylation and trimethylation of H3K9, H3K27 and H4K20 [102].

As ribosome production is intimately linked with cellular proliferation, rDNA transcription is tightly regulated in response to the needs and energy status of the cell. In the 1980s, increased nucleolar size was identified as a cytological feature of cancer cells [103]. Additionally, growth-dependent signalling pathways, oncogenes and tumour suppressors [104-108] converge on ribosome biogenesis and modulate transcriptional output, thus it is not surprising that cancers have increased rRNA production [109,110].

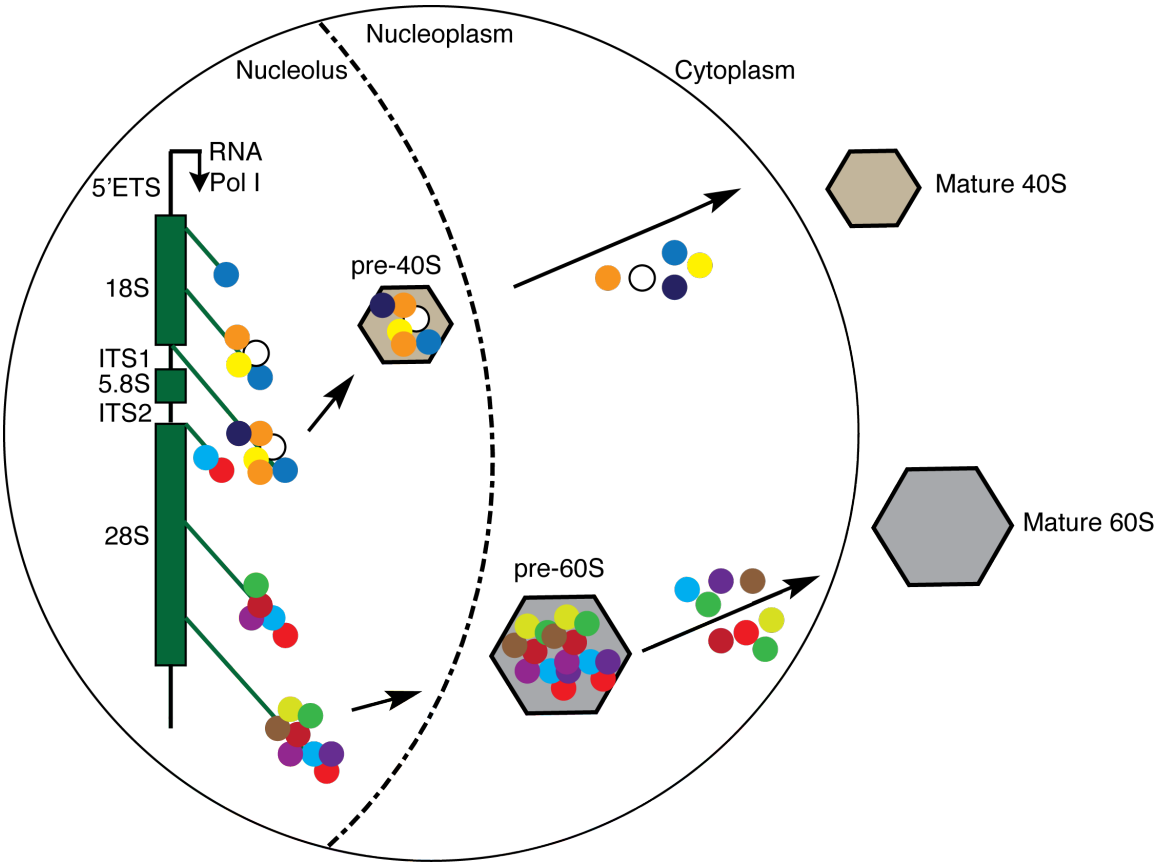

Figure 5. Eukaryotic ribosome biogenesis is a multi-step process.

Ribosome biogenesis is initiated in nucleolar organizer regions, where the rRNAs are synthesized. RNA polymerase I transcribes three of the four rRNAs (18S, 5.8S and 28S) as a single transcript. The fourth rRNA (5S) is transcribed in the nucleus by RNA polymerase III (not shown). The 18S, 5.8S and 28S are interspersed with non-coding sequences, 5'ETS (external transcribed spacer), ITS1 (internal transcribed spacer), ITS2 and 3'ETS. Branches from the rDNA represent rRNA at different times through transcription. Processing proteins/complexes (coloured circles) arrive almost immediately as rRNA emerges. The pre-40S and pre-60S subunits mature in separate pathways with their own unique complement of assembly and processing proteins. These factors transit through the nucleus with the pre-ribosomes. The transient collection of processing factors becomes less complex as maturation progresses. Pre-ribosomes are exported through nuclear pores by export factors. Final maturation steps occur in the cytoplasm. Factors involved in the maturation of ribosomal subunits are recycled (returned to the nucleolus for continuous ribosome synthesis).

1.6.2 Ribosome assembly, maturation and export.

The assembly and maturation of the two ribosomal subunits is coordinated process, initiated in the nucleolus and finished with final maturation in the cytoplasm.

The 40S subunit consists of the 18S rRNA and 32 ribosomal proteins (RPSs), whereas the 60S consists of the 28S, 5.8S and 5S rRNAs and 47 ribosomal proteins (RPLs). Over 200 transient pre-rRNA processing proteins have been identified in humans [94], however as previously unknown pre-ribosomal associated proteins are identified this list will surely grow. Included in this diverse collection are endonucleases, helicases, chaperones and scaffold proteins. Additionally, snoRNAs guide rRNA modifications, which are thought to contribute to folding and ribosomal interactions. Protein complexes that form with C/D box snoRNAs are associated with 2'O-ribose methylation, whereas H/ACA box snoRNA complexes mediate pseudouridinylation. Thus, a diverse collection of scaffolds, and enzyme activities that post-translationally modify both the protein and rRNA are needed to generate a functional ribosome.

The recruitment of ribosomal assembly factors must be carefully coordinated. The arrival and departure of factors occurs as a hierarchical process that is spatially and temporally regulated [111,112]. The small subunit (SSU) processome arrives almost immediately as the 5' end of the rRNA transcript that emerges from RNA polymerase I, forming the 90S pre-ribosomal complex. This complex consists of a combination of structural ribosomal proteins and processing factors that mediate the first rRNA cleavage events [113]. RPLs and 60S processing factors do not associate with these early events and are only recruited at a later point as RNA polymerase I nears or transits the 28S transcript [114]. The pre-40S and pre-60S complexes mature separately, and as the subunits mature, the non-ribosomal protein content decreases and the processing and assembly factors recycle back to the nucleolus to participate in new rounds of ribosome assembly. When the subunits reach the nuclear membrane, export factors mediate their passage through the nuclear pore. The final steps of maturation occur in the cytoplasm as export proteins dissociate and the last ribosomal proteins are placed in the structure.

1.6.3 Cryo-EM provides molecular detail of ribosome assembly.

The model of ribosome assembly has largely come from biochemical and genetic experiments in yeast. Despite this, spatial relationships between pre-ribosome assembly factors and the key assembly events responsible for subunit maturation remain unclear. Recent advances in 3D cryo-electron microscopy (cryo-EM) have allowed the

visualization of complex structures and we now are beginning to understand the molecular details of pre-40S and pre-60S ribosome assembly.

Recently, Kornprobst et al. determined the structure of the 90S pre-ribosome using cryo-EM [115]. Features of the molecule were mapped by fitting data from other studies to determine the location of different proteins and RNAs in the 90S complex. Intriguingly, the UTP protein complexes act as a chaperone-like complex, encasing the nascent rRNA, so that it can be processed, assembled and loaded with ribosomal proteins. The authors also demonstrate different states of 18S rRNA folding, supporting the model of hierarchical assembly.

Insight into the late stages of pre-60S assembly has also recently been revealed. Wu et al. enriched the pre-60S ribosomes containing the GTPase Nog2, which is recruited to the pre-60S in the nucleolus and is present during most of the nucleoplasmic assembly stages [116]. The structures provide mechanistic detail for three major remodelling events preceding nuclear export: rotation of the 5S ribonucleoprotein, construction of the active centre and ITS2 removal. Additionally, the location and structure of over 20 assembly factors were mapped with these data as well [116].

Together, these reports provide three-dimensional architecture of early pre-40S assembly, as well as the latest stages of pre-60S maturation. Targeting other pre-ribosomal assembly stages will provide further mechanistic insight into the complexity of ribosome assembly and shed light on the functions of other assembly factors.

1.7 Nucleolin.

Nucleolin is a highly abundant nucleolar protein, making up approximately 10% of non-histone protein content of the nucleolus [117]. Nucleolin can also be found in regions of the nucleus, cytoplasm and plasma membrane. Structurally, it contains an N-terminal acidic domain, four central RNA recognition motifs (RRMs) and a C-terminal glycine-arginine rich region (RGG) (Figure 4). Nucleolin is a truly multi-functional protein, having been shown to regulate a number of cellular processes. The following sections will focus on nucleolin's role in ribosome biogenesis. While not discussed in detail in this dissertation, it should be noted that nucleolin has additional functions in mRNA translation and turnover [118,119], viral entry and replication [120,121], DNA damage and chromatin dynamics [79,122]. Interestingly, nucleolin also localizes to the

cell surface in a number of cancer cells and is a target for cancer therapies. These therapies include the aptamer AS1411, which binds to nucleolin on the cell surface and is internalized, decreasing cellular proliferation through bcl-2 mRNA destabilization and Rac1 activation [123,124]. The tumour-homing peptide F3 is also internalized by cell-surface nucleolin and could be used for drug delivery [125]. For more information on these additional functions, please refer to [126-128].

1.7.1 rDNA regulation.

Much of the recent attention of nucleolin in ribosome biogenesis has focused on its role in rDNA transcription. While early studies utilizing microinjection of nucleolin protein or anti-serum suggested a repressive role in RNA polymerase I transcription [129,130], more recent depletion studies *in vivo* yielded contradictory results [131-133]. First, conditional knockout and siRNA depletion experiments demonstrated that decreased nucleolin levels are directly correlated to low RNA polymerase I transcription of rDNA [131,132]. Second, depletion of nucleolin also results in nucleolar disruption and cell cycle arrest [133]. Mechanistically, nucleolin regulation of rDNA transcription involves alterations to chromatin architecture. Cong et al. established that depletion of nucleolin resulted in changes in the epigenetic landscape where activating histone marks (H4K12ac, H3K4me3) are decreased, and repressive marks (H3K9me2) are increased [134]. Nucleolin appears to prevent the recruitment of silencing complexes, including TTF-1 and the NoRC, preventing the formation of a repressive environment. These results collectively demonstrate that nucleolin is an activator of RNA polymerase I transcription.

1.7.2 Histone chaperone and nucleosome remodelling.

The N-terminal domain of nucleolin contains acidic stretches characteristic of histone chaperones [135]. It has been proposed that nucleolin histone chaperone activity facilitates RNA polymerase I transcription by destabilizing nucleosomes through the transient release of histones [134]. Indeed, nucleolin exhibits FACT-like histone chaperone activity [79]. Both nucleolin and FACT dissociate the histone H2A/H2B dimer, facilitating RNA polymerase transiting through nucleosomes *in vitro*. Not

surprisingly, FACT and nucleolin occupy active rDNA repeats suggesting a common role in aiding transcriptional elongation [136].

Additionally, nucleolin is able to promote nucleosome remodelling through SWI/SNF and ACF [79]. These complexes modify chromatin architecture by sliding nucleosomes allowing regulatory machinery to access DNA. Interestingly, nucleolin is able to stimulate sliding of nucleosomes containing the histone variant macroH2A. Nucleolin and macroH2A act antagonistically on rDNA, as nucleolin promotes transcription, while macroH2A mediates repression [137].

1.7.3 RNA binding, ribosomal processing and assembly.

The role of nucleolin in ribosome maturation has received much attention since its first description in the 1970s [138,139]. Initial studies identified nucleolin as nucleolar localized and associated with pre-ribosomal particles [117,140].

The Bouvet and Amalric groups have since extensively described the role of nucleolin in early pre-rRNA processing. Nucleolin represents one of the first proteins recruited to the 5'ETS, and promotes the first rRNA processing step *in vitro* [141]. Nucleolin's interaction with a conserved 11 nucleotide stem-loop sequence (termed 'evolutionary conserved motif' or ECM) lies 5 nt downstream of the cleavage site and is required for its processing [142]. Notably, all four RRMs are required to interact with the ECM [143].

In addition to the ECM, nucleolin also interacts with a 68 nucleotide conserved stem-loop sequence termed the 'nucleolin recognition element' or NRE [144]. This interaction has been thoroughly studied with *in vitro* gel shift assays [145,146]. In contrast to binding to the ECM, only RRMs 1-2 are required for nucleolin to bind the NRE. These assays are in full agreement with a co-structure that shows surfaces from both RRM1 and RRM2 interact with the NRE RNA loop [147]. Since putative NRE motifs are found throughout the 47S rRNA transcript, these likely provide nucleolin with recruitment landmarks to mediate additional processing or assembly events for the small and large subunits [148].

Nucleolin may also function in ribosome assembly and export. Nucleolin interacts with ribosomal proteins through its C-terminal RGG domain [149]. In light of this, ribosomal proteins could serve as a docking platform for nucleolin to be recruited to pre-

ribosomes to aid assembly. Alternatively, nucleolin may interact with rRNA, acting as a bridge to deliver ribosomal proteins. Nucleolin also shuttles between the nucleus and cytoplasm [150], thus its interaction with ribosomal proteins could come after subunit assembly to facilitate export of ribosomal subunits.

Despite nucleolin's abundance in the nucleolus and its association with multiple RNAs and proteins in both the small and large pre-ribosomal subunits [140], its precise function downstream of the 5'ETS cleavage is unclear. Depletion of nucleolin only results in a minor effect in rRNA processing, with a 20% decrease in 32S to 28S maturation [132,134]. Therefore, nucleolin does not play an integral role in the RNA processing aspect of ribosome assembly. Nucleolin may instead interact with rRNA and associate with pre-ribosomes to protect rRNA and prevent improper modification or contacts.

Alternatively, nucleolin's interaction with pre-ribosomes may not be directly related to ribosome biogenesis. Rather it is possible that it is a mechanism of nucleolar sequestration. This is evident by nucleolin re-localizing from the nucleolus to the nucleoplasm and cytoplasm after cellular stresses, such as RNA polymerase I inhibition, heat shock and DNA damage [151,152]. The redistribution of nucleolin to the nucleoplasm under heat shock functions to sequester RPA away from sites of DNA synthesis, inhibiting DNA replication [152]. Additionally, treatment of cells with DNA damage agents re-localizes nucleolin to the nucleoplasm in a p53 dependent manner [151]. Together, these reports suggest nucleolin may be a stress response factor.

1.7.4 G-quadruplex DNA.

G-quadruplexes are stacked structures that form in single stranded guanine rich sequences (Figure 6). Computational analyses of the human genome reveal the potential for upwards of 300,000 G-quadruplex forming sequences [153]. Interestingly, G-quadruplexes are not random, occurring in functional regions of the genome such as telomeres, replication origins and gene promoters. Recent G-quadruplex ChIP-seq revealed they are directly correlated with low nucleosome occupancy and are present in highly transcribed genes [154].

Two reports from the Maizels lab demonstrate that nucleolin is a G-quadruplex binding protein *in vitro* [155,156]. Thus it appears nucleolin binds both RNA and DNA

with secondary structure. The G-quadruplex sequences used in these studies were derived from rDNA, telomeric and immunoglobulin switch recombination regions. While confirmation of nucleolin binding to each of these locations via G-quadruplexes *in vivo* is currently lacking, there is evidence of nucleolin regulating c-Myc transcription through a G-quadruplex in its promoter. The nuclease-hypersensitivity element (NHE III_1) is a G-rich sequence upstream of the P1 promoter, controlling c-Myc transcription [157]. In support of G-quadruplex regulation of c-Myc, a small molecule that stabilizes G-quadruplexes represses c-Myc transcription *in vivo* [158]. Nucleolin binds with high affinity to the c-Myc G-quadruplex *in vitro* and enriches in the NHE III_1 region *in vivo* by ChIP [159,160]. Additionally, nucleolin over-expression represses c-Myc transcription in reporter assays *in vivo* [159].

Together this data supports nucleolin as a G-quadruplex binding protein capable of regulating RNA polymerase II transcribed genes. Comparison of nucleolin and G-quadruplex ChIP-seq datasets may shed light on the potential of nucleolin regulating other genes through a similar mechanism. This is especially relevant to rDNA, as the nucleolar-targeting molecule CX-3543 selectively disrupts nucleolin/G-quadruplexes, inhibiting RNA pol I transcription [161]. G-quadruplexes may therefore provide a recruitment surface for nucleolin, bringing its acidic chaperone domain in proximity of histones to aid rDNA transcription.

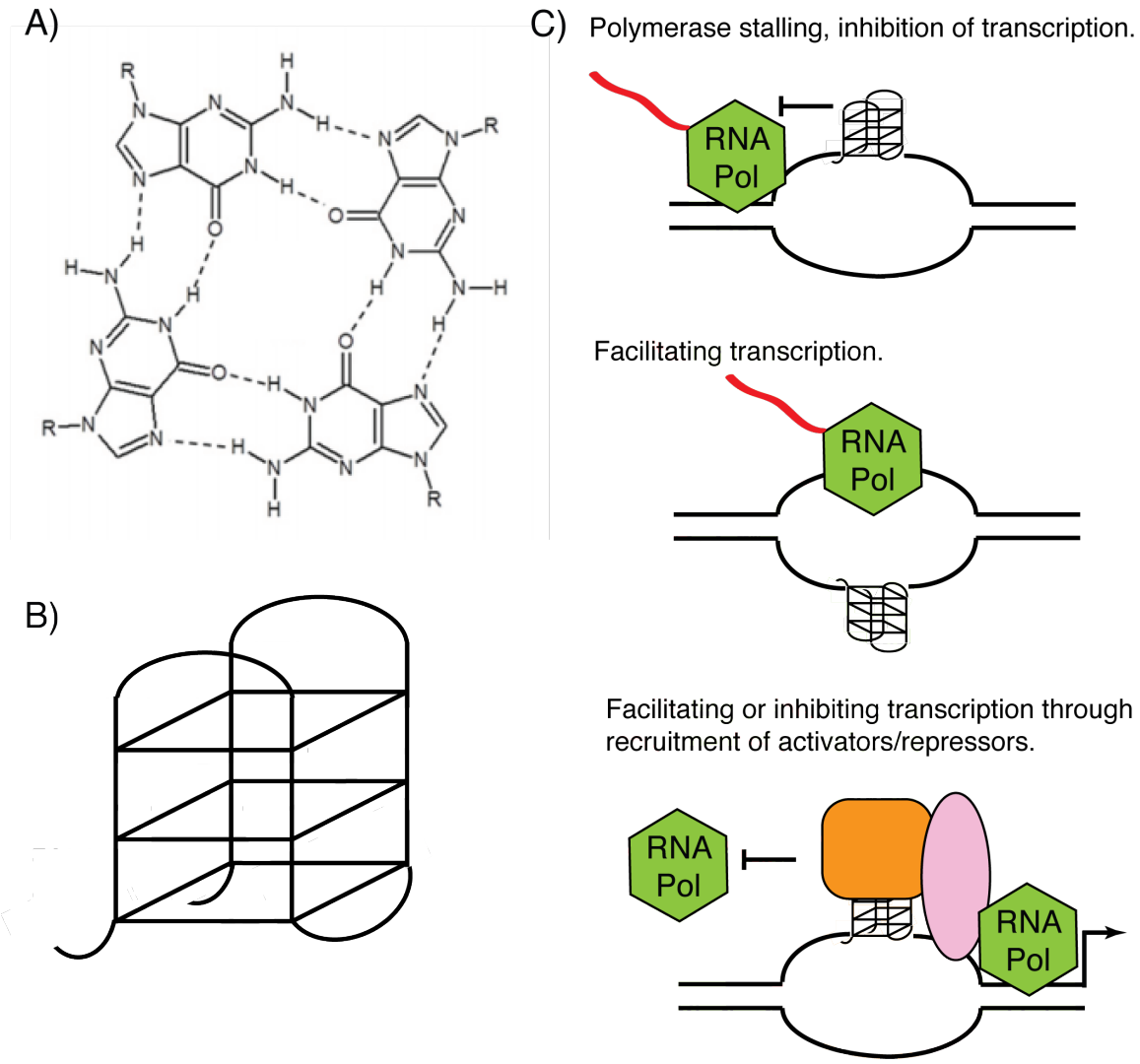

Figure 6. G-quadruplexes are regulatory elements in chromatin.

A) Orientation of four guanines arranged into a quartet structure. B) Representation of a stacked G-quadruplex structure. C) Potential mechanisms for G-quadruplexes to regulate transcription. Top: RNA polymerase blocked by G-quadruplex structure in transcribed strand. Middle: G-quadruplex in the non-transcribed strand facilitates RNA polymerase passage. Bottom: G-quadruplex binding proteins can block or stimulate recruitment of transcriptional machinery.

1.8 Further details and practical considerations of the study of PPIs.

Understanding the mechanisms by which PPIs function is imperative for defining their roles in biological processes. As such, a number of considerations must be taken when studying this class of enzyme. The domain architectures of PPIs are important for both substrate interactions and function and once recruited to their substrates, PPIs can

act in a catalytic-dependent or –independent manner. Differentiating between these mechanisms is challenging and requires tools to accurately separate these properties. The following sections will highlight the considerations, methods and tools required to study PPIs.

1.8.1 Domain architectures of PPIs.

The domain architecture of PPIs vary widely from just a single isomerase domain, to large proteins with multiple isomerase and accessory domains [33]. For example, FKBP12 contains just a single PPI domain, whereas FKBP52 contains three tetratricopeptide repeats (TPR), and two FKBP isomerase domains. Accessory domains provide an interaction surface, directing the PPI to substrates. For example: Pin1's WW domain interacts with specific phosphorylated S/T-P motifs in substrates [162,163] and Fpr4's NL domain binds its substrate histone H3 [8]. Additionally, FKBP52's TPR domain is required for an interaction with the transcription factor IRF-4, placing its PPI activity to modulate DNA binding [164]. Therefore, accessory domains serve as a surface to mediate interactions with substrate.

Remarkably, the opposite mechanism, where PPI action establishes a binding epitope for an accessory domain, has also been demonstrated. The cyclophilin Cyp33 promotes a *cis* to *trans* isomerization of P1629 between the PHD3 and Bromo domains of MLL1. This induces a structural rearrangement, revealing a previously occluded PHD3 binding surface for the RRM of Cyp33 [9]. It is thought the binding of Cyp33 to MLL1 mediates a switch from activator to repressor through altered affinity of PHD3 for H3K4me3 [9,44] and recruitment of co-repressors [165]. Cyp33's initial recruitment is not through an interaction with its substrate, MLL1, but possibly through RNA [9], which stimulates PPI activity [166]. Thus, accessory domains are not the only method to recruit PPIs to substrates.

While above examples demonstrate that accessory domains in prolyl isomerases can mediate protein interactions before or after PPI activity, it is important to appreciate that the PPI domain itself also provides an interaction surface. Perhaps the best illustration of this is the fact single domain isomerases (ie. Yeast Cpr1, Cpr2 and Fpr1, Fpr2), have discrete protein-interactomes [74,76] and seemingly unique functions based on their genetic interactions [167]. Single domain PPIs from higher organisms display

non-overlapping functions as well. These enzymes are likely recruited as a consequence of the biochemical attributes of the domain. Features such as surface charge and structure can help to recruit enzymes to their substrates. In support of this, Davis et al. systematically compared the solution structures of 15 human cyclophilin domains, revealing extensive differences in domain charge and structure [168]. In addition to the highly conserved residues in the catalytic pocket, Davis et al. identified diversity in a second pocket conferring some substrate specificity and wide variations in surface features. Almost certainly, the same principle applies to the FKBP family and I have highlighted the PPI domain surface charge of FKBP12, FKBP25 and FKBP52 (Figure 7). Differences in the globular domain structure and surface charge distribution between these three FKBP domains illustrate that these PPIs have divergences that are certain to influence interactions.

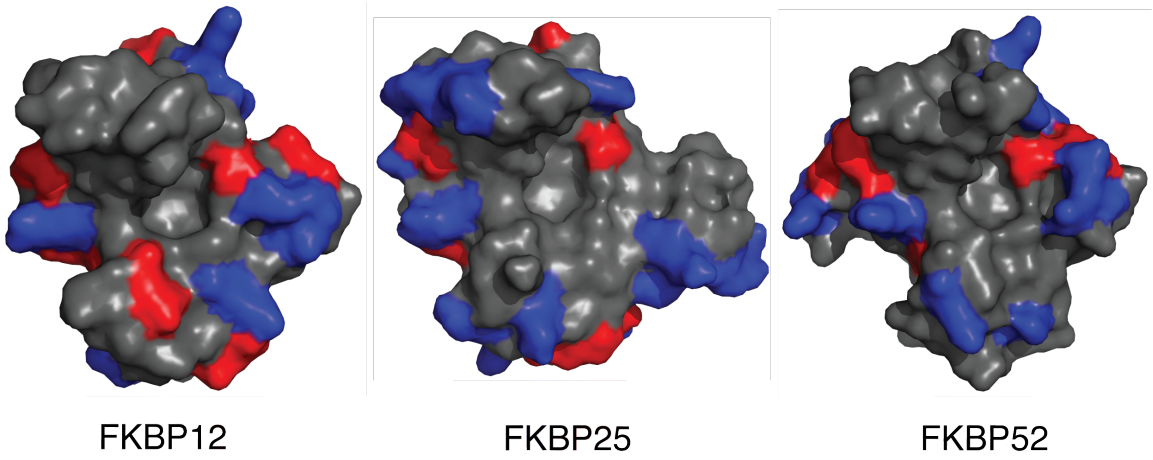

Figure 7. Surface charge density differs between human FKBPs.

Structures of the FKBP domains facing the catalytic pocket of FKBP12 (left), FKBP25 (middle) and FKBP52 FK1 (right) displaying charged surface patches (Acidic-red, basic-blue). Images were rendered in PyMOL.

1.8.2 FKBP PPI domains have catalytic and non-catalytic functions.

Although the naming of PPIs came as a result of their observed enzymatic activity, catalytic PPI domains also exhibit functions independent of isomerase activity.

As such, PPIs have been demonstrated to possess both catalytic-dependent and independent functions.

As described above, FKBP12 and its modulation of the ryanodine receptor represent one of the best-studied examples of non-catalytic regulation by a PPI. However, FKBP12's association with membranes is not limited to ion channels. FKBP12 has also been shown to promote the depalmitoylation and trafficking of H-Ras from the plasma membrane to the Golgi [169]. It is thought that this occurs through prolyl isomerization of P179 in H-Ras, as demonstrated with FK506 treatment and mutagenesis. Consequently, inhibiting the action of FKBP12 yields enhanced Ras signalling at the plasma membrane.

FKBP52 represents a second example of a PPI possessing both catalytic and non-catalytic functions. FKBP52 associates with steroid hormone complexes, such as the glucocorticoid receptor (GR), and can promote its nuclear translocation [170]. Riggs et al. used a yeast reporter model to show expression of FKBP52 enhances steroid hormone potentiation, speculating a prolyl isomerase-dependent mechanism [171]. However, further analysis with additional catalytic mutants revealed a loop overhanging FKBP52's catalytic pocket mediates an interaction with GR and induces potentiation in a non-catalytic manner [172].

Additionally, the action of FKBP51 and FKBP52 possess antagonistic roles in transcriptional regulation [69]. FKBP51 forms a complex with cytoplasmic RelA (a NF-kB family member), inhibiting its nuclear localization. However, upon RelA stimulation, FKBP52 exchanges with FKBP51 and promotes the activation of NF-kB target genes. Interestingly, FKBP51's cytoplasmic sequestration of RelA is insensitive to FK506 suggesting a catalytic independent mechanism. In contrast, FK506 and catalytic mutants inhibit FKBP52's function and point to a prolyl isomerase dependent mechanism activating RelA.

Taken together, these examples demonstrate that PPIs and more specifically, FKBP domains, do have functions that are independent of prolyl-isomerase activity. This is an important consideration that is often overlooked in the study of PPIs. I will discuss distinguishing between these catalytic and non-catalytic functions in Chapter 2.

1.8.3 Measuring prolyl isomerase activity.

The biggest challenge in studying prolyl isomerases is the limited means to observe the non-covalent *cis-trans* modification of a proline substrate. The initial studies that demonstrated prolyl isomerization utilized protein folding as a means to measure activity [23]. Differences in rates between unfolded, intermediate and folded structures dependent on prolyl isomerization could be determined spectrophotometrically, and subsequent mutagenesis and structural work identified these proline targets.

Fischer et al. developed an assay to measure the activity of these PPI enzymes towards proline containing peptide substrates [173] (Figure 8). This assay takes advantage of chymotrypsin only being able to cleave a phenylalanine in a Xaa-P-F-pNA peptide (Xaa is any amino acid) when the proline is in the *trans* conformation. This assay has been extensively used to determine the activity of PPIs towards different substrate sequences [16,174]. A solvent-jump system that increases the initial *cis*-proline population has improved this assay [24]. However there are still a number of issues [175]. First, kinetic analysis can only be measured in the *cis-trans* direction. Secondly, the peptide substrate does not represent a native sequence as it only contains amino acids N-terminal (usually four) to the target proline. It is now appreciated that amino acids C-terminal to the proline impact isomerization. Initial experiments using chymotrypsin-coupled isomerization assays revealed Fpr4 to be active against histone H3 P30 and P38, but not P16 peptides [8]. Using NMR to measure the activity of Fpr4 towards histone H3 decapeptides (containing residues both N- and C-terminal to the target proline), Monneau et al. revealed a discrepancy in isomerization of the P16 peptide [176]. Fpr4 was active towards the P16 peptide only with C-terminal amino acids present, suggesting the importance of these residues in enzymatic activity. Finally, the use of a protease to cleave the substrate peptide may also digest the prolyl isomerase [177].

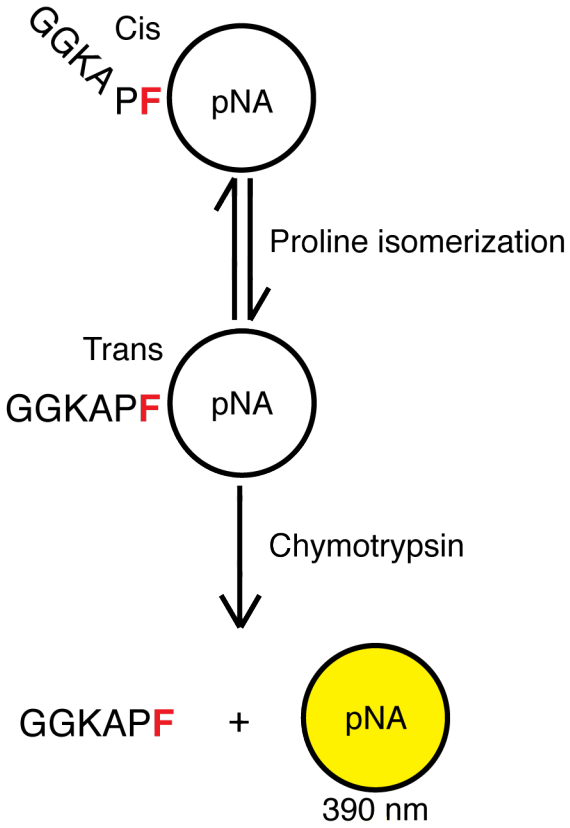

Figure 8. Schematic of chymotrypsin-coupled prolyl isomerase assay.

Substrate peptide linked to p-nitroanaline (pNA) is stored in a TFA/LiCl solution, promoting the formation of the cis-isomer. Chymotrypsin can only cleave the phenylalanine in the *trans* conformation. Isomerization from *cis* to *trans* is measured by addition of substrate to samples with or without PPI. Release of pNA by chymotrypsin is directly proportional to the rate of isomerization. pNA release is measured in real time using a spectrophotometer.

NMR is the preferred method to determine isomerase activity. Spectra contain distinct amide peak shifts for both the *cis* and *trans* isomers and rates can be measured at equilibrium in both directions [178]. Additionally, unlike the chymotrypsin-coupled assay, NMR is not limited to a peptide substrate and prolyl isomerization can be visualized in proteins as well. However, this requires assigning amide peaks, which can be difficult for large proteins. Another major drawback of NMR is the requirement of high protein concentrations.

1.8.5 Targeting catalytic activity.

Identifying post-translational modifications on proteins is essential for understanding their mechanism of action in biological processes. Following covalent modifications, such as methylation, phosphorylation and acetylation, comes with relative ease. The addition of a 'chemical signature' to a protein can be detected through mass spectrometry, antibodies and radioactivity. The same however, cannot be utilized when studying prolyl isomerization, which is a dynamic and non-covalent modification. As such, mass spectrometry and radioactivity cannot be used. Additionally, while there is now an example of proline *cis/trans* specific antibodies for phosphorylated Pin1 substrate, p-tau [179], developing similar antibodies for unphosphorylated FKBP substrates has not yet been successful in our lab. Of course, this approach requires prior knowledge of the prolyl substrate.

The study of prolyl isomerization is therefore contingent on the identification of gain or loss of function phenotypes that are dependent on these enzymes' activity. This has relied on two methods: 1. Genetic inhibition through the use of site directed mutagenesis, and 2. Chemical inhibition by way of small molecule drugs. Despite the wide use of these techniques, each is not without flaws.

Chemical inhibition of the FKBP family can be achieved with FK506 and rapamycin. While these molecules are widely used, three major shortfalls exist that cannot be overlooked when implementing inhibition in cellular assays. First, rapamycin and FK506 occupy the hydrophobic pocket of FKBPs and have the potential to abrogate interactions that may require the catalytic pocket or the surfaces surrounding the cavity [172]. A second shortfall is gain of the functions when treating cells with the inhibitors. As discussed above, the impact of FK506 and CsA inhibiting calcineurin has been well documented [37]. Additionally, rapamycin forms a ternary complex with FKBP12 and mTOR, inhibiting mTOR's kinase activity and downstream signalling [62]. Finally, both FK506 and rapamycin are not able to distinguish between individual FKBPs in a complex cellular environment. For example, FKBP12 and FKBP25 have comparable affinities for rapamycin (0.2 nM for FKBP12 vs. 0.9 nM for FKBP25 [80,180]). While they are specific for FKBPs, they have the potential to target more than one in cells; therefore, assigning phenotypes to an individual enzyme proves difficult with the use of inhibitors

alone. As FK506 and rapamycin are both still used as immunosuppressants today, the above shortfalls also translate to a clinical setting. These molecules achieve immune suppression through FKBP12 binding calcineurin and mTOR, yet knowledge of how inhibition affects the other seventeen FKBPs in humans is not known. Given FKBP12 and FKBP25 have similar affinities for rapamycin, treatment will target both enzymes and the consequence of inhibiting FKBP25 in this context is not known.

To overcome the limitations of using inhibitors, mutations that abolish catalytic activity provides alternative means to analyze a single enzyme. However, mutagenesis is not without flaws. A significant shortfall of mutagenesis is the potential of unforeseen structural consequences, which can impact both catalytic and non-catalytic functions. This will be discussed in more detail in Chapter 2.

1.9 Research objectives.

At the time this thesis work began, the functions of FKBP25 could be summarized as follows.

Yang et al. had shown that FKBP25 interacts with histone modifying enzymes and regulates the DNA binding of YY1 [82]. The Burakoff lab had shown FKBP25 co-purifies with nucleolin [78], a protein functioning as a histone chaperone and in ribosome biology [79,132,141,149]. Our lab also knew that FKBP25 localized to the nucleus and interacted with chromatin. These results of course suggested chromatin proximal functions similar to that of yeast Fpr4; raising the possibility of FKBP25 mediating gene regulation through isomerization of histone prolines. Additionally, the overlapping nature of Fpr4 and nucleolin in ribosome biogenesis provide a link to this process.

Therefore, based on the combined evidence in the literature, I hypothesized that FKBP25 was a functional ortholog of Fpr4 with possible contributions to at least two biological processes: regulating a) the chromatin landscape by targeted prolyl isomerization of histones (and likely other chromatin-associated proteins), and b) promoting ribosome biogenesis and the maturation of ribosomal subunits, through an as yet unidentified mechanism.

To test these hypotheses, my primary research objective was to use a proteomics approach to define FKBP25's interactome. My logic was that a view of stable FKBP25 protein interactions would provide insight into the processes in which FKBP25 participates, and potential substrates and functions of the prolyl isomerase domain. This work led to ribosome biogenesis of the 60S subunit and the potential substrate nucleolin, respectively. This will be described in Chapters 3 and 4.

At the onset of this project, I anticipated that upon the completion of my proteomics screens, I would have a need to assay whether FKBP25 catalyzed the isomerization of prolines in interacting proteins. To enable this work, I created and characterized a set of loss-of-function mutants of FKBP25. These experiments generated critical tools and insight for the study of FKBP25 and its interactions, and are described first in this thesis, in Chapter 2.

Chapter 2. Mutagenesis as a tool to distinguish the catalytic and non-catalytic functions of FKBP25.

This chapter was adapted in part from the publication:

Gudavicius, G., Soufari, H., Upadhyay, S.K., Mackereth, C.D. & Nelson C.J. (2013) Resolving the functions of peptidylprolyl isomerases: insights from the mutagenesis of the nuclear FKBP25 enzyme. *Biochemical Society Transactions* 41 (3): 761-768.

Contributions to this work: The above publication was written by GG under the guidance of CN. Experimentation (design and figures) was carried out by GG with the exception of NMR in Figures 11b, 12c,d. NMR was performed by HS, SKU and CDM.

2.1 Introduction.

Prolyl isomerases have both catalytic (ie. prolyl isomerization) and non-catalytic (ie. binding) functions, however distinguishing between these mechanisms is a significant challenge. Discrimination requires tools that can accurately separate the two properties. Currently, the use of small molecule inhibitors and loss of function point mutations provide the main approaches to studying prolyl isomerases, however as described in Chapter 1, each is not without drawbacks.

At the outset of this work, genetic inhibition had yet to be used in assaying FKBP25 function. Ochocka et al. identified the need for FKBP25's isomerase domain to promote MDM2 degradation, however only rapamycin was used to assay the catalytic dependence of FKBP25 *in vivo* [70]. Due to the confounding factors associated with the use of inhibitors, complementing small molecule inhibitors with genetic inhibition would provide a more complete assessment of the importance of the FKBP active site to putative biological functions. Therefore, because I anticipated that my proteomic interaction screens would generate putative substrates, I saw a need to prepare a toolset of catalytically inactive mutants of FKBP25.

The residues constituting the catalytic pocket of FKBPs possess a high degree of conservation, however their impact and role in prolyl isomerization cannot be fully

inferred by simply comparing sequence or substrate interactions. While only a few studies have assessed the impact of these conserved residues on catalytic activity [172,181,182], there is a surprising lack of structural understanding as to how these mutants contribute to activity and domain structure.

Here, I targeted three conserved catalytic residues in FKBP25 for mutation and structural analysis. I found that mutation at each of these sites ablates catalytic activity *in vitro*, however this occurs through completely different mechanisms. One mutation generates a loss of function phenotype as a result of domain unfolding, whereas two other mutations ablated catalytic activity while maintaining FKBP domain structure. The mutants described in this Chapter therefore provide a useful toolset to facilitate the dissection of FKBP25's catalytic and non-catalytic functions.

2.2 Results.

2.2.1 Mutation of FKBP25 F145 ablates catalytic activity by domain unfolding.

I initially focused on FKBP25 F145 to target for mutagenesis for a number of reasons. F145 constitutes a part of the hydrophobic catalytic pocket, its aromatic side chain is directed towards the center of the pocket and it is a conserved residue across FKBPs (Figure 9). Additionally, others have identified the importance of this residue for catalytic activity of other FKBPs [172,181,182] (Table 1). Notably, mutation of the analogous residue in Fpr4 is catalytically inactive *in vitro* and has been utilized in Fpr4 functional studies [8,72,73].

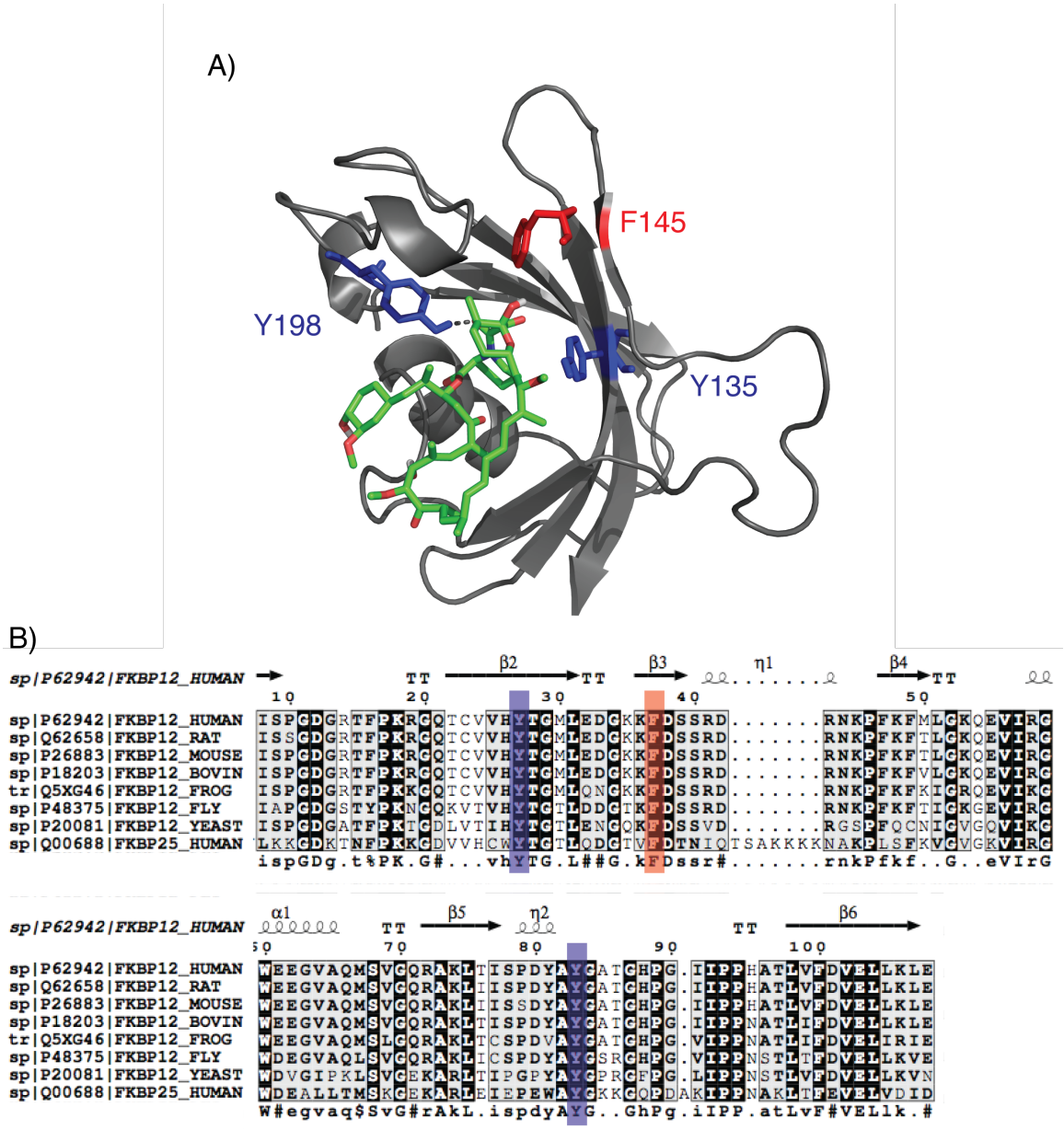

Figure 9. FKBP25 Y135, F145 and Y198 are conserved residues in the catalytic pocket.

A) Structure of the FKBP domain of FKBP25 with rapamycin (green) occupying the catalytic site (PDB: 1PBK). The side chains of Y135, F145 and Y198 are shown and are directed towards the pocket. B) Sequence alignment of FKBP12 from yeast to human and the isomerase domain of human FKBP25. Y135, F145 and Y198 are highlighted and are conserved between FKBP12 and FKBP25. Image of FKBP25 structure was generated with PyMOL. Sequence alignment was generated using T-Coffee.

Table 1. Summary of conserved residue positions in the FKBP domain of FKBP25, FKBP12 and FKBP52.
Catalytic activities determined by *in vitro* chymotrypsin-coupled prolyl isomerase assay of FKBP12 and FKBP52 are represented as: +, catalytically active or -, <10% activity). ND, not determined.

FKBP25 Position	FKBP12	Catalytic Activity	FKBP52	Catalytic Activity
Wildtype	Wildtype	+ [a]	Wildtype	+ [c]
F145	F36L	+ [a]	F67Y	- [c]
FD145	FD36DV	ND	FD67DV	- [c]
D146	D37V	- [a]	D68V	ND
W169	W59A	- [a]	W90L	- [c]
F199	F99Y	- [b]	F130Y	- [c]
Y135/Y198	Y26F/Y82F	- [a]	Y57F/Y113F	ND

a. Decenzo et al. (1996)
b. Tradler et al. (1997)
c. Riggs et al. (2007)

To assess the importance of F145 in the catalytic activity of FKBP25, I first performed chymotrypsin-coupled prolyl isomerization assays against histone H3 proline peptide substrates (Figure 10a). Wildtype FKBP25 was active against both the H3-P16 and H3-P30 peptides, but not H3-P38, whereas mutation of F145 to alanine (F145A) ablated catalytic activity against the same substrates. Therefore, F145 is a critical residue for the isomerase activity of FKBP25.

When purifying wildtype and F145A FKBP25 by size exclusion chromatography, strikingly different elution patterns are observed; FKBP25 F145A eluted at a molecular weight approximately double that of the wildtype protein (Figure 10b). Pre-treatment of the F145A protein with a reducing agent (TCEP) prior to separation shifted the elution profile towards a monomeric species, suggesting a disulfide bond as the source of dimer formation (Figure 10c). FKBP25 contains a single cysteine (C133) that is buried in the hydrophobic core of the globular catalytic domain. Thus, mutation of F145 must expose C133 as a consequence of local or large structural changes.

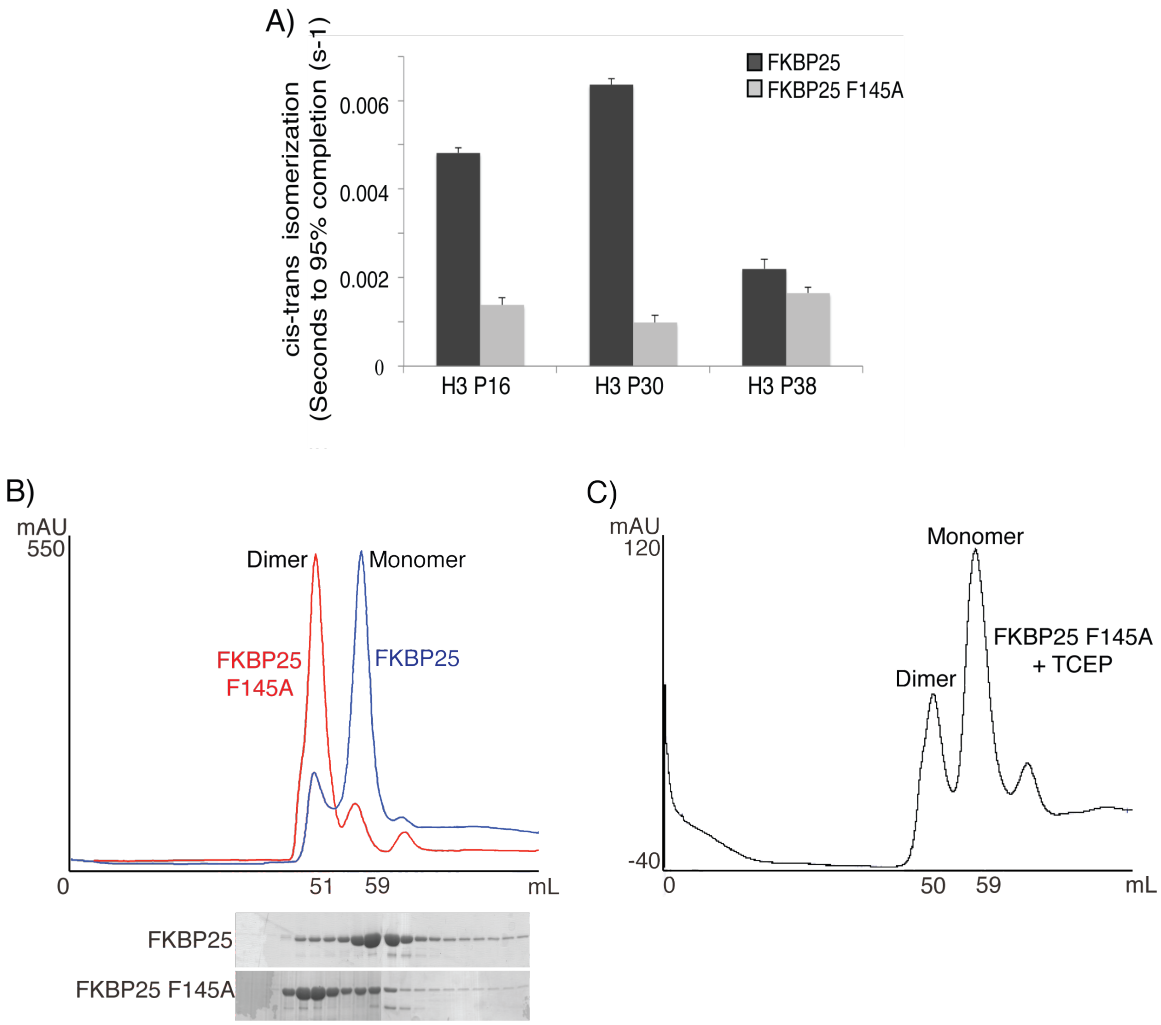

Figure 10. FKBP25 F145A is catalytically inactive and elutes as a dimer by size exclusion chromatography.
A) Synthetic peptides H3-P16 (GGKAPF-pNA); H3-P30 (RKSAPF-pNA); H3-P38 (GVKKPF-pNA), were incubated with wildtype or F145A FKBP25 and isomerase activity measured by absorbance at 390 nm. Rate was determined by time to reach 95% completion. Assays were performed with at least two separate protein preparations in triplicate and averaged. B) Elution profiles of wildtype (blue) and F145A (red) FKBP25 separated by size exclusion chromatography. Below are the corresponding protein fractions separated by SDS-PAGE and coomassie stained. C) Elution profile of FKBP25 F145A pre-treated with TCEP prior to separation by size exclusion chromatography.

Consistent with a structural change of the PPI domain, limited trypsin digestion of purified FKBP25 revealed the F145A mutant is more susceptible to proteolysis than the wildtype protein (Figure 11a). This is further supported with HSQC-NMR (Heteronuclear Single Quantum Coherence Nuclear Magnetic Resonance spectroscopy) of wildtype and

F145A FKBP25. Mutation of F145 conferred unfolding of the catalytic domain, as observed by the amide shifts converging on 8.0-8.4 ppm, indicating an unstructured peptide (Figure 11b). Cross-peaks for the BTHB and linker (aa 1-107) of FKBP25 are unaffected upon mutation of F145 confirming the destabilization only occurs in the FKBP domain (C. Mackereth, personal communication, data not shown). Together, these data reveal the loss of catalytic activity upon mutation of F145 is due to domain unfolding.

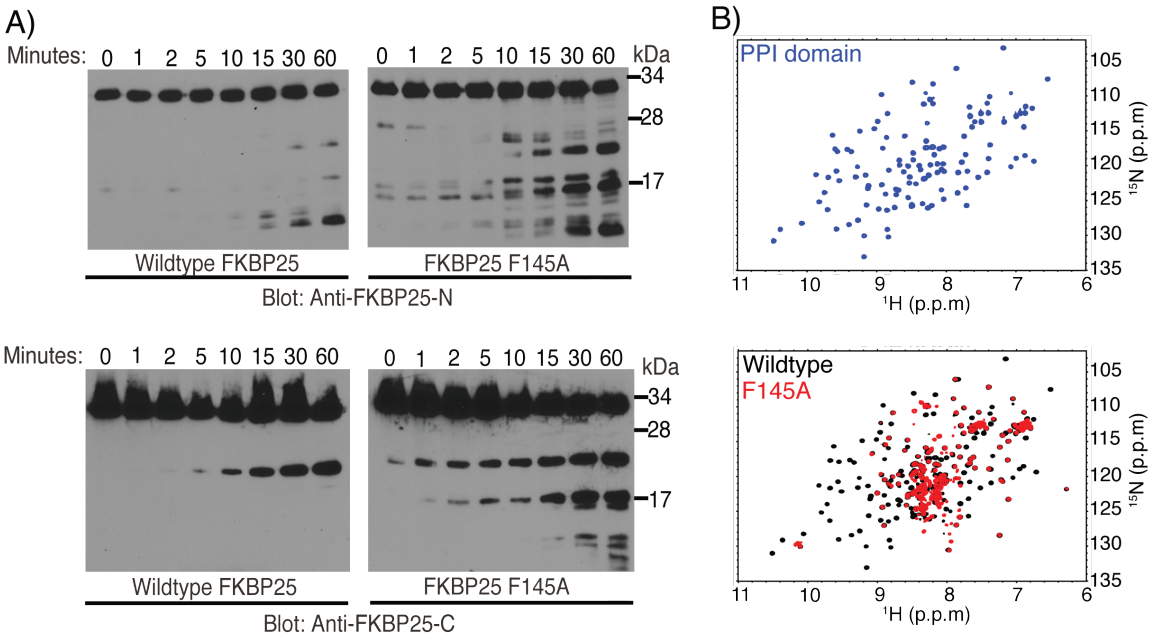

Figure 11. Mutation of FKBP25 F145A induces domain unfolding.
A) Trypsin digestion of wildtype and F145A FKBP25 was performed at 37°C and aliquots were taken at the indicated time points up to 1 hour. Samples were subjected to western blotting with antibodies reactive to the N- and C-termini of FKBP25. B) $^{1}H/^{15}N$ HSQC-NMR spectra of wildtype FKBP25 PPI domain (top) and overlay of wildtype PPI domain (black) and F145A PPI domain (red) (bottom). Cross-peaks correspond to amide nitrogens in the peptide backbone and side chain residues of glutamine and asparagine.

2.2.2 FKBP25 Y135F and Y198F maintain domain structure and are catalytically inactive.

The observation that mutation at F145 induced domain instability invokes the question: can catalytic activity be disrupted without affecting domain structure? This is an important consideration given that there are examples of non-catalytic functions

mediated by PPI domains. Interpreting a loss of function with the F145A mutant can only be interpreted as a requirement of the PPI domain, and cannot distinguish between catalytic-dependence and independence due to loss of domain structure. Therefore, a catalytically inactive mutant that maintains the proper FKBP fold could address the shortfalls of the F145A protein.

To answer this, I targeted two additional sites (Y135 and Y198) in FKBP25's PPI domain for mutagenesis. These tyrosines are also highly conserved residues comprising the FKBP catalytic pocket (Figure 9b), and their mutation in FKBP12 rendered it catalytically inactive *in vitro* (Table 1). This implied these positions in FKBP25 are likely important for catalytic function. Indeed, the side chains of both tyrosines are directed towards the center of the active site and make contacts with rapamycin in the structure (Figure 9a). Specifically, Y198 forms a hydrogen bond with the carbonyl oxygen of the substrate peptide bond to be isomerized, whereas Y135 is directed towards the pocket and is poised to potentially interact with amino acids adjacent to the substrate proline.

By chymotrypsin-coupled prolyl isomerase assay, FKBP25 Y135F and Y198F are catalytically inactive *in vitro* against the H3-P16 peptide (Figure 12a). However, unlike FKBP25 F145A, the Y135F and Y198F mutants do not disrupt FKBP domain fold. Since I found that cysteine-dimer formation is a good readout for domain unfolding of the F145A protein, I used a simple non-reducing SDS-PAGE to assay domain stability Y135 and Y198 mutants. In this assay, nearly all wildtype FKBP25 migrated as a monomeric species, whereas the F145A mutant is a mixture of monomer and dimer (Figure 12b). By contrast, Y135F and Y198F proteins run predominantly as monomers, similar to wildtype FKBP25. HSQC-NMR of these tyrosine mutants confirmed they remain folded and do not result in the same domain instability observed with the F145A protein (Figure 12c-d). These data demonstrate that mutation of Y135 and Y198 ablate catalytic activity without disrupting the major fold of the FKBP domain.

The identification of key tyrosine residues in FKBP25 integral for catalytic activity provides insight into a possible regulatory mechanism by phosphorylation. Olsen et al. identified pY198 in a screen to define the phospho-proteome as a function of the cell cycle [183]. I have also confirmed pY198 by treating HEK293 cells with phosphatase inhibitors and analyzing FKBP25 phosphorylation with mass spectrometry (Figure 13a).

To identify the impact of a negative charge on the environment surrounding Y198, I created a phospho-mimetic mutation to a glutamate (Y198E). By non-reducing SDS-PAGE, FKBP25 Y198E formed a cysteine-dimer similar to the F145A protein (Figure 13b), indicating that a single negative charge at this location destabilized the FKBP domain. Whether phosphorylation at Y198 has functional significance *in vivo* still has to be determined. However my data predict that phosphorylation of either tyrosine, which would introduce two negative charges, would very likely unfold and inactivate the FKBP domain removing both catalytic and non-catalytic functions.

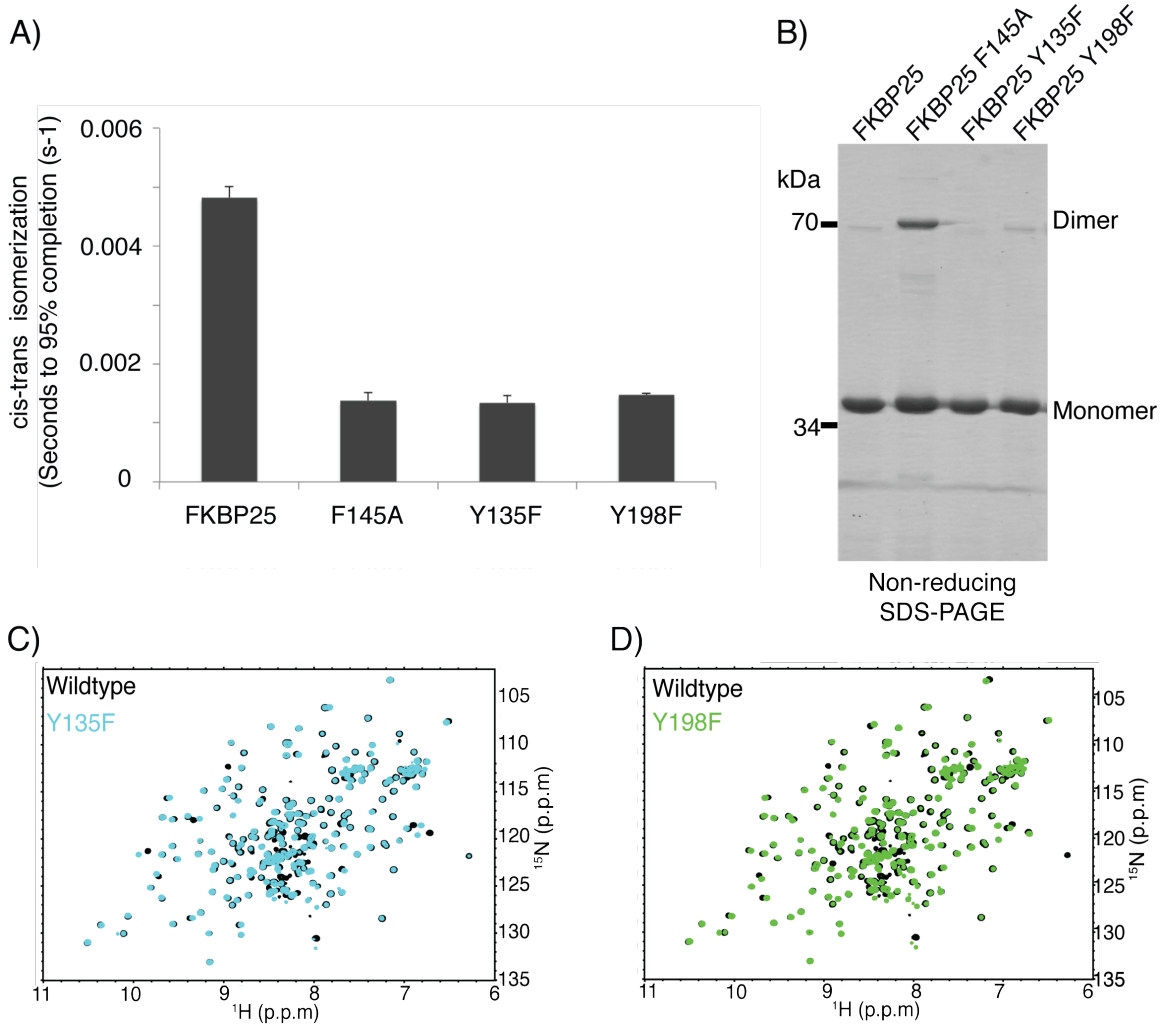

Figure 12. FKBP25 Y135F and Y198F ablate catalytic activity and maintain domain fold.

A) Synthetic H3-P16 peptide (GGKAPF-pNA) was incubated with wildtype, F145A, Y135F or Y198F FKBP25 and isomerase activity measured by absorbance at 390 nm. Rate was determined by time to reach 95% completion. Assays were performed with at least two separate protein preparations in triplicate and averaged. B) FKBP25 protein (wildtype, F145A, Y135F and Y198F) separated by non-reducing SDS-PAGE and coomassie stained. C) $^{1}H/^{15}N$ HSQC-NMR spectra overlay of wildtype FKBP25 PPI domain (black) and Y135F PPI domain (blue). D) $^{1}H/^{15}N$ HSQC-NMR spectra overlay of wildtype FKBP25 PPI domain (black) and Y198F PPI domain (green).

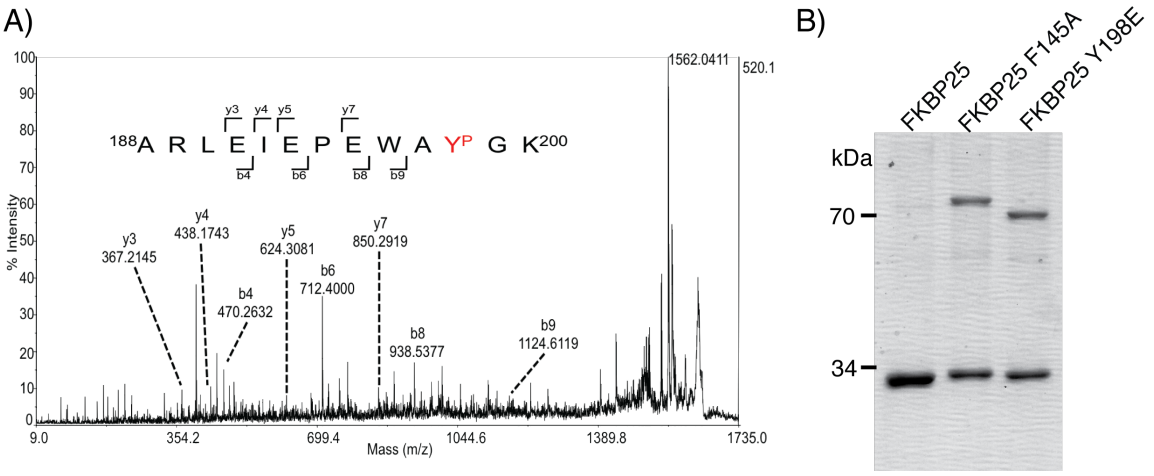

Figure 13. FKBP25 is phosphorylated at Y198.
A) MS/MS spectrum of 1561.90 ion corresponding to amino acids 188-200 of FKBP25 digested with trypsin. Inset represents the peptide sequence and b and y ions are shown. B) Non-reducing SDS-PAGE of FKBP25 mutant proteins separated by SDS-PAGE and coomassie stained.

2.2.3 FKBP25 catalytic activity is not required for protein-protein interactions *in vivo*.

As described in the Introduction, accessory domains do not solely mediate the protein interactions of prolyl isomerases. FKBP12, for example, interacts with the ryanodine receptor [65]. Additionally in the case of Cyp33, isomerase activity is required to establish a binding surface on MLL1 [9]. Thus, I next sought to determine whether FKBP25's protein interactions require catalytic activity or the FKBP fold.

Wildtype and mutant FKBP25 were immunoprecipitated from HEK293 cells and eluted material was separated by SDS-PAGE and western blotted or silver stained. Comparing bands between wildtype and mutant samples, there does not appear to be any significant change in protein interactions upon loss of catalytic activity (Figure 14a, b).

This is not necessarily a surprise, as the BTHB and linker of FKBP25 has been shown to interact with YY1, HDAC1 and HDAC2 [82], as well as nucleolin (Figure 14b) and likely represents the major protein interaction surface for FKBP25. These results do not rule out the possibility of FKBP25's PPI domain and/or activity being required to mediate protein interactions, however it suggests that like Pin1, features of the accessory domain mediate most protein interactions.

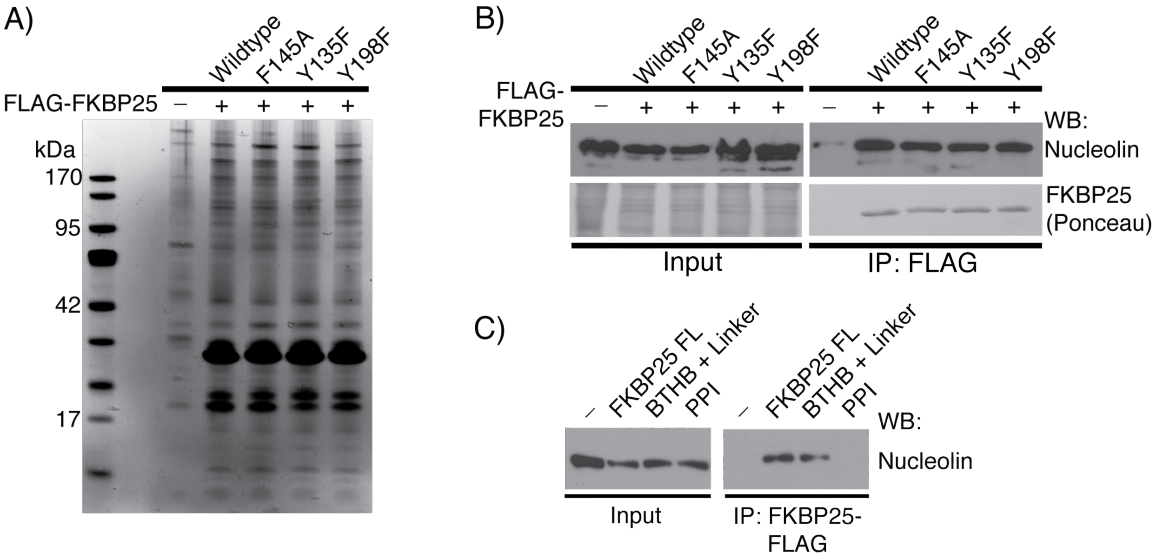

Figure 14. FKBP25 catalytic activity is not required for protein-interactions.
A) Immunoprecipitations of FKBP25 wildtype and mutants separated by SDS-PAGE and silver stained. B) Immunoprecipitation and western blot of FKBP25 wildtype and mutants. C) Immunoprecipitation and western blot of FKBP25 domains.

2.3 Discussion.

One of the greatest challenges in studying prolyl isomerase enzymes is being able to distinguish between catalytic (prolyl isomerization) and non-catalytic (protein/nucleic acid binding, etc.) functions. Mutagenesis provides a tool to dissect these functions of PPIs, however as illustrated in this Chapter, structural insight is essential when performing mutagenesis, as unforeseen structural consequences can be overlooked.

Mutation of F145 in FKBP25 ablated prolyl isomerase activity *in vitro* as a consequence of domain unfolding. Despite the lack of structural information for other FKBP mutants, it appears this observation is not specific to FKBP25. For example, Fpr4

F323A confers some degree of domain unfolding (C. Mackereth, personal communication). FKBP52 may also exhibit domain unfolding with a FD67/68DV mutation, as it inhibits steroid hormone potentiation, while other FKBP52 catalytic-null mutants do not affect signalling [171,172], though this has yet to be confirmed structurally. Moreover, mutation of FKBP12 W59 to valine results in dimer formation as well [184], however it was not reported whether the dimer is a result structural changes and exposure of cysteine. This suggests that mutation of the catalytic phenylalanine may not be the only site in FKBPs that is important for maintaining domain integrity. The impact of catalytic mutagenesis on the unfolding of FKBPs (and potentially cyclophilins, parvulins as well) may therefore be under represented. The majority of FKBP mutant structures use X-ray crystallography, where crystal packing may stabilize partially unfolded proteins giving the appearance of a properly folded structure. Ideally, 'in solution' techniques such as NMR or hydrogen-deuterium exchange mass spectrometry (HDX) should be used to determine whether mutation has significant impact on protein fold and stability.

Another point to consider when assessing the F145A protein is the actual extent of unfolding in the PPI domain. By HSQC-NMR, the majority of cross-peaks are shifted towards the region of the spectra indicating an unstructured peptide. HDX experiments with wildtype and F145A FKBP25 (Appendix Figure 32) confer similar results compared to our NMR data (Figure 11, 12). The F145A protein is significantly more accessible to deuterium incorporation (56 residues protected) than wildtype FKBP25 (73 residues protected) (Appendix Figure 32). Surprisingly, the addition of rapamycin is able to bind and restore the fold of the F145A protein. Therefore, FKBP25 F145A may not be completely unfolded, but represent an intermediate structure that can still be coordinated by substrate. In light of this, protein interactions in the proximity of FKBP25's catalytic pocket might contribute to folding the F145A mutant. Perhaps interacting proteins coordinating F145A structure can explain the lack of differences observed in co-immunoprecipitated proteins between wildtype and F145A (Figure 14).

While caution must be taken when utilizing mutants conferring domain instability, these mutants can provide valuable functional insight. When used in

combination with catalytically inactive mutants that do not impact domain structure (ie. Y135F, Y198F), catalytic and non-catalytic functions can potentially be distinguishable.

Whether non-catalytic functions of FKBP25 can be distinguished with these mutants still needs to be explored. Currently, the only known function of the catalytic domain of FKBP25 is that it promotes the self-ubiquitination and degradation of MDM2. As the experiments carried out by Ochocka et al. utilized transfected plasmids to over-express FKBP25 [70], the mutant proteins would be amendable to these cellular assays. If isomerase activity is required, auto-ubiquitination of MDM2 would not occur with either the F145 or Y135/198 mutants. Alternatively, if MDM2 ubiquitination is observed with only the Y135/198 mutants and not F145A, features of the FKBP domain would be the driving factor for the effect. The use of catalytically inactive FKBP25 instead of rapamycin treatment eliminates confounding factors, such as mTOR, which may converge on MDM2 and p53 [185,186]. As new functions for FKBP25 are discovered, the tools I have developed will undoubtedly provide insight into the role of FKBP25 in the cell.

While I have focused on the effects of mutagenesis on FKBP25 in this study, the same domain destabilization appears to occur with other FKBPs [171,172,184,187] and may therefore be used as a general tool to study this family of prolyl isomerases. Isomerase independent functions for FKBP12 and FKBP52 have been reported, thus transfer of these tools to other FKBPs may shed light on non-catalytic functions of these enzymes as well. Despite the use of genetic inhibition in cyclophilins and parvulins, insight into the structural effects of their mutation has yet to be reported. Whether a similar system can be transferred to cyclophilins or parvulins represents a future avenue to explore.

2.4 Methods.

Cell culture.

HEK293 Flp-In T-Rex cells (Life Technologies) were maintained in DMEM containing 10% FBS and Penicillin/Streptomycin at 37^{o}C in 5% CO_2. For tetracycline inducible cells, FKBP25 was cloned into pcDNA5/FRT/TO (Life Technologies) containing a

tetracycline-regulated, hybrid CMV/TetO2 promoter and a triple FLAG epitope tag. Stable cell lines were constructed as per manufacturers recommendations.

Mutagenesis.

Mutagenesis was performed on the parent pET FKBP25 vector using oligos described in Appendix. For site directed mutagenesis, PCR reactions were assembled in 25 mL volumes containing 2.5 mL 10X buffer, 1 mL forward and reverse primer (0.8 mM final), 1 mL DMSO, 1 mL 10 mM each dNTPs, 50-100 ng parent vector and 1 mL Pfu DNA polymerase (Thermo Scientific). The mutagenesis PCR program consisted of an initial denaturation step at 94^{o}C for 2 minutes, followed by 22 cycles of: 94^{o}C for 1 minute; 55^{o}C for 1 minute; and 68^{o}C for 16 minutes, with a final extension of 68^{o}C for 10 minutes. Mutagenesis was confirmed by sequencing.

Protein expression and purification.

Escherichia coli BL21 RIL strains containing pET 6-His encoding: FKBP25, FKBP25 F145A, FKBP25 Y135F, FKBP25 Y198F, Y198E were diluted 1:50 from overnight cultures into LB broth. Cells were grown to an OD_{600} of approximately 0.6. Protein expression was induced with 1 mM IPTG at 37^{o}C for 3 hours. Cells were harvested by centrifugation and resuspended in nickel binding/wash buffer (50 mM NaH_2PO_4, 300 mM NaCl, 20 mM imidazole, pH 8), incubated on ice for 10 minutes and lysed by sonication (10 pulses of 30 seconds). Extracts were cleared by centrifugation at 10,000 rpm for 10 minutes. Cleared lysates were added to pre-washed Nickel-NTA agarose beads (Qiagen) and incubated at 4^{o}C with nutating for 1.5 hours. Following binding, beads were washed three times for 10 minutes in 5 mL wash buffer. Proteins were eluted twice with elution buffer (50 mM NaH_2PO_4, 300 mM NaCl, 250 mM imidazole, pH 8) for 10 minutes in 2 mL volumes. Eluted protein was pooled and dialyzed against PBS with 10% glycerol. For size exclusion chromatography, 6-his purified FKBP25 was separated with a HiLoad 16/60 Superdex 75 prep grade column on a GE AKTAprime plus FPLC. Fractions were collected in 1 mL volumes and separated by SDS-PAGE to compare A_{254} absorbance traces with protein elution. To reduce samples, TCEP was added to column buffer and purified protein to a final concentration of 0.5 mM.

Proline isomerase assay.

Proline isomerase assay was performed as described previously [22,24]. Synthetic histone proline peptides (H3-P16: GGKAPF-pNA; H3-P30: RKSAPF-pNA; H3-P38: GVKKPF-pNA) were prepared in 0.45 mM LiCl/TFA at a concentration of 7.8 mM. Purified 6His-FKBP25 proteins were prepared to a concentration of 4 mM. Assays were assembled with 30 mL FKBP25 (3 mg), 10 mL synthetic peptide, 50 mL chymotrypsin (30 mM final) per 1 mL reaction. The progress of the assay was monitored in real time at 390 nm with a Varian Cary 50 UV-Vis Spectrophotometer. Assays were performed in triplicate and averaged for each FKBP25 protein. Isomerase activity was calculated by the time to reach 95% of the maximal absorbance.

SDS-PAGE.
SDS-PAGE was performed as per standard procedures. For non-reducing sample preparation, purified FKBP25 was diluted with 4X SDS loading buffer without reducing agent (200 mM Tris pH 6.8, 8% SDS, 0.4% bromophenol blue, 40% glycerol). Gels were electrophoresed for 1 hour at 200 V and stained with Coomassie Brilliant Blue R250.

Immunoprecipitation.
HEK293 cells (~$3x10^7$ cells) were lysed in 0.75 mL immunoprecipitation (IP) buffer (50 mM Tris pH8, 150 mM NaCl, 0.5% IGEPAL, 0.5% Triton X100, 2 mM EDTA, 1 μg/mL leupeptin, 1 μg/mL aprotinin and 1 μg/mL pepstatin), vortexed for 3 seconds and incubated on ice for 10 minutes. Insoluble material was pelleted at 10,000 rpm for 10 minutes. Soluble extracts were added to pre-washed EZ-view Red ANTI-FLAG M2 Affinity gel beads (Sigma). After binding, beads were washed three times in IP buffer (0.75 mL IP buffer was added to beads and nutated for 5 minutes, then centrifuged at 1000 rpm for 1 minute). FLAG-complexes were eluted with 1.25 mg/mL 3x FLAG peptide (Sigma) by nutating for 15 minutes at 4^oC.

Western blot.
Eluted proteins were resolved by SDS-PAGE and transferred to a nitrocellulose membrane. Membranes were blocked in 10% skim milk for 30 minutes and probed in primary antibody overnight at 4^oC. Antibodies and dilutions used were: anti-FKBP25-N (Raised against amino acids 3-18) and anti-FKBP25-C (Raised against amino acids 201-224), anti-nucleolin (Abcam ab22758). Blots were washed three times for 10 minutes in

TBST (TBS + 0.1% Tween-20) and incubated in secondary antibody for 1-2 hours at room temperature. Horseradish peroxidase conjugated anti-rabbit (GE) secondary antibody was used at 1:5,000. Proteins were detected by chemiluminescence (Millipore) and exposed to film.

Limited proteolysis.
Purified 6-his FKBP25 and FKBP25 F145A were first diluted to 0.1 mg/mL and pre-treated with TCEP (10 mM final) for 10 minutes at room temperature to disrupt cysteine dimers. Trypsin (10 ng) was added to each protein (reaction volume 50 mL) and allowed to digest at 37^{o}C for the various times. At each time point, 5 mL of protein was removed from the digestion reaction and stopped by addition of SDS loading buffer and boiling.

Mass spectrometry.
HEK293 FLAG-FKBP25 cells were grown to ~70% confluent. $NaVO_4$ was added to media at a final concentration of 5mM, incubated 24 hours and cells were harvest by scraping. Nuclear extract was prepared by hypotonic lysis of cells in buffer A (10mM Tris pH 8, 1.5mM $MgCl_2$, 10mM NaCl, 0.5mM DTT, 5mM $NaVO_4$, protease inhibitors), incubated 10 minutes and vortexed 10 seconds prior to pelleting at 15,000rpm for 1 minute. The pellet was resuspended in buffer B (20mM Tris pH 8, 25% glycerol, 420mM NaCl, 1.5mM $MgCl_2$, 0.2 mM EDTA, 0.5mM DTT, 5mM $NaVO_4$, protease inhibitors), incubated on ice 20 minutes and centrifuged at 15,000rpm for 2 minutes. FLAG-FKBP25 was purified as above and resolved on NuPAGE Novex 4-12% Bis-Tris Gradient gels at 150 V for approximately 1.5 hours and stained in Coomassie G250. After destaining (25% methanol, 14.2% glacial acetic acid), bands were excised from the gel using a sterile razor, cut in half and placed in microfuge tubes. Gel slices were washed with 100 mL of sterile dH_2O for 5 minutes at 37^{o}C, shaking at 400 rpm. dH_2O was discarded and the wash was repeated. 50 mL of 50 mM ammonium bicarbonate and 50 mL of 100% acetonitrile were added and samples were incubated at 37 ^{o}C at 400 rpm for 5 minutes in a thermomixer. The solution was discarded and washing repeated (3-8 times) until gel slices were colorless. Slices were subjected to two 5 minute washes in 100 mL acetonitrile, frozen at -80^{o}C for 20 minutes, and lyophilized. Samples were incubated in 100 mL acetonitrile for 5 minutes, the solution discarded and wash repeated. Tubes

containing gel slices were cooled on ice for 30 minutes and 20 ml of acetonitrile containing 0.5 mg of sequencing grade trypsin (Promega) added to the gel slices and samples kept on ice for 30 minutes. The trypsin solution was discarded and 40 mL ammonium bicarbonate was added and samples incubated overnight in a thermomixer at 37^{o}C and 400 rpm. The following day 50 mL of acetonitrile was added to each digest and samples were incubated for 10 minutes. The solution containing digested peptides was removed to a new microfuge tube. Gel slices were washed in 30 mL for 10 minutes followed by addition of 50 mL acetonitrile and further incubation for 10 minutes. This solution was decanted and pooled with the first extraction. Samples were lyophilized until dry and reconstituted with 10 mL 0.1% triflouro-acetic acid. Samples were spotted on Applied Biosystems stainless steel MALDI plate in duplicate, overlaid with 1 mL a-cyano matrix and analyzed using Applied Biosystems 4800 MALDI-TOF/TOF mass spectrometers at the UVic Genome BC Proteomics Centre.

Chapter 3. FKBP25 interacts with RNA-engaged nucleolin and the pre-60S ribosomal subunit.

This chapter was adapted in part from the publication:

Gudavicius, G., Dilworth, D., Serpa, J.J., Sessler, N., Petrotchenko, E.V., Borchers, C.H. & Nelson C.J. (2014) The prolyl isomerase, FKBP25, interacts with RNA-engaged nucleolin and the pre-60S ribosomal subunit. *RNA* 20 (7): 1014-22.

Contributions to this work: The above publication was written by GG under the guidance of CN. Experimentation (design and figures) was carried out by GG with the following exceptions. JJS, NS, EP, CHB provided mass spectrometry services; DD analyzed data for in-solution experiments and prepared the data represented in Figure 15b and Table 2. DD performed experiments and prepared data in Figure 16a, 17 and 22.

3.1 Introduction.

Identifying the substrates and functions of PPIs can prove a formidable task, and as described in Chapter 1, FKBP25 is not exempt. As the prolyl isomerase activity of PPIs cannot be monitored directly in a cellular environment, understanding where these enzymes localize and defining interacting proteins can provide insight into potential functions. For example, Cyp33 was first identified as an MLL1 interacting protein by a yeast-two hybrid screen, which led to the observation that Cyp33 altered the expression of MLL1 target genes [188]. Additionally, Pin1 was first reported to interact with the mitotic kinase NIMA, which subsequently led an implication in cell cycle regulation [48]. Therefore, defining the interactomes of PPIs will highlight biological process, and potentially reveal likely substrates.

Indeed, this methodology was used for the human parvulin, Par14, which revealed its interacting proteins to function in ribosome biogenesis [189]. While Par14 has since been implicated in pre-rRNA processing [190], its substrates and mechanism affecting rRNA maturation has yet to be explored. Thus, this approach can provide insight into the functions of PPIs, however additional techniques must be used to identify the direct targets.

While FKBP25 localizes to the nucleus and is chromatin-associated [81,82], only a handful of interaction partners have been described. These were identified by yeast-two hybrid, GST-pulldown or immunoprecipitation [70,78,82], and mass spectrometry analyses of FKBP25 interacting proteins had yet to be performed. Therefore, defining the interactome of FKBP25 can provide insight into its localization and potential substrates for regulation by prolyl isomerization.

Here, I perform the first unbiased proteomic screen to define FKBP25's interactome. The majority of proteins that co-purify with FKBP25 are annotated as nuclear and/or nucleolar factors, supporting previous data predicting FKBP25 as a nuclear enzyme. I find that the majority of these interacting proteins are involved in either ribosome biogenesis or chromatin biology. I focus on the interaction between FKBP25 and the top-hit in my screen, nucleolin, and demonstrate a direct interaction between these proteins only occurs in the presence of rRNA. Moreover, this interaction occurs specifically on the immature 60S ribosomal subunit. These results support a model where FKBP25 acts to chaperone the protein content of the large ribosomal subunit, as it is assembled and transits from the nucleolus to the cytoplasm.

3.2 Results.

3.2.1 FKBP25 protein interactions occur in the nucleus.

To gain insight into the cellular functions of FKBP25, I first performed a proteomic characterization of its interacting proteins. Using HEK293 cells stably expressing 3x-FLAG-FKBP25, I enriched FKBP25 and its associated proteins by anti-FLAG immunoprecipitation and separated the material by SDS-PAGE. I found a significant number of interacting proteins that are unique to FKBP25 and absent in the no FLAG control sample (Figure 15a). I then performed two unbiased mass spectrometry methods to characterize proteins that co-purify with 3x-FLAG-FKBP25: an in-gel trypsin digestion of 18 prominent bands followed by MALDI-TOF-TOF, as well as an in-solution trypsin digestion followed by Orbitrap LC/MS analysis. Together, these methods identified 18 and 104 proteins, respectively, which represents 111 unique FKBP25 interacting factors (Table 2, 3). Nucleolin was the only protein identified in the screens that has previously been shown to associate with FKBP25, while the other 110 proteins represent novel interactions. We performed a functional annotation and enrichment

analysis using Database for Annotation, Visualization and Integrated Discovery v6.7 (DAVID) [191,192], which is summarized in Figure 15b. From this analysis, ribosome-related ontologies represented the top hits, encompassing 61 proteins interacting with FKBP25.

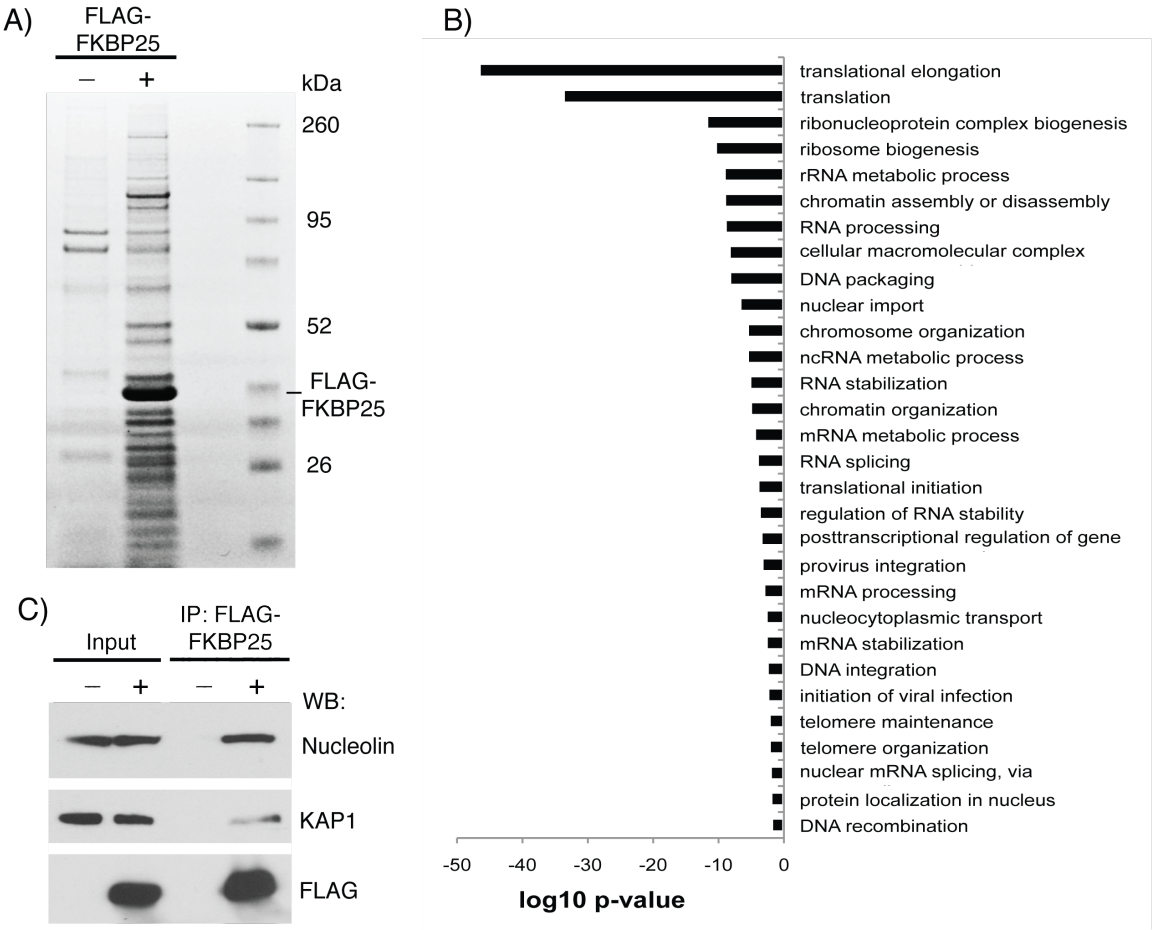

Figure 15. FKBP25 interacts with ribosomal and chromatin-associated factors.
A) Coomassie stained SDS-PAGE of FKBP25-FLAG immunoprecipitations performed from HEK293 cells. B) Functional annotation and enrichment analysis of FKBP25 interacting proteins identified from two mass spectrometry experiments. C) Western blots of FKBP25-FLAG immunoprecipitations from HEK293 cells probing for most abundant (nucleolin) and least abundant (KAP1) identified from in-gel MS.

Table 2. MALDI-TOF-TOF identification of FKBP25 interacting proteins from whole cell extract.

Protein Name	Uniprot Accession	Theorectical MW (kDa)	Gel Silce MW (kDa)	Peptides	Cellular Function
Myb-binding protein 1A	Q9BQG0	149	146	5	transcription, ribosome biogenesis
ATP-dependent RNA helicase A	Q08211	141	146	3	ribosome biogenesis, transcription
Poly [ADP-ribose] polymerase 1	P09874	113	116	6	DNA repair, chromatin dynamics, ribosome biogenesis
KRAB-associated protein 1	Q13263	88	98	2	transcription
Nucleolin	P19338	76	98	14	ribosome biogenesis, transcription, chromatin dynamics
Nucleolar RNA helicase Gu	Q9NR30	89	98	4	ribosome biogenesis, transcription
Nucleolin	P19338	76	76	11	ribosome biogenesis, transcription, chromatin dynamics
Replication protein A 70 kDa DNA-binding subu	P27694	68	68	8	DNA repair, DNA replication
60S ribosomal protein L4	P36578	48	49	9	ribosome biogenesis
60S ribosomal protein L3	P39023	46	46	7	ribosome biogenesis
60S ribosomal protein L8	P62917	28	30	4	ribosome biogenesis
60S ribosomal protein L13	P26373	24	29	3	ribosome biogenesis
60S ribosomal protein L14	P50914	24	29	2	ribosome biogenesis
60S ribosomal protein L19	P84098	23	29	2	ribosome biogenesis
60S ribosomal protein L23a	P62750	17	23	4	ribosome biogenesis
60S ribosomal protein L26	P61254	17	23	2	ribosome biogenesis
60S ribosomal protein L23	P62829	15	22	4	ribosome biogenesis
Heterogeneous nuclear ribonucleoprotein U	Q00839	90	100	3	transcription, chromatin dynamics
40S ribosomal protein S4, X isoform	P62701	30	31	2	ribosome biogenesis

Table 3. Orbitrap identification of FKBP25 interacting proteins from nuclear extract.

Proteins with enrichment less than 2 were excluded.

Accession	Description	Mass (Da)	Empty Vector Control IP			FLAG-FKBP25 IP			Enrichment Relative to Empty Vector
			Num. of significant matches	Num. of significant sequences	Score	Num. of significant matches	Num. of significant sequences	Score	
Q00688|FKBP3_HUMAN	Peptidyl-prolyl cis-trans isomerase FKBP3 OS=Homo sapiens GN=FKBP3 PE=1 SV=1	25161	4	2	54	231	10	5108	57.8
P11388|TOP2A_HUMAN	DNA topoisomerase 2-alpha OS=Homo sapiens GN=TOP2A PE=1 SV=3	174276	1	1	1	42	18	1563	42.0
Q9BQG0|MBB1A_HUMAN	Myb-binding protein 1A OS=Homo sapiens GN=MYBBP1A PE=1 SV=2	148762	1	1	23	21	12	675	21.0
Q9BQE3|TBA1C_HUMAN	Tubulin alpha-1C chain OS=Homo sapiens GN=TUBA1C PE=1 SV=1	49863	1	1	1	19	9	611	19.0
Q9NR30|DDX21_HUMAN	Nucleolar RNA helicase 2 OS=Homo sapiens GN=DDX21 PE=1 SV=5	87290	2	1	65	29	13	661	14.5
Q9BQ39|DDX50_HUMAN	ATP-dependent RNA helicase DDX50 OS=Homo sapiens GN=DDX50 PE=1 SV=1	82514	1	1	1	13	4	462	13.0
P06899|H2B1J_HUMAN	Histone H2B type 1-J OS=Homo sapiens GN=HIST1H2BJ PE=1 SV=3	13896	1	1	1	12	3	494	12.0
P11387|TOP1_HUMAN	DNA topoisomerase 1 OS=Homo sapiens GN=TOP1 PE=1 SV=2	90669	1	1	1	11	5	214	11.0
P39023|RL3_HUMAN	60S ribosomal protein L3 OS=Homo sapiens GN=RPL3 PE=1 SV=2	46080	3	2	46	30	6	782	10.0
P17066|HSP76_HUMAN	Heat shock 70 kDa protein 6 OS=Homo sapiens GN=HSPA6 PE=1 SV=2	70984	1	1	1	9	4	299	9.0
P46778|RL21_HUMAN	60S ribosomal protein L21 OS=Homo sapiens GN=RPL21 PE=1 SV=2	18553	1	1	1	9	4	197	9.0
P46087|NOP2_HUMAN	Putative ribosomal RNA methyltransferase NOP2 OS=Homo sapiens GN=NOP2 PE=1 SV=2	89247	1	1	1	8	5	213	8.0
P07237|PDIA1_HUMAN	Protein disulfide-isomerase OS=Homo sapiens GN=P4HB PE=1 SV=3	57081	1	1	55	7	3	194	7.0
P61313|RL15_HUMAN	60S ribosomal protein L15 OS=Homo sapiens GN=RPL15 PE=1 SV=2	24131	1	1	1	7	4	235	7.0
P78527|PRKDC_HUMAN	DNA-dependent protein kinase catalytic subunit OS=Homo sapiens GN=PRKDC PE=1 SV=3	468788	1	1	1	7	4	292	7.0
Q02880|TOP2B_HUMAN	DNA topoisomerase 2-beta OS=Homo sapiens GN=TOP2B PE=1 SV=3	183152	1	1	1	7	4	353	7.0
P04908|H2A1B_HUMAN	Histone H2A type 1-B/E OS=Homo sapiens GN=HIST1H2AB PE=1 SV=2	14127	1	1	1	6	3	154	6.0
P0C0S5|H2AZ_HUMAN	Histone H2A.Z OS=Homo sapiens GN=H2AFZ PE=1 SV=2	13545	1	1	1	6	3	167	6.0
P62263|RS14_HUMAN	40S ribosomal protein S14 OS=Homo sapiens GN=RPS14 PE=1 SV=3	16263	1	1	1	6	3	192	6.0
Q49A26|GLYR1_HUMAN	Putative oxidoreductase GLYR1 OS=Homo sapiens GN=GLYR1 PE=1 SV=3	60518	1	1	1	6	3	257	6.0
Q9Y2X3|NOP58_HUMAN	Nucleolar protein 58 OS=Homo sapiens GN=NOP58 PE=1 SV=1	59541	1	1	67	6	2	287	6.0
P19013|K2C4_HUMAN	Keratin, type II cytoskeletal 4 OS=Homo sapiens GN=KRT4 PE=1 SV=4	57250	1	1	1	5	4	108	5.0
Q5SSJ5|HP1B3_HUMAN	Heterochromatin protein 1-binding protein 3 OS=Homo sapiens GN=HP1BP3 PE=1 SV=1	61169	1	1	1	5	4	59	5.0
Q96SB4|SRPK1_HUMAN	SRSF protein kinase 1 OS=Homo sapiens GN=SRPK1 PE=1 SV=2	74278	1	1	1	5	2	70	5.0
Q9NRI5|DISC1_HUMAN	Disrupted in schizophrenia 1 protein OS=Homo sapiens GN=DISC1 PE=1 SV=3	93552	1	1	1	5	1	49	5.0
P32969|RL9_HUMAN	60S ribosomal protein L9 OS=Homo sapiens GN=RPL9 PE=1 SV=1	21850	3	2	95	14	4	623	4.7
P46783|RS10_HUMAN	40S ribosomal protein S10 OS=Homo sapiens GN=RPS10 PE=1 SV=1	18886	1	1	1	4	2	164	4.0
P62266|RS23_HUMAN	40S ribosomal protein S23 OS=Homo sapiens GN=RPS23 PE=1 SV=3	15798	1	1	26	4	2	133	4.0
P62937|PPIA_HUMAN	Peptidyl-prolyl cis-trans isomerase A OS=Homo sapiens GN=PPIA PE=1 SV=2	18001	1	1	1	4	2	88	4.0
Q13868|EXOS2_HUMAN	Exosome complex component RRP4 OS=Homo sapiens GN=EXOSC2 PE=1 SV=2	32768	1	1	1	4	1	154	4.0
Q6NVV1|R13AX_HUMAN	Putative 60S ribosomal protein L13a-like MGC87657 OS=Homo sapiens PE=5 SV=1	12127	1	1	20	4	2	103	4.0
Q8NC51|PAIRB_HUMAN	Plasminogen activator inhibitor 1 RNA-binding protein OS=Homo sapiens GN=SERBP1 PE=	44938	1	1	62	4	3	148	4.0
Q92522|H1X_HUMAN	Histone H1x OS=Homo sapiens GN=H1FX PE=1 SV=1	22474	2	1	97	8	4	242	4.0
Q92922|SMRC1_HUMAN	SWI/SNF complex subunit SMARCC1 OS=Homo sapiens GN=SMARCC1 PE=1 SV=3	122790	1	1	1	4	1	211	4.0
Q9NW13|RBM28_HUMAN	RNA-binding protein 28 OS=Homo sapiens GN=RBM28 PE=1 SV=3	85685	1	1	1	4	1	161	4.0
Q9UKN8|TF3C4_HUMAN	General transcription factor 3C polypeptide 4 OS=Homo sapiens GN=GTF3C4 PE=1 SV=2	91923	1	1	35	4	1	241	4.0
Q9Y3U8|RL36_HUMAN	60S ribosomal protein L36 OS=Homo sapiens GN=RPL36 PE=1 SV=3	12246	1	1	1	4	1	157	4.0
P46782|RS5_HUMAN	40S ribosomal protein S5 OS=Homo sapiens GN=RPS5 PE=1 SV=4	22862	3	2	183	11	3	351	3.7
P46777|RL5_HUMAN	60S ribosomal protein L5 OS=Homo sapiens GN=RPL5 PE=1 SV=3	34341	2	1	113	7	5	137	3.5
P62081|RS7_HUMAN	40S ribosomal protein S7 OS=Homo sapiens GN=RPS7 PE=1 SV=1	22113	3	2	114	10	4	234	3.3
O00303|EIF3F_HUMAN	Eukaryotic translation initiation factor 3 subunit F OS=Homo sapiens GN=EIF3F PE=1 SV=1	37540	1	1	1	3	1	251	3.0
O15131|IMA5_HUMAN	Importin subunit alpha-6 OS=Homo sapiens GN=KPNA5 PE=1 SV=2	60311	1	1	1	3	1	37	3.0
P09874|PARP1_HUMAN	Poly [ADP-ribose] polymerase 1 OS=Homo sapiens GN=PARP1 PE=1 SV=4	113012	1	1	1	3	2	118	3.0
P12956|XRCC6_HUMAN	X-ray repair cross-complementing protein 6 OS=Homo sapiens GN=XRCC6 PE=1 SV=2	69799	1	1	1	3	1	79	3.0
P27635|RL10_HUMAN	60S ribosomal protein L10 OS=Homo sapiens GN=RPL10 PE=1 SV=4	24588	1	1	1	3	3	103	3.0
P58107|EPIPL_HUMAN	Epiplakin OS=Homo sapiens GN=EPPK1 PE=1 SV=2	555279	1	1	1	3	1	59	3.0
P84243|H33_HUMAN	Histone H3.3 OS=Homo sapiens GN=H3F3A PE=1 SV=2	15318	1	1	1	3	2	73	3.0
Q02388|CO7A1_HUMAN	Collagen alpha-1(VII) chain OS=Homo sapiens GN=COL7A1 PE=1 SV=2	295041	1	1	1	3	1	41	3.0
Q5RKV6|EXOS6_HUMAN	Exosome complex component MTR3 OS=Homo sapiens GN=EXOSC6 PE=1 SV=1	28218	1	1	1	3	2	62	3.0
Q86U86|PB1_HUMAN	Protein polybromo-1 OS=Homo sapiens GN=PBRM1 PE=1 SV=1	192825	1	1	1	3	1	53	3.0
Q8TAQ2|SMRC2_HUMAN	SWI/SNF complex subunit SMARCC2 OS=Homo sapiens GN=SMARCC2 PE=1 SV=1	132797	1	1	1	3	1	145	3.0
Q92499|DDX1_HUMAN	ATP-dependent RNA helicase DDX1 OS=Homo sapiens GN=DDX1 PE=1 SV=2	82380	2	1	135	6	2	277	3.0
Q9NZI8|IF2B1_HUMAN	Insulin-like growth factor 2 mRNA-binding protein 1 OS=Homo sapiens GN=IGF2BP1 PE=1	63441	1	1	1	3	2	156	3.0
P18124|RL7_HUMAN	60S ribosomal protein L7 OS=Homo sapiens GN=RPL7 PE=1 SV=1	29207	4	2	120	11	5	235	2.8

Table 3 cont'd.

Accession	Description	Mass (Da)	Empty Vector Control IP			FLAG-FKBP25 IP			Enrichm
			Num. of significant matches	Num. of significant sequences	Score	Num. of significant matches	Num. of significant sequences	Score	Relativ Empt Vect
P78347|GTF2I_HUMAN	General transcription factor II-I OS=Homo sapiens GN=GTF2I PE=1 SV=2	112346	13	6	437	35	16	883	2.7
Q5QNW6|H2B2F_HUMAN	Histone H2B type 2-F OS=Homo sapiens GN=HIST2H2BF PE=1 SV=3	13912	5	2	226	13	4	505	2.6
P05386|RLA1_HUMAN	60S acidic ribosomal protein P1 OS=Homo sapiens GN=RPLP1 PE=1 SV=1	11507	2	1	81	5	2	190	2.5
P26373|RL13_HUMAN	60S ribosomal protein L13 OS=Homo sapiens GN=RPL13 PE=1 SV=4	24247	4	2	79	10	4	231	2.5
P46781|RS9_HUMAN	40S ribosomal protein S9 OS=Homo sapiens GN=RPS9 PE=1 SV=3	22578	6	3	109	15	8	145	2.5
P61247|RS3A_HUMAN	40S ribosomal protein S3a OS=Homo sapiens GN=RPS3A PE=1 SV=2	29926	4	2	166	10	5	266	2.5
P83731|RL24_HUMAN	60S ribosomal protein L24 OS=Homo sapiens GN=RPL24 PE=1 SV=1	17768	2	1	124	5	2	232	2.5
Q96AV8|E2F7_HUMAN	Transcription factor E2F7 OS=Homo sapiens GN=E2F7 PE=1 SV=3	99826	2	1	45	5	3	191	2.5
P19338|NUCL_HUMAN	Nucleolin OS=Homo sapiens GN=NCL PE=1 SV=3	76568	15	8	538	34	14	1382	2.3
Q02878|RL6_HUMAN	60S ribosomal protein L6 OS=Homo sapiens GN=RPL6 PE=1 SV=3	32708	9	5	272	20	9	666	2.2
O00422|SAP18_HUMAN	Histone deacetylase complex subunit SAP18 OS=Homo sapiens GN=SAP18 PE=1 SV=1	17550	2	1	92	4	2	155	2.0
O00567|NOP56_HUMAN	Nucleolar protein 56 OS=Homo sapiens GN=NOP56 PE=1 SV=4	66009	1	1	1	2	1	152	2.0
O00629|IMA4_HUMAN	Importin subunit alpha-4 OS=Homo sapiens GN=KPNA4 PE=1 SV=1	57851	1	1	1	2	1	89	2.0
O75475|PSIP1_HUMAN	PC4 and SFRS1-interacting protein OS=Homo sapiens GN=PSIP1 PE=1 SV=1	60067	1	1	1	2	1	76	2.0
P04085|PDGFA_HUMAN	Platelet-derived growth factor subunit A OS=Homo sapiens GN=PDGFA PE=1 SV=1	24028	1	1	1	2	1	160	2.0
P06493|CDK1_HUMAN	Cyclin-dependent kinase 1 OS=Homo sapiens GN=CDK1 PE=1 SV=3	34074	1	1	1	2	1	137	2.0
P06737|PYGL_HUMAN	Glycogen phosphorylase, liver form OS=Homo sapiens GN=PYGL PE=1 SV=4	97087	1	1	29	2	1	31	2.0
P06748|NPM_HUMAN	Nucleophosmin OS=Homo sapiens GN=NPM1 PE=1 SV=2	32555	1	1	1	2	1	91	2.0
P07305|H10_HUMAN	Histone H1.0 OS=Homo sapiens GN=H1F0 PE=1 SV=3	20850	1	1	1	2	1	138	2.0
P07477|TRY1_HUMAN	Trypsin-1 OS=Homo sapiens GN=PRSS1 PE=1 SV=1	26541	1	1	41	2	1	77	2.0
P26196|DDX6_HUMAN	Probable ATP-dependent RNA helicase DDX6 OS=Homo sapiens GN=DDX6 PE=1 SV=2	54382	1	1	1	2	1	94	2.0
P40227|TCPZ_HUMAN	T-complex protein 1 subunit zeta OS=Homo sapiens GN=CCT6A PE=1 SV=3	57988	1	1	1	2	1	74	2.0
P42285|SK2L2_HUMAN	Superkiller viralicidic activity 2-like 2 OS=Homo sapiens GN=SKIV2L2 PE=1 SV=3	117729	1	1	1	2	1	49	2.0
P46013|KI67_HUMAN	Antigen KI-67 OS=Homo sapiens GN=MKI67 PE=1 SV=2	358474	1	1	1	2	1	43	2.0
P46776|RL27A_HUMAN	60S ribosomal protein L27a OS=Homo sapiens GN=RPL27A PE=1 SV=2	16551	1	1	1	2	1	88	2.0
P46779|RL28_HUMAN	60S ribosomal protein L28 OS=Homo sapiens GN=RPL28 PE=1 SV=3	15738	1	1	1	2	1	70	2.0
P49137|MAPK2_HUMAN	MAP kinase-activated protein kinase 2 OS=Homo sapiens GN=MAPKAPK2 PE=1 SV=1	45538	1	1	1	2	1	85	2.0
P61353|RL27_HUMAN	60S ribosomal protein L27 OS=Homo sapiens GN=RPL27 PE=1 SV=2	15788	4	2	59	8	4	101	2.0
P62304|RUXE_HUMAN	Small nuclear ribonucleoprotein E OS=Homo sapiens GN=SNRPE PE=1 SV=1	10797	1	1	38	2	1	49	2.0
P62829|RL23_HUMAN	60S ribosomal protein L23 OS=Homo sapiens GN=RPL23 PE=1 SV=1	14856	1	1	1	2	1	140	2.0
P62851|RS25_HUMAN	40S ribosomal protein S25 OS=Homo sapiens GN=RPS25 PE=1 SV=1	13734	3	2	74	6	3	115	2.0
P62888|RL30_HUMAN	60S ribosomal protein L30 OS=Homo sapiens GN=RPL30 PE=1 SV=2	12776	1	1	1	2	1	82	2.0
P62917|RL8_HUMAN	60S ribosomal protein L8 OS=Homo sapiens GN=RPL8 PE=1 SV=2	28007	4	2	166	8	4	216	2.0
P62987|RL40_HUMAN	Ubiquitin-60S ribosomal protein L40 OS=Homo sapiens GN=UBA52 PE=1 SV=2	14719	1	1	1	2	1	49	2.0
P63162|RSMN_HUMAN	Small nuclear ribonucleoprotein-associated protein N OS=Homo sapiens GN=SNRPN PE=1	24598	1	1	1	2	1	87	2.0
P84098|RL19_HUMAN	60S ribosomal protein L19 OS=Homo sapiens GN=RPL19 PE=1 SV=1	23451	2	1	152	4	2	211	2.0
Q02543|RL18A_HUMAN	60S ribosomal protein L18a OS=Homo sapiens GN=RPL18A PE=1 SV=2	20749	1	1	31	2	1	48	2.0
Q13247|SRSF6_HUMAN	Serine/arginine-rich splicing factor 6 OS=Homo sapiens GN=SRSF6 PE=1 SV=2	39563	1	1	1	2	1	54	2.0
Q4ADV7|RIC1_HUMAN	Protein RIC1 homolog OS=Homo sapiens GN=KIAA1432 PE=1 SV=2	159199	1	1	1	2	1	21	2.0
Q52LJ0|FA98B_HUMAN	Protein FAM98B OS=Homo sapiens GN=FAM98B PE=1 SV=1	37167	1	1	40	2	1	57	2.0
Q8N684|CPSF7_HUMAN	Cleavage and polyadenylation specificity factor subunit 7 OS=Homo sapiens GN=CPSF7 PE	52018	1	1	1	2	1	202	2.0
Q8WW22|DNJA4_HUMAN	DnaJ homolog subfamily A member 4 OS=Homo sapiens GN=DNAJA4 PE=1 SV=1	44769	1	1	1	2	1	43	2.0
Q96P11|NSUN5_HUMAN	Putative methyltransferase NSUN5 OS=Homo sapiens GN=NSUN5 PE=1 SV=2	46662	1	1	1	2	1	170	2.0
Q99613|EIF3C_HUMAN	Eukaryotic translation initiation factor 3 subunit C OS=Homo sapiens GN=EIF3C PE=1 SV=	105278	2	1	47	4	1	130	2.0
Q9H0U9|TSYL1_HUMAN	Testis-specific Y-encoded-like protein 1 OS=Homo sapiens GN=TSPYL1 PE=1 SV=3	49162	1	1	1	2	1	256	2.0
Q9NQT4|EXOS5_HUMAN	Exosome complex component RRP46 OS=Homo sapiens GN=EXOSC5 PE=1 SV=1	25233	1	1	1	2	1	44	2.0
Q9NX58|LYAR_HUMAN	Cell growth-regulating nucleolar protein OS=Homo sapiens GN=LYAR PE=1 SV=2	43588	1	1	1	2	1	78	2.0
Q9NZK5|CECR1_HUMAN	Adenosine deaminase CECR1 OS=Homo sapiens GN=CECR1 PE=1 SV=2	58895	1	1	1	2	1	36	2.0
Q9UJV9|DDX41_HUMAN	Probable ATP-dependent RNA helicase DDX41 OS=Homo sapiens GN=DDX41 PE=1 SV=2	69793	1	1	1	2	2	28	2.0
Q9ULU4|PKCB1_HUMAN	Protein kinase C-binding protein 1 OS=Homo sapiens GN=ZMYND8 PE=1 SV=2	131610	1	1	1	2	1	158	2.0

A number of these factors are involved in the transcriptional regulation of rDNA. This indicates that the ribosomal and chromatin gene ontologies may not be separate functions. The top two hits, DNA topoisomerase 2α (Top2α) and Mybbp1a have contrasting functions in RNA Pol I transcription. Top2α associates with active rDNA and mediates *de novo* assembly of the RNA Pol I pre-initiation complex, whereas Mybbp1a contributes to maintaining a repressed environment through recruitment of HDAC1 and HDAC2 [193,194]. Furthermore, I found a histone chaperone (nucleophosmin) and two members of the SWI/SNF nucleosome-remodelling complex, that act to positively regulate rDNA transcription through changes to the chromatin environment [195,196]. Additionally, nucleolin is highly enriched and represented the top-hit in the dataset. As described in the Introduction, nucleolin contributes to rDNA transcriptional regulation, but also to ribosome biogenesis.

I found 36 structural ribosomal proteins (27 RPLs, 9 RPSs) as well as proteins involved in ribosomal subunit maturation, which are required for rRNA processing or ribosome assembly. These include the RNA helicases, DDX21 and DDX1, which significantly impair rRNA processing upon their depletion [156,197]. Furthermore, two members of a C/D box snoRNA complex, Nop56 and Nop58, impair processing and assembly as well [94,198]. Together, the abundance of these ribosome biogenesis associated factors suggests a role for FKBP25 in rDNA transcriptional regulation and/or pre-ribosome assembly.

In addition to the ribosomal factors, I found a number of chromatin-associated proteins involved in the DNA damage response. A major reorganization of chromatin is needed upon damage to prepare for DNA repair. KAP1 normally maintains a heterochromatic environment and is phosphorylated by ATM upon DNA insults, triggering a relaxation of chromatin [199]. Moreover, PARP1 is activated upon DNA breaks and modifies the environment with poly-ADP-ribose, serving as a scaffold to recruit repair machinery [200]. Nucleolin has also been linked to DNA repair through its histone chaperone activity [122,128]. The ssDNA binding protein, RPA1, also has extensive functions in DNA metabolism (Reviewed in [201]), and is integral in protecting ssDNA during replication and DNA repair. The combination of DNA damage response factors, chromatin remodellers and histone proteins in the FKBP25 interactome dataset strongly suggest roles for FKBP25 in chromatin biology.

To validate the mass spectrometry results, I immunoprecipitated FKBP25 and performed western blots for the most abundant (nucleolin) and least abundant (KAP1) proteins identified by in-gel digestion based on the number of peptides detected. I confirmed these proteins specifically interact with FKBP25 (Figure 15c). Since I have not confirmed all of FKBP25's interacting proteins, it is possible some are due to non-specific interactions. It is noteworthy that the previously published FKBP25 interactions between YY1, HDAC1/2 and MDM2 were not detected in my data. This discrepancy may be a result of relatively weak interactions, and differences in my purification conditions. KAP1 for example, was only detected in the in-gel dataset (2 peptides), whereas the more thorough in-solution screen failed to detect any peptides. Despite this, I detected KAP1 interacting with FKBP25 by western blot, confirming the proteins on the

low end of the detection limit are likely missing from the dataset. Thus, this list should be interpreted with caution, as it is almost certainly not comprehensive. Alternatively, these differences could be explained by a cell type dependency. Although I used HEK293 cells, Ochocka et al. used a combination of MCF-7, U2OS, H1299 and HTC116 cells, whereas Yang et al. used Jurkat and HeLa cells [70,82].

I next sought to determine where FKBP25's protein interactions occur in the cell. Given the abundance of nucleolar proteins interacting with FKBP25 I first wanted to confirm its presence in the nuclear sub-compartment. Subcellular fractionation revealed the majority of FKBP25 localizes to the cytoplasm, at least in HEK293 cells, however a proportion can be isolated from the nucleus and nucleolus (Figure 16a). I then purified FKBP25 complexes from whole cell, cytoplasmic and nuclear extracts and separated the material by SDS-PAGE (Figure 16b). In support of FKBP25's interactions occurring in the nucleus, I observed few interacting proteins with cytoplasmic FKBP25, whereas the nuclear FKBP25 material is comparable to the interactions from whole cell extract. This is further supported by FKBP25 interacting with nucleolin in the nucleus and not the cytoplasmic fraction (Figure 16c). Additionally, we performed chromatin immunoprecipitations (ChIP) for FKBP25 and nucleolin (Figure 17). Our data supports FKBP25 associating with rDNA chromatin in the nucleolus, and possessing a similar localization as nucleolin.

Together this data suggests possible functions for FKBP25 in ribosome biogenesis and rDNA chromatin regulation. The presence of FKBP25 interacting with ribosomal factors is intriguing as there are no reports of nucleolar functions of FKBP25. Although FKBP25 has been shown to associate with nucleolin, it has only been speculated to be involved in ribosome biogenesis and this has yet to be explored.

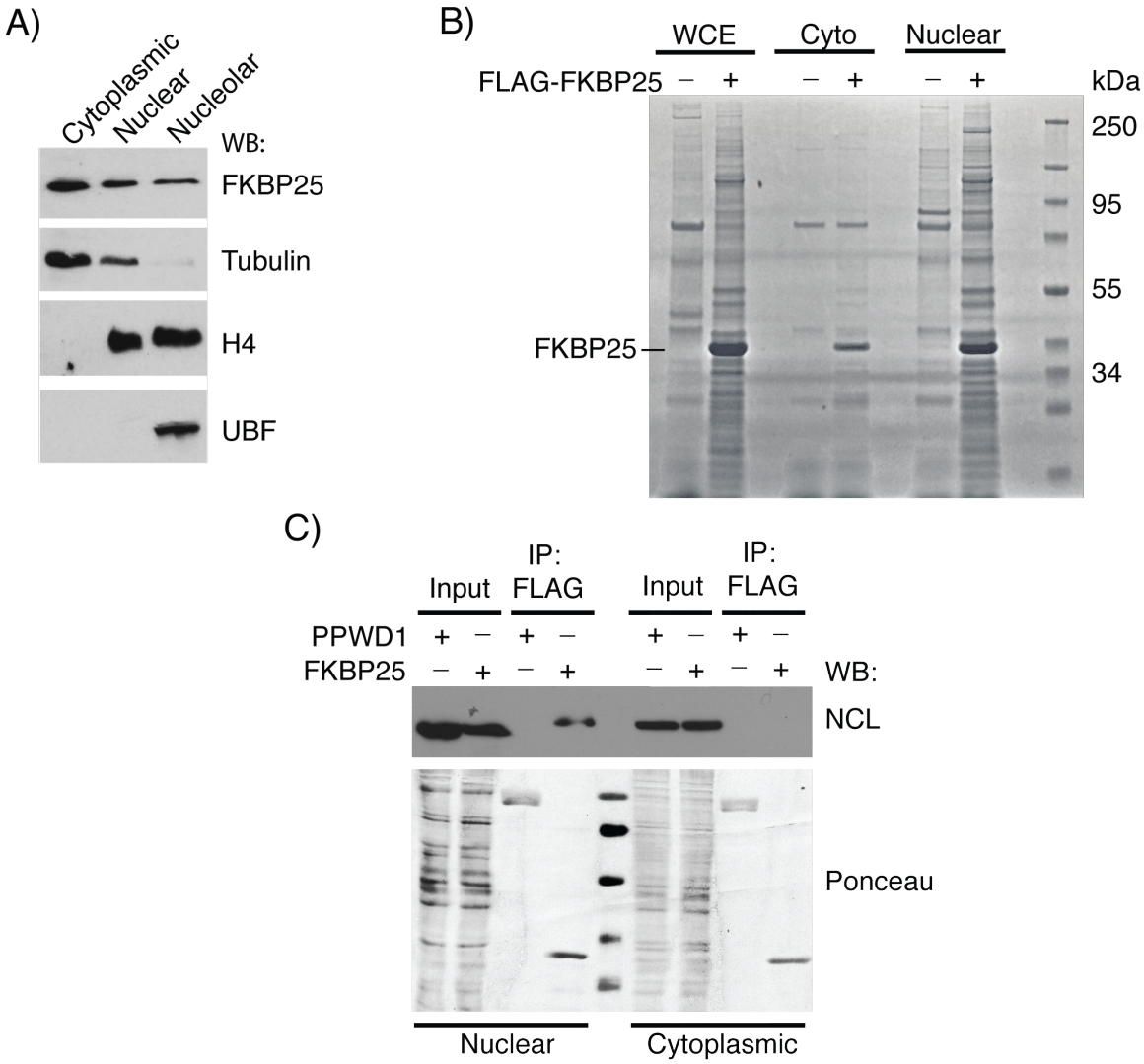

Figure 16. FKBP25's protein interactions occur mainly in the nucleus.
A) Western blots of subcellular fractionation of HEK293 cells. Markers are: Tubulin, cytoplasm; H4, nucleus/nucleolus; and UBF, nucleolus. B) FKBP25 immunoprecipitations from whole cell (WCE), cytoplasmic and nuclear extract separated by SDS-PAGE and silver stained. C) Western blot of FKBP25 immunoprecipitations from nuclear and cytoplasmic extracts. PPWD1 is a nuclear protein control.

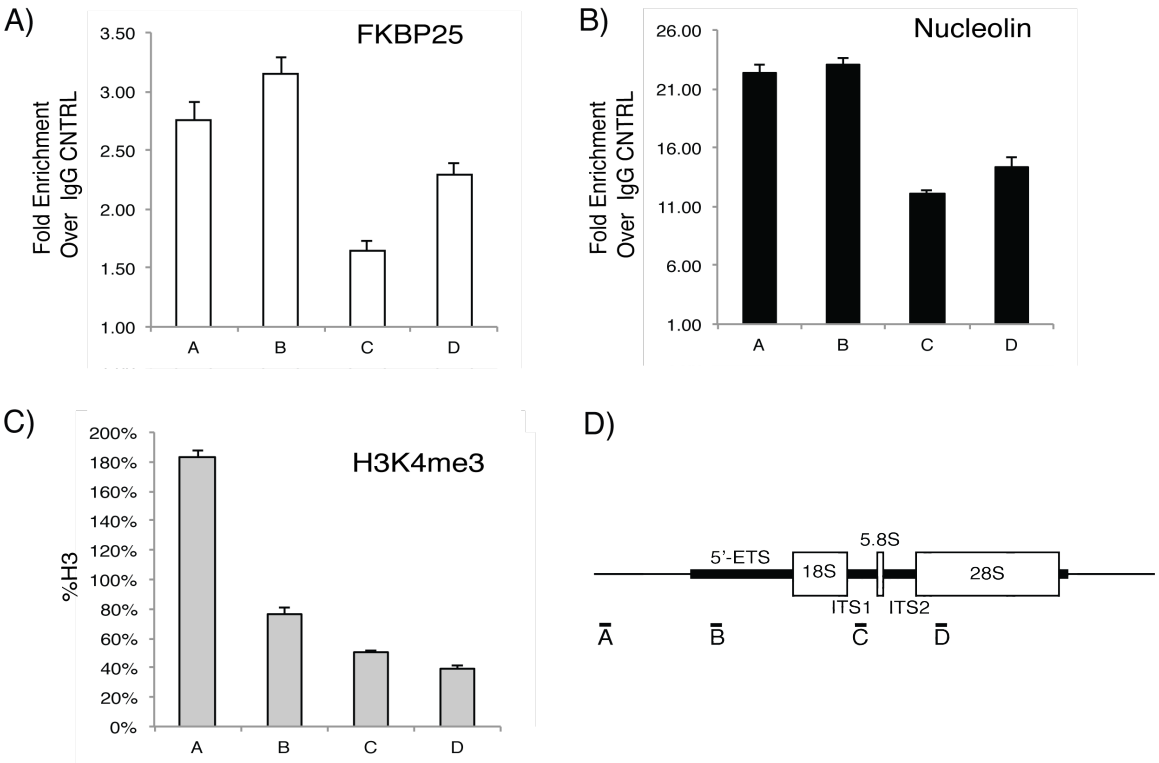

Figure 17. FKBP25 occupies rDNA.
Chromatin immunoprecipitation with (A) FKBP25, (B) nucleolin and (C) H3 was performed in HEK293 cells. Enrichment was analyzed by qPCR. D. Schematic of the rDNA locus. Areas below the schematic correspond to regions amplified in qPCR.

3.2.2 The interaction between FKBP25 and nucleolin is dependent on 28S rRNA.

Given the abundance of ribosome biogenesis factors associating with FKBP25, I sought to determine the nature of FKBP25's interaction with the ribosome. Nucleolin represented one of the most abundant FKBP25 interacting proteins, as observed by western blot and through the number of peptides identified with mass spectrometry, indicating the potential of a direct interaction.

To determine if FKBP25 and nucleolin directly interact *in vitro*, I performed pulldowns of GST-FKBP25 against nucleolin. In these assays, I used a construct containing nucleolin RRM1-4 and the RGG motif (referred to nucleolin hereafter in this section); as we, and others [202,203] were unable to express full-length protein in bacteria. In the pulldown assays, I found FKBP25 and nucleolin interact, albeit weakly (Figure 18a, left). Additionally, the interaction with nucleolin could not be recapitulated with either the BTHB-Linker (aa 1-107) or the isomerase domain of FKBP25 (aa 108-224), suggesting the full-length protein is required to form the interaction. As the

nucleolin construct used in the pulldown assays did not contain the acidic N-terminus, I performed reciprocal pulldowns using a series of GST-nucleolin domain constructs [204] (Figure 18b, bottom) against full-length FKBP25. I confirmed that the interaction surface of nucleolin lies in RRM1-2 and not the acidic regions (Figure 18b).

The identification of a weak interaction between FKBP25 and nucleolin did not reflect my observations from immunoprecipitations and mass spectrometry. I speculated that either a nucleic acid or protein was necessary to mediate the interaction. Given the number of RNA-associated proteins interacting with FKBP25, I hypothesized that the interaction between the two proteins may be enhanced upon the addition of RNA.

I first assayed this by performing immunoprecipitations for FKBP25 from cellular extracts pre-treated with RNase A to deplete total RNA. In support of my hypothesis, FKBP25 fails to enrich nucleolin in RNase-treated material, whereas the interaction is robust in the control mock RNase treatment (Figure 18c). Thus, RNA is necessary to mediate an interaction between FKBP25 and nucleolin *in vivo*.

In order to identify the RNA species that facilitates the FKBP25-nucleolin interaction, I performed RNA immunoprecipitations (RIP). FKBP25 complexes were immunoprecipitated, and the RNA content was extracted and separated by agarose gel, revealing a strong band the same size as the 28S rRNA (Figure 18d). This suggested rRNA mediates the FKBP25-nucleolin interaction *in vivo*.

These results can be interpreted two ways. First, FKBP25 and nucleolin may not interact in a direct manner per se, but are both present within an RNase-sensitive complex - potentially the ribosome. Alternatively, since nucleolin is an RNA-binding protein, FKBP25 may interact specifically with an RNA-engaged form of nucleolin.

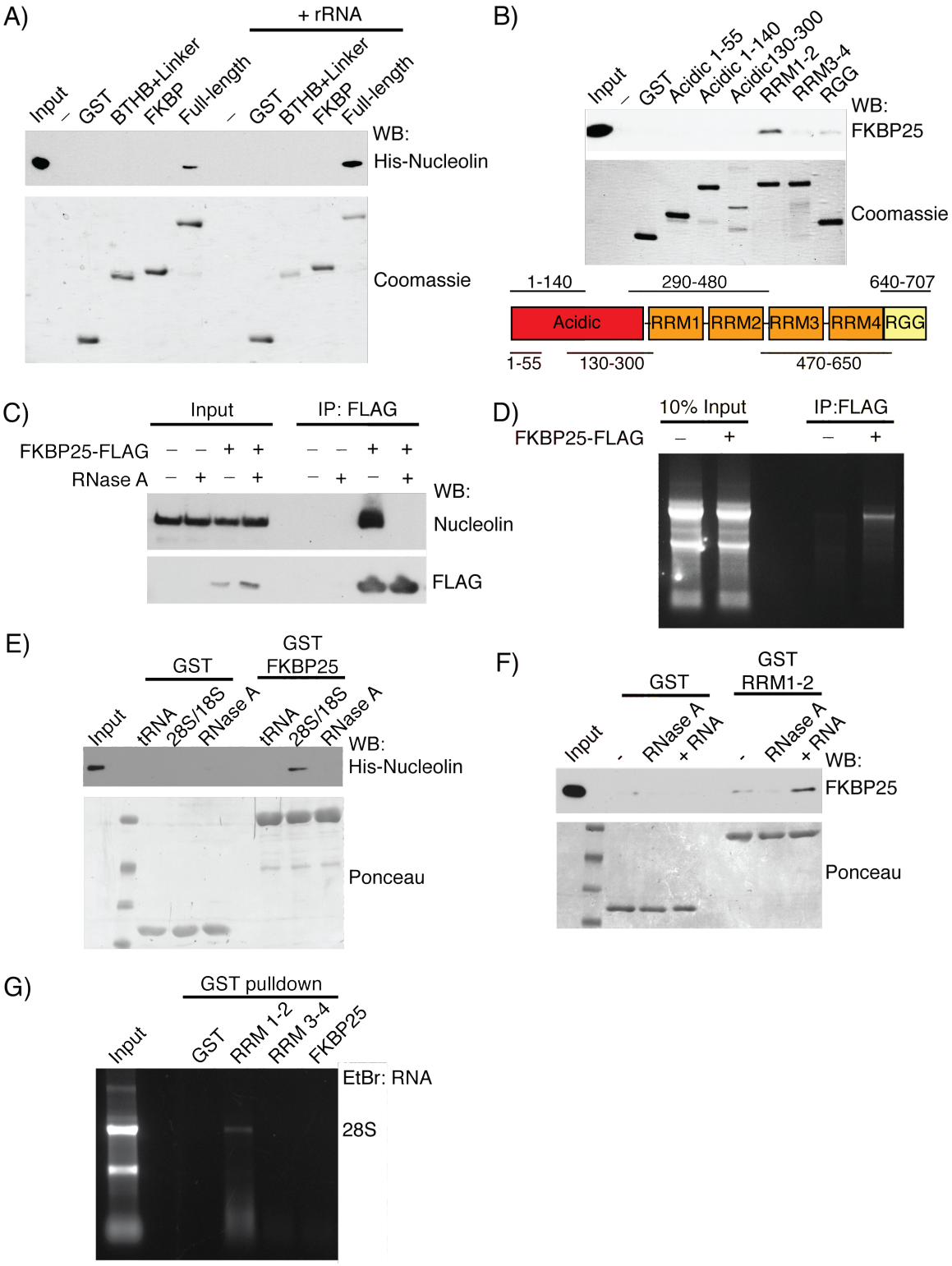

Figure 18. FKBP25 interacts with nucleolin RRM1-2 and requires 28S rRNA.
A) GST pulldown assays of FKBP25 full-length, BTHB+Linker (aa 1-107) and FKBP (aa 108-224) against nucleolin RRM1-4RGG. Pulldowns were performed with and without the addition of rRNA. B) GST pulldown assays using GST-nucleolin domain

deletion series against full-length FKBP25. C) FKBP25-FLAG immunoprecipitations from HEK293 nuclear extracts with and without pre-treatment with RNase A. D) Trizol extracted RNA from FKBP25-FLAG immunoprecipitations from HEK293 nuclear material electrophoresed on a denaturing formaldehyde-agarose gel. E) GST pulldown assays using GST-FKBP25 (full-length) against 6-His nucleolin RRM1-4RGG in the presence of tRNA, rRNA or RNase A. F) GST pulldown assays using GST-nucleolin RRM1-2 (aa 290-480) against full-length FKBP25 in the presence and absence of RNase A, and supplemented with total RNA extracted from HEK293 cells. G) GST pulldowns of GST, nucleolin RRM1-2, nucleolin RRM3-4 and FKBP25 in the presence of total RNA. Interacting RNA was extracted with Trizol and separated on a denaturing formaldehyde-agarose gel.

To distinguish between these possibilities, pulldown assays were repeated and supplemented with purified rRNA. With the addition of rRNA, I observed an increase in the amount of nucleolin recovered with full-length GST-FKBP25, while the separate domains could not form an interaction with nucleolin regardless of the presence of rRNA (Figure 18a, right). To address whether any RNA could mediate the FKBP25/nucleolin interaction, I performed the same assays in the presence of an equal molar amount of tRNA or 28S/18S rRNA. Only rRNA can mediate the interaction and I detect no interaction in the presence of tRNA (Figure 18e). Moreover, reciprocal pulldowns confirms rRNA enhances the interaction between FKBP25 and nucleolin RRM1-2 (Figure 18f).

I also sought to ensure RRM1-2 specifically interacts with the 28S. I performed pulldowns of RRM1-2, RRM3-4 and FKBP25 with rRNA added to the assays and the interacting RNAs were extracted and separated on an agarose gel. RRM1-2 specifically enriches the 28S rRNA, whereas RRM3-4 and FKBP25 had no detectable interacting RNAs (Figure 18g). This confirms FKBP25 is not interacting with the 28S itself, and the RNA is not just bridging the interaction with nucleolin. Together these assays support a model where FKBP25 forms a specific complex with RNA-engaged nucleolin, and is not mediated by other factors.

The identification of the 28S rRNA associating with FKBP25 from nuclear extracts was not unexpected, as I identified 27 ribosomal proteins of the large subunit in the mass spectrometry dataset. However, as FKBP25's interaction with the ribosomal associated factors occurs in the nuclear compartment, this rRNA species may represent

an immature form. To confirm the presence of the 28S rRNA and to directly test whether FKBP25 interacts with pre-processed rRNAs, I reverse transcribed the interacting RNAs from FKBP25 RIP material and the abundance of these transcripts were determined by qPCR (Figure 19). I did not detect an enrichment of the 5'ETS and 18S, whereas the ITS1 had minimal enrichment. The absence of these species was expected, as FKBP25 does not appear to associate with the small ribosomal subunit or 18S rRNA (Figure 19). In contrast, both the ITS2 and the 28S transcripts were enriched. While the 28S was significantly more abundant than ITS2 in the RIP material, this distribution was expected as the amount of 28S in the nucleus significantly outnumbers the pre-processed ITS2-28S transcript. Thus, FKBP25 is recruited to nascent rRNA downstream or near ITS2, and associates with pre-28S rRNA in the nucleus.

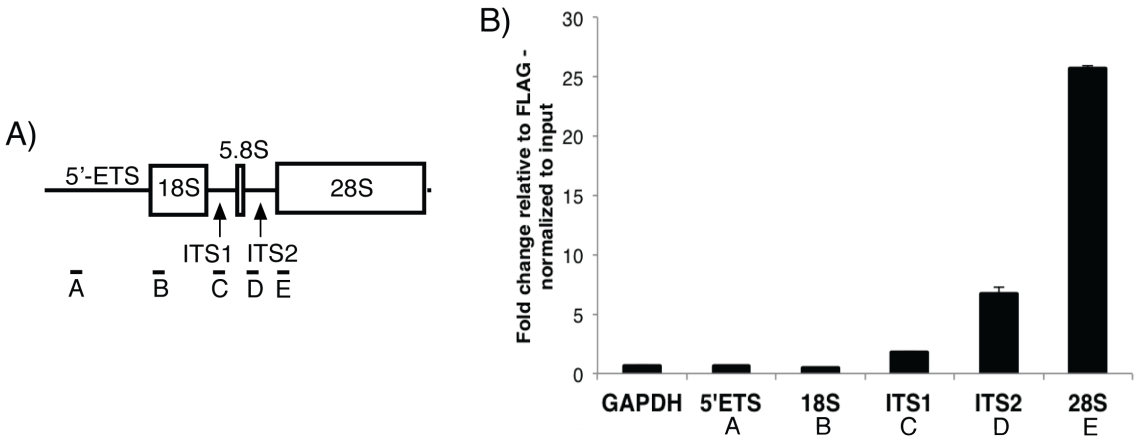

Figure 19. FKBP25 interacts with ITS2 and 28S rRNA.
A) Schematic of the 47S rRNA transcript. Below are locations of primers used for qPCR. B) qPCR analysis of reverse transcribed RNA extracted from FKBP25-FLAG immunoprecipitations from HEK293 nuclear extract. GAPDH is used as a control.

3.2.3 FKBP25 transiently associates with the pre-60S ribosomal subunit in the nucleus.

Ribosome processing factors transiently associate with structural ribosomal proteins and rRNA in the nucleus during 40S and 60S assembly. My data supports FKBP25 interacting with both nucleolin and 28S rRNAs, including those yet to be fully processed (ie. still contain ITS2 sequences). The latter association, and the presence of

ribosome biogenesis factors in FKBP25 immunoprecipitates raise the question of whether FKBP25 interacts with pre-ribosomes. To resolve whether FKBP25 associates with the mature or immature 60S ribosomal subunit, I performed sucrose density ultracentrifugation to separate large macromolecular complexes from smaller protein complexes. First, I subjected cytoplasmic extract to a sucrose gradient centrifugation and followed FKBP25 and nucleolin in the separated fractions by western blot. I was unable to identify an association between FKBP25 and mature ribosomes in the cytoplasm (Figure 20a). Similarly, nucleolin does not interact with mature ribosomes in my experiments which is consistent with previous reports that nucleolin interacts with pre-ribosomes [140].

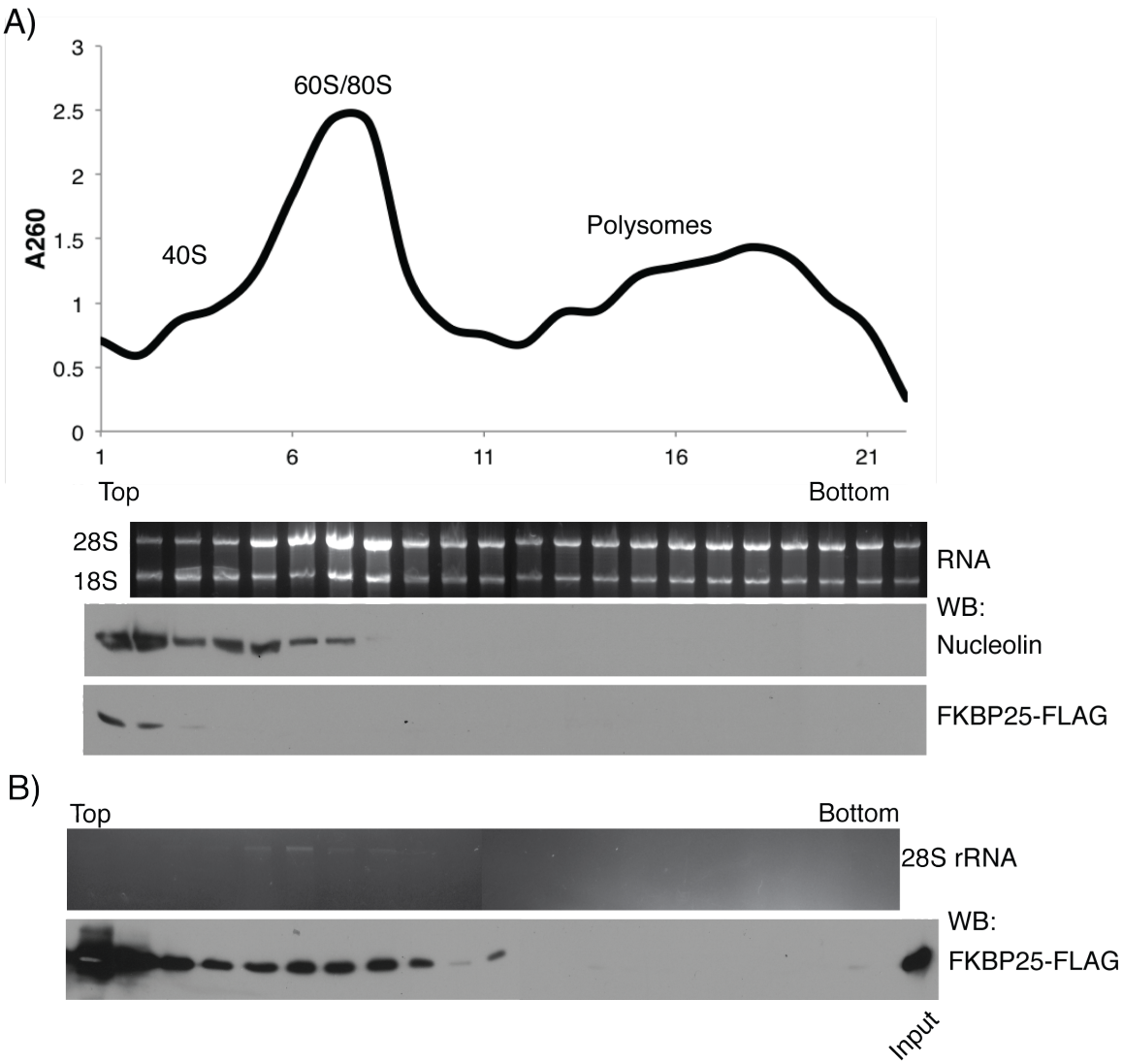

Figure 20. FKBP25 does not associate with translating cytoplasmic ribosomes.
A) Sucrose gradient ultracentrifugation of cytoplasmic extract from HEK293 cells expressing FLAG-FKBP25. RNA and protein were extracted from each fraction and were resolved by denaturing-formaldehyde gel electrophoresis or SDS-PAGE and western blot. B) Sucrose density gradient ultracentrifugation of FLAG-FKBP25 immunoprecipitate from cytoplasmic extract. RNA and protein were extracted from each fraction and were resolved by denaturing-formaldehyde gel electrophoresis or SDS-PAGE and western blot.

To separate pre-40S from pre-60S, the same experiment was performed using nuclear extract to enrich for immature ribosomal species prior to export to the cytoplasm. Nucleolin was present in every fraction collected (Figure 21a); however abundance of nucleolin in peaks encompassing the pre-40S and pre-60S did not appear to differ.

Despite nucleolin's co-fractionation with pre-ribosomes, I was unable to identify FKBP25 in any fraction that contained pre-40S or pre-60S ribosomal species (Figure 21a). I speculated that the interaction between FKBP25 and nascent ribosomes could be disrupted by centrifugation, which explained the lack of FKBP25 entering the gradient. Alternatively, FKBP25 may interact with a sub-population of pre-ribosomes. To address this possibility, FKBP25 enriched material was subjected to sucrose density ultracentrifugation. The majority of immune-captured FKBP25 was found at the top of the gradient, however a longer exposure revealed fractions containing FKBP25, nucleolin and 28S rRNA (Figure 21b). This confirmed that a fraction of FKBP25 sediments with the pre-60S ribosome, and the remainder sediments with lower molecular weight material. The lower molecular weight species could represent other FKBP25 associated entities, such as chromatin-associated complexes.

To determine if FKBP25 interacts with the mature 60S subunit or translating ribosomes, I performed immunoprecipitations of FKBP25 from cytoplasmic material (Figure 20b). Although FKBP25 does enrich a small amount of 28S rRNA, I speculate a portion of nuclear FKBP25 may not dissociate and transits with the pre-60S across the nuclear membrane to the cytoplasm. Alternatively, FKBP25 may be involved in the final cytoplasmic maturation steps of the 60S. The absence of 18S rRNA in this material confirms that FKBP25 does not associate with mature, translating ribosomes in the cytoplasm.

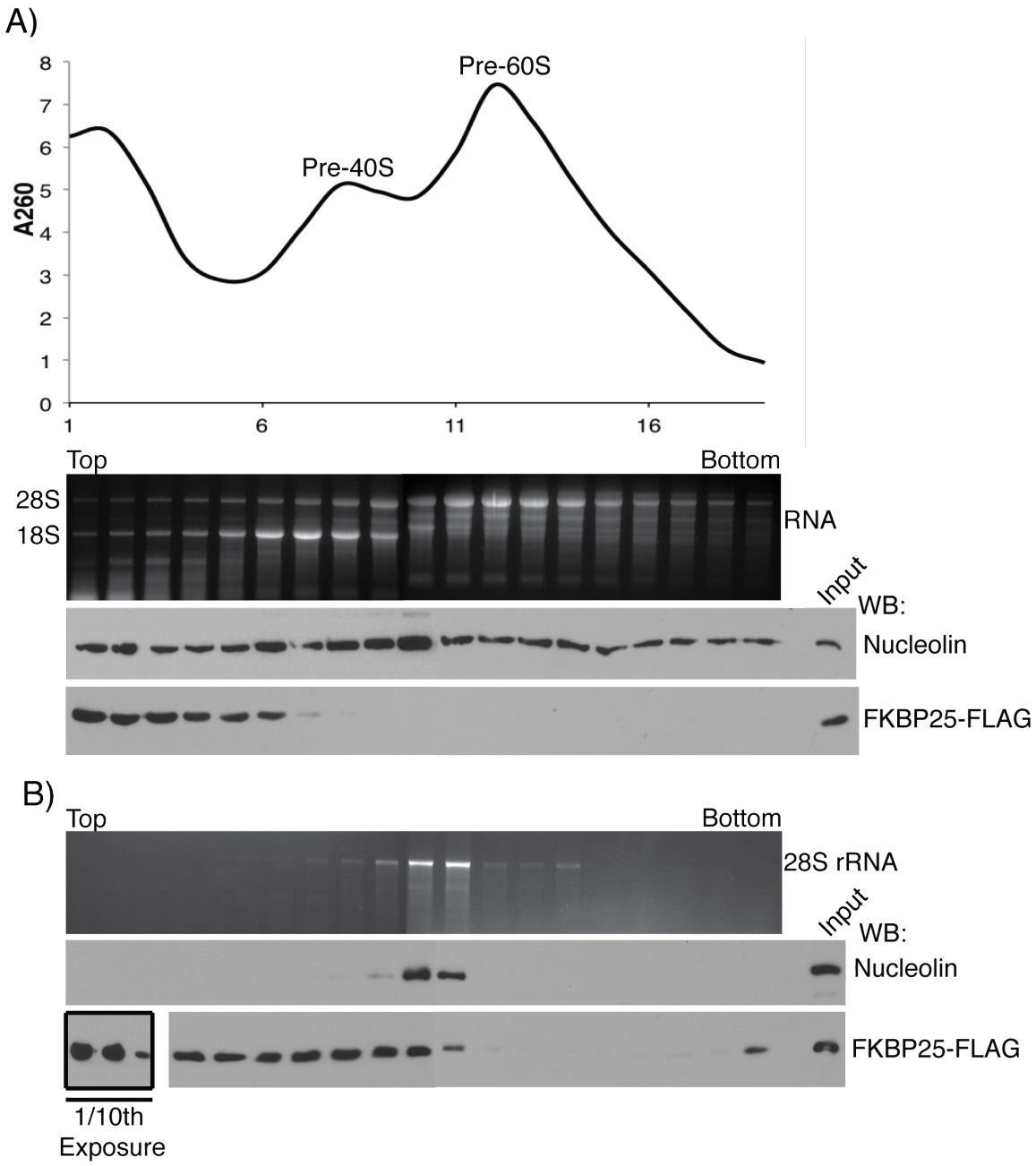

Figure 21. FKBP25 interacts with the pre-60S ribosome in the presence of nucleolin. A) Sucrose density gradient ultracentrifugation of HEK293 nuclear extract. RNA and protein were extracted from each fraction and were resolved by denaturing-formaldehyde gel electrophoresis or SDS-PAGE and western blot. B) Sucrose density gradient ultracentrifugation of FLAG-FKBP25 immunoprecipitate from HEK293 cells. RNA and protein were extracted from each fraction and were resolved by denaturing-formaldehyde gel electrophoresis or SDS-PAGE and western blot.

3.2.4 FKBP25 does not affect steady state levels or processing rates of rRNA intermediates.

The presence of FKBP25 associating with a pre-60S ribosomal species led me to speculate that FKBP25 may affect ribosome maturation. This is most easily monitored by following the processing of rRNA, which occurs in well-defined steps. I explored this in collaboration with David Dilworth, who at the time was performing FKBP25 knockdown and over-expression experiments. We performed northern blots on total RNA isolated from cells depleted of FKBP25. We detected no major change of any processed transcript level upon knockdown of FKBP25 (Figure 22a). Similarly, we observed no major differences in transcript levels of any processed stage upon over-expression of FKBP25 in comparison to the control (Figure 22b). Thus, the depletion or over-expression of FKBP25 does not affect processing of rRNA steady state levels.

As a control to ensure that we could detect changes in rRNA processing, we treated cells with rapamycin, which is well documented to affect rRNA processing through mTOR [205]. Consistent with previous reports, we observe a rapamycin-induced accumulation of the 30S transcript (Figure 22c).

These experiments show that FKBP25 does not have a major impact on rRNA processing and suggest FKBP25 may act in a manner that does not directly involve or affect the maturation of rRNAs.

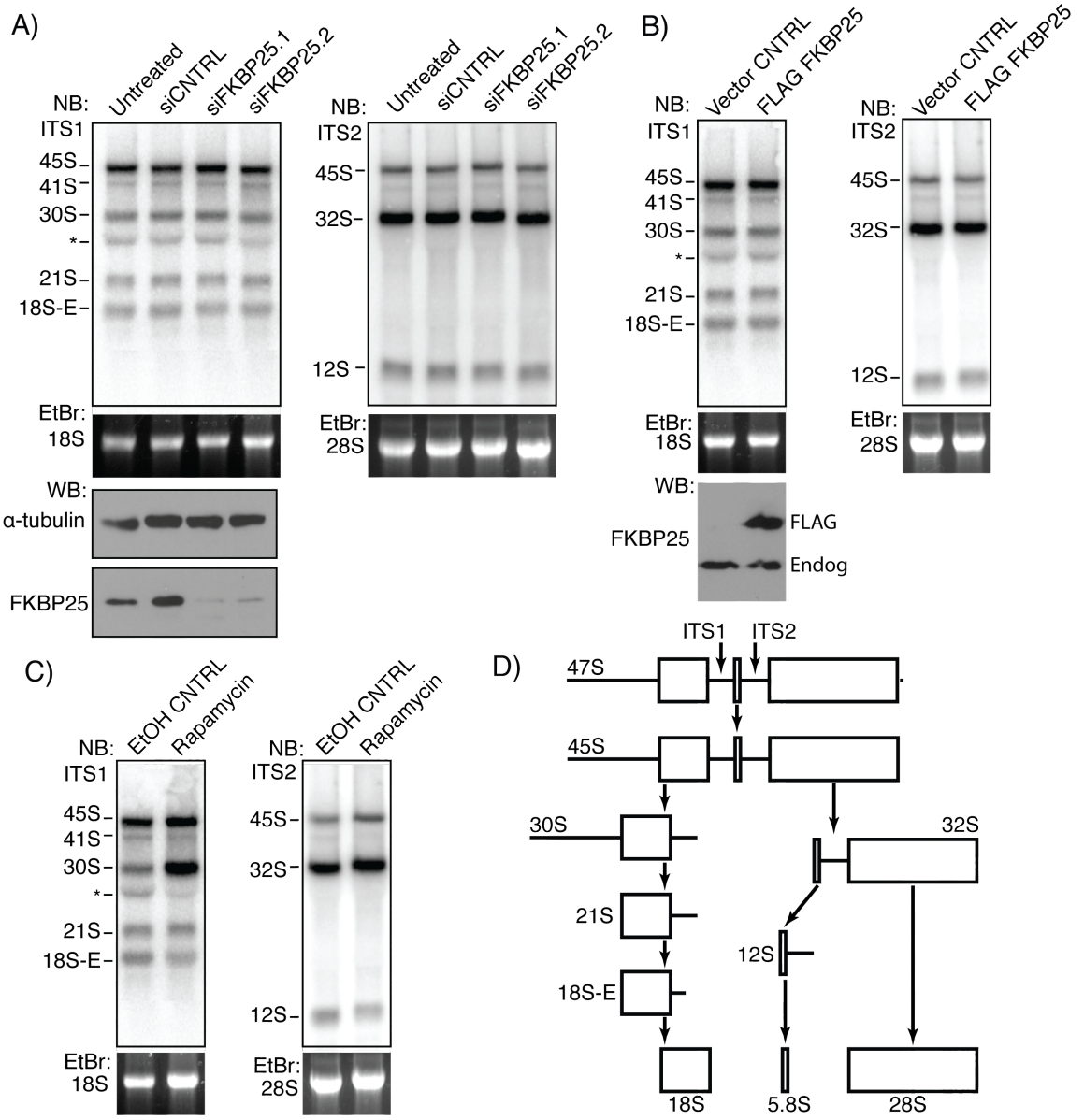

Figure 22. Over-expression or knockdown of FKBP25 does not affect steady state levels of pre-rRNA intermediates.

A) Northern blot of RNA extracted from untransfected HEK293 cells or HEK293 cells transfected with control siRNA or FKBP25-targetting siRNA. Blots were probed for ITS1 (Left) or ITS2 (Right). Extracts were western blotted for FKBP25 to verify knockdown. B) Northern blot of RNA extracted from HEK293 from control and cells over-expressing FLAG-FKBP25. Blots were probed for ITS1 (Left) or ITS2 (Right). C) Northern blot of HEK293 cells treated with vehicle or rapamycin probed for ITS1 (Left) or ITS2 (Right). Cells were treated with rapamycin or ethanol control for 6 hours at 100 nM. D) Schematic of rRNA processing steps. * denotes non-specific signal.

3.3 Discussion.

The results presented herein significantly advance the understanding of where FKBP25 functions in the nucleus. Through two mass spectrometry screens I identified 110 novel interacting proteins for FKBP25 (Table 2, 3). Over half of these proteins are implicated in ribosome biogenesis, including rDNA transcriptional regulators, structural ribosomal proteins and ribosome assembly factors.

The list of FKBP25 interacting proteins suggested two areas for FKBP25 to function in ribosome biogenesis: chromatin and ribosome assembly. Nucleolin represented one of the most abundant interacting proteins for FKBP25 and provided a link to both chromatin and ribosome biogenesis, thus I sought to understand where these proteins might function in the pathway. I demonstrated that the 28S rRNA is necessary and sufficient for FKBP25 and nucleolin to interact and this interaction occurs on the pre-60S ribosomal subunit. This indicated that FKBP25 might be involved in maturation of the large ribosomal subunit.

The FKBP25 interactome dataset supports a potential role in ribosome assembly based on the presence of ribosomal factors that have distinct functions in 60S maturation. For example, nucleophosmin has dual roles in rRNA processing and subunit export. This is evident when depleting nucleophosmin, as there is a lag in processing from the 32S to mature 28S form [206]. Nucleophosmin also interacts with RPL5 and is involved in 60S export from the nucleus through this association [207,208]. Moreover, the RNA helicase Mtr4 (SKIV2L2) has been implicated in processing of the 5.8S rRNA [209]. This processing step requires the RNA exosome [210,211], of which I found three core components in my FKBP25 interactome dataset (Mtr3, Rrp46, Rrp4). Additionally, depletion of the yeast homolog of RBM28 prevents accumulation of the mature 60S ribosomal subunits by impeding pre-rRNA processing [212].

Although our data suggests FKBP25 levels have no effect on processing of rRNA intermediates, the general consensus is that pre-ribosome associated factors function in maturation of the subunits. FKBP25 is an exception to this, but it is not the only example. Despite its association with the SSU processome and abundance with both the pre-40S and pre-60S subunits, nucleolin has no effect on rRNA processing [132,134].

Additionally, the rRNA methyltransferase Nop2 also enriches with pre-ribosomes, yet its depletion has no impact on processing rates or subunit maturation [94].

It is possible that FKBP25 does participate in rRNA processing but it is complemented by another protein. Indeed, there are examples of this in ribosome biogenesis. Depletion of the RNA helicase DDX17 has no effect on rRNA processing, however depletion in concert with another helicase DDX5 impairs 28S processing [213]. With many pre-ribosome associated proteins having shared activities (ie. helicase, methyltransferase, etc.), there are potentially other redundancies. While FKBP25 is the only pre-ribosome associated FKBP in humans, it is not the only PPI. Par14 can be detected with pre-ribosomes more readily than FKBP25 [189,190]. It is noteworthy that Par14 is not detected interacting with FKBP25, despite it being previously reported as a component of the maturing 60S subunit.

While I was unable to attribute FKBP25 to a specific function in ribosome biogenesis, the data described here provides insight into where FKBP25 is recruited in the complex pathway.

The first aspect of the pathway I can rule out is rDNA transcriptional regulation by FKBP25. Although we were able to enrich FKBP25 at rDNA in the nucleolus, we did not detect any change in 47S rRNA levels upon depletion or over-expression of FKBP25 (Figure 22). Depletion of nucleolin significantly impairs RNA polymerase I transcription at rDNA [132,134], thus it is unlikely that FKBP25 modulates transcription directly or through regulating nucleolin.

Additionally, I can rule out FKBP25 functioning in the earliest stages of assembly based on a few observations. First, FKBP25 RNA immunoprecipitations did not enrich sequences from the 5'ETS, 18S or ITS1 (Figure 19). Second, of the 70+ proteins constituting the small subunit processome, only four interacted with FKBP25 from the MS screen (Nop56, Nop58, Mybbp1a and nucleolin) [214]. These proteins also enriched with the pre-60S subunit and are implicated in its assembly as well [94,132,140,215]. Therefore it is unlikely FKBP25 is an undiscovered member of this complex. Finally, although a small number of RPS proteins enriched in the FKBP25 interactome dataset,

these are likely bridged through an interaction with nucleolin, which is known to interact with ribosomal proteins through its RGG domain [149].

The interpretation of the data described above suggests FKBP25 is recruited to the pre-60S subunit, at the earliest, after the A_2 processing event separating the 18S and 28S branches of the pathway. The exact mechanism of recruitment is not clear, however it is likely nucleolin contributes to FKBP25's recruitment through binding the 28S rRNA. It is interesting to note that despite nucleolin interacting with the pre-40S subunit, the nucleolin-FKBP25 interaction can only be detected on the immature large subunit. Therefore, rRNA sequence or structural factors may contribute to FKBP25 recruitment. Additionally, FKBP25 may transit with the pre-60S subunit across the nuclear membrane. From the FKBP25 interaction screens, I found low enrichment of two of the eight RPLs (RPL10, RPLP1) that are integrated into the large subunit in the cytoplasm. However, the lack of proteins involved in pre-60S nuclear export interacting with FKBP25 suggests the majority of FKBP25 may dissociate before nuclear export. Together, this data suggests FKBP25 is recruited sometime after the A_2 cleavage and dissociates prior to nuclear export.

Ultimately, the limiting factor for identifying the function of FKBP25 is its low abundance in pre-60S subunits. The sheer number of non-FKBP25 associated pre-ribosomes may mask any alterations in ribosome assembly or function. My data suggests FKBP25 is a sub-stoichiometric component of the emerging 60S ribosomal subunit meaning it may visit each ribosome on a temporary basis or confer a specialized function to a subset of pre-ribosomes.

Ribosome heterogeneity has recently become appreciated as a mechanism to regulate how the genomic template is translated into functional proteins [216]. This can come by a number of mechanisms, such as post-translational modifications to ribosomal proteins and rRNA. Beaudin-Baillieu et al. have demonstrated that deletion of snoRNAs in yeast that guide rRNA pseudouridinylation and methylation lead to defects in translational accuracy in reading frame maintenance and termination [217]. In humans, increased expression of rRNA methyltransferase fibrillarin leads to a similar effect resulting in decreased translational fidelity [218]. As these rRNA modifications are

enriched in functional regions of the ribosome and contribute to folding, changes in rRNA modification drastically impact function [219,220]. Thus, FKBP25 may act on a subset of pre-ribosomes, altering the structure or orientation of the 60S subunit.

Perhaps one mechanism by which FKBP25 can modulate pre-ribosome function, composition or structure is through recruitment or displacement of specific transient assembly proteins. Building on the reported role of FKBP25 promoting YY1-DNA binding, a similar chaperone function for FKBP25 may exist by recruiting proteins to the pre-60S ribosome. Therefore, I propose the function of FKBP25 may be to regulate protein-RNA interactions, aiding their recruitment or displacement from the pre-ribosome to ensure the progression of ribosome biogenesis. As FKBP25 associates with proteins integral in rRNA modification and processing, recruiting these proteins to their substrates and proper location is essential. In Chapter 4, I will address the *in vitro* role of FKBP25 in nucleolin-RNA binding to shed light on this hypothesis.

3.4 Methods.

Cell lines and transfections.

HEK293 Flp-In T-Rex cells (Life Technologies) were maintained in DMEM containing 10% FBS and Pen/Strep at 37^{o}C in 5% CO_2. For tetracycline inducible cells, FKBP25 and PPWD1 were cloned into pcDNA5/FRT/TO (Life Technologies) containing a tetracycline-regulated, hybrid CMV/TetO2 promoter and a triple FLAG epitope tag. Stable cell lines were constructed as per manufacturers recommendations. Cells were transfected overnight using Lipofectamine 2000 (Life Technologies) in 6-well dishes as per manufacturers recommendations with either 60nM siRNA or pcDNA5/FRT/TO 3×-FLAG FKBP25 vector. Cells were split in the morning 1:4 and incubated for 48hrs. In the case of cells transfected with pcDNA5/FRT/TO 3×-FLAG-FKBP25, 0.1μg/ml tetracycline was added to the media to induce expression of the transgene.

Immunoprecipitation and western blot.

For whole cell extraction, HEK293 cells (~3×10^7 cells) were lysed in 0.75 mL immunoprecipitation (IP) buffer (50 mM Tris pH8, 150 mM NaCl, 0.5% IGEPAL, 0.5% Triton X100, 2 mM EDTA, 1 μg/mL leupeptin, 1 μg/mL aprotinin and 1 μg/mL pepstatin), vortexed for 3 seconds and incubated on ice for 10 minutes. Insoluble material

was pelleted at 10,000 rpm for 10 minutes. Cytoplasmic and nuclear extractions are described below for sucrose density ultracentrifugation. Extract were normalized for total protein and buffers were compensated to wash buffer conditions prior to immunoprecipitation. Soluble extracts were added to pre-washed EZ-view Red ANTI-FLAG M2 Affinity gel beads (Sigma F2426). For RNase A treated extracts, 100 μg RNase A (Qiagen) was added to extracts (2-3 mg) and incubated at 37°C for 5 minutes prior to addition of FLAG beads. IPs were incubated at 4°C for 1.5 hours with nutating. After binding, beads were washed three times in IP buffer (0.75 mL IP buffer was added to beads and nutated for 5 minutes, then centrifuged at 1000 rpm for 1 minute). FLAG-complexes were eluted with 1.25 μg/μL 3× FLAG peptide (Sigma F4799) by nutating for 15 minutes at 4°C. For western blotting, eluted proteins were resolved by SDS-PAGE and transferred to a nitrocellulose membrane. Membranes were blocked in 10% skim milk for 30 minutes and probed in primary antibody overnight at 4°C. Antibodies and dilutions used were: 1/50,000 anti-FLAG M2 antibody (Sigma F1804); 1/5,000 anti-Nucleolin (Abcam ab22758); 1/1,000 anti-TIF1β (KAP1) (Santa Cruz sc-33186); 1/1000 anti-His probe (Santa Cruz sc-803) anti-UBF (Santa Cruz sc-13125X); anti-H3 (Abcam ab1791), anti-αTubulin (Rockland 600-401-880) and anti-FKBP25 (Raised against amino acids 3-18). Blots were washed three times for 10 minutes in TBST (TBS + 0.1% Tween-20) and incubated in secondary antibody for 1-2 hours at room temperature. Horseradish peroxidase conjugated anti-mouse (GE NXA931) or anti-rabbit (GE NA934) secondary antibody was used at 1:5,000. Proteins were detected by chemiluminescence (Millipore WBLUF0500) and exposed to film.

Mass spectrometry.

FKBP25 was immunoprecipitated with anti-FLAG as described above. For in-gel experiments, FKBP25 was immunoprecipitated from whole cell extracts. For in-solution experiments, FKBP25 was immunoprecipitated from nuclear extract. For in-gel digestion, immunoprecipitated samples were resolved on NuPAGE Novex 4-12% Bis-Tris Gradient gels at 150 V for approximately 1.5 hours and stained in Coomassie G250. After destaining (25% methanol, 14.2% glacial acetic acid), bands were excised from the gel using a sterile razor, cut in half and placed in microfuge tubes. Gel slices were washed with 100 μL of sterile dH_2O for 5 minutes at 37°C, shaking at 400 rpm. dH_2O was

discarded and the wash was repeated. 50 μL of 50 mM ammonium bicarbonate (ABC) and 50 μL of 100% acetonitrile were added and samples were incubated at 37 ^{o}C at 400 rpm for 5 minutes in a thermomixer. The solution was discarded and washing repeated (3-8 times) until gel slices were colorless. Slices were subjected to two 5 minute washes in 100 μL acetonitrile, frozen at -80^{o}C for 20 minutes, and lyophilized. Samples were incubated in 100 μL acetonitrile for 5 minutes, the solution discarded and wash repeated. Tubes containing gel slices were cooled on ice for 30 minutes and 20 μl of acetonitrile containing 0.5 μg of sequencing grade trypsin (Promega) added to the gel slices and samples kept on ice for 30 minutes. The trypsin solution was discarded and 40 μL ammonium bicarbonate was added and samples incubated overnight in a thermomixer at 37^{o}C and 400 rpm. The following day 50 μL of acetonitrile was added to each digest and samples were incubated for 10 minutes. The solution containing digested peptides was removed to a new microfuge tube. Gel slices were washed in 30 μL for 10 minutes followed by addition of 50 μL acetonitrile and further incubation for 10 minutes. This solution was decanted and pooled with the first extraction. Samples were lyophilized until dry and reconstituted with 10 μL 0.1% triflouro-acetic acid. Samples were spotted on Applied Biosystems stainless steel MALDI plate in duplicate, overlaid with 1 μL α-cyano matrix and analyzed using Applied Biosystems 4800 MALDI-TOF/TOF mass spectrometers at the UVic Genome BC Proteomics Centre. Results were analyzed by Mascot MS/MS ion search. For in solution digests, FKBP25 enriched material was incubated with 1 μg trypsin overnight at 37^{o}C in TBS and lyophilized until dry. Peptides were resuspended in water and ZipTips (Millipore) were used to clean up samples. Peptides were flown on an Orbitrap LTQ mass spectrometer (Thermo Scientific). MS searches were performed using MASCOT. Enrichment was assed by the number of significant peptides identified relative to an empty vector control. Functional enrichment analysis was performed for all proteins with greater than twofold enrichment as well as proteins identified by the in-gel digest method using DAVID (Database for Annotation, Visualization and Integrated Discovery version 6.7, DAVID) with a p-value cut-off of < 0.5. Gene ontology terms were then submitted to the REVIGO [221] (reduce and visualize Gene ontologies) server and summarized using a similarity cut-off of 0.4 and

Resnik's semantic similarity measure. Refer to Appendix Table 4 for data.

Cellular fractionation.

Cellular fractionation to isolate cytoplasmic, nuclear, nucleolar components was performed as described previously [222] (http://www.lamondlab.com/pdf/CellFractionation.pdf). Briefly, cells were lysed in a hypotonic buffer with dounce homogenization yielding the cytoplasmic fraction. The nuclear fraction was isolated using a series of centrifugations over sucrose cushions and sonication. Finally, nucleoli were isolated by centrifugation of the nuclear fraction. Extracts were normalized for total protein and resolved by SDS-PAGE and western blotted as described below.

Chromatin Immunoprecipitation.

Cells were cross-linked with 1% formaldehyde for 10 minutes at room temperature and the reaction quenched with the addition of glycine to 0.175 M with an additional 5 minute incubation at room temperature. Cross-linked and washed cells were then harvested and resuspended in nuclei isolation buffer (5 mM PIPES pH 8.0, 85 mM KCl, 0.5% NP-40, and protease inhibitors) and dounce homogenized to isolate nuclei. Nuclei were pelleted for 10 minutes at 1500 rpm in a swing bucket rotor and resuspended in micrococcal nuclease (MNase) digestion buffer (50 mM Tris-HCl pH 8.0, 5 mM $CaCl_2$, and protease inhibitors). Chromatin was digested by incubation with 50 U of MNase (Worthington) for 5 minutes at 37^{o}C. Digestion was stopped by the addition of an equal volume of ice-cold 2x lysis buffer (100 mM Tris-HCl pH 8.0, 20 mM EDTA pH 8.0, and 2% SDS). Samples were then flash frozen in liquid nitrogen and stored at -80^{o}C. A small aliquot was held and the cross-links reversed by heating at 65^{o}C overnight to assess the extent of MNase digestion and quantify the concentration of input chromatin. Prior to immunoprecipitation, chromatin samples were cleared of SDS and debris by centrifugation at 12,000 rpm for 10 minutes, diluted in dilution buffer (1% Triton X-100, 2 mM EDTA, 150 mM NaCl, 20 mM Tris-HCl (pH 8.0), and protease inhibitors) to 0.1 μg/μl chromatin, and pre-cleared by mixing with protein A/G agarose beads (Thermo Scientific) for 2 hours at 4^{o}C. Pre-cleared solubilized chromatin samples were incubated with 5 μg of either anti-FKBP25 (Raised against amino acids 3-18), anti-histone

H3K4me3 (Abcam ab8580), anti-nucleolin (Abcam ab22758), or rabbit IgG (Rockland) for 2 hours at 4°C. Protein A/G beads were added for 3 hours at 4°C to precipitate immune complexes. Beads were then washed three times with wash buffer (0.1% SDS, 1% Triton X-100, 2 mM EDTA, 150 mM NaCl, 20 mM Tris-HCl pH 8.0, and protease inhibitors) and once with a final high salt wash buffer (0.1% SDS, 1% Triton X-100, 2 mM EDTA, 500 mM NaCl, 20 mM Tris-HCl pH 8.0, and protease inhibitors), and eluted by incubation with elution buffer (50 mM Tris-HCl pH 8.0, 10 mM EDTA) for 30min at 30°C. To reverse cross-links, samples were incubated overnight at 65°C with 5 μg/ml RNase A (Qiagen). DNA was purified by PCR purification spin column (BioBasic) and quantitative PCR analysis performed as described in methods section.

Protein expression and GST pulldown assays.

Escherichia coli BL21 RIL strains containing pGEX5x1 encoding: GST; GST-FKBP25 FL (1-224); GST-FKBP25 NTD (1-107); GST-FKBP25 PPI (108-224); GST-NCL 1-55, GST-NCL 1-140, GST-NCL 130-300; GST-NCL 290-480; GST-NCL 470-650; GST-NCL 640-707 (NCL series a gift from O. Becherel), pET 6-His FKBP25 (1-224) and pET15b encoding 6-His nucleolin RRM-RGG (308-710) were expressed and lysed as described previously. Proteins were normalized by SDS-PAGE. For each pulldown reaction, 500 μL binding buffer, 100 μg BSA, RNase inhibitors and GST/6-His protein extracts were added. Equal molar amounts of tRNA or rRNA containing of 18S and 28S transcripts purified from sucrose gradient ultracentrifugation or 100 ng RNase A was added to the corresponding samples. Samples were nutated for 1.5 hours at 4°C, then added to pre-washed Glutathione-Agarose beads (Qiagen) and allowed to bind for another hour. Protein bound beads were washed three times and resuspended in SDS loading buffer. Proteins were separated by SDS-PAGE and immunoblotted as described above.

RNA immunoprecipitation and qPCR.

FLAG immunoprecipitations were performed as described above. RNA was extracted from eluates with TRIzol as per manufacturers recommendations. Purified RNA was reverse transcribed using a cDNA kit (Applied Biosystems) with random hexamers as per manufacturers recommendations. qPCR reactions (20 μL per reaction) contained 10 μL

2X Maxima SYBR Green qPCR Master Mix (Thermo Scientific K0253), 1.25 μM ROX (Thermo Scientific R1371), 0.5 μM oligos, 7.5 μL dsH_2O and 2 μL diluted template cDNA. qPCR reactions were run on a Stratagene MX3000p real-time qPCR system (Agilent Technologies). The thermocycle program included an initial activation step at 95°C (10 minutes) and 40 cycles of 95°C denaturation (15 sec), 60°C annealing (30 sec). Specificity of target amplification was analyzed by no DNA template controls and subjecting completed runs to melting curve analysis. Data was analyzed by normalizing IP samples to 10% input samples and then calculating the fold change over FLAG (-) control sample. Oligonucleotides used for qPCR are described in the Appendix.

Sucrose density gradient ultracentrifugation.

For preparation of cytoplasmic extracts, HEK293 cells were pre-incubated for 10 minutes at 37^{o}C in the presence of 100 μg/ml cycloheximide in the media. Following treatment, cells were washed once in cold PBS and extracts were extracted as described previously. Extracts were overlaid on a 10-50% sucrose gradient with conditions equivalent to nuclear extract except for the presence of cycloheximide. Immunoprecipitation of FKBP25 from cytoplasmic extract was performed as above with buffer compensated to wash buffer conditions. Extracts were overlaid on 10-50% sucrose gradients made up in immunoprecipitation wash buffer without detergent.

For nuclear extracts, sucrose density gradient ultracentrifugation was performed as previously described [223]. Cell pellets were resuspended in 1 mL buffer A (16.7 mM Tris pH 8, 50 mM NaCl, 1.67 mM $MgCl_2$, 0.1% Triton X-100, 1 μg/mL leupeptin, 1 μg/mL aprotinin and 1 μg/mL pepstatin), vortexed 10 seconds and incubated on ice for 5 minutes. Extracts were centrifuged at 1000g for 5 minutes. The pellet was washed once more in buffer A as above. To extract the nuclear material, the pellet was sonicated 3 x 20 seconds in 0.5 mL sonication buffer containing 25 mM Tris pH 8, 100 mM KCl, 2 mM EDTA, 1 mM DTT, 0.05% IGEPAL, 1 μg/mL leupeptin, 1 μg/mL aprotinin and 1 μg/mL pepstatin and 10 units RNase inhibitor. Nuclear material was overlaid on 10-30% sucrose gradients containing 25 mM Tris pH 8, 100 mM KCl, 2 mM EDTA and 1 mM DTT. Gradients were centrifuged at 36,000 rpm for 3 hours at 4^{o}C using a Beckman L8-70M ultracentrifuge and SW41Ti rotor. Immunoprecipitated FLAG-FKBP25 complexes were prepared as above and overlaid on a 10-30% sucrose gradient with buffer conditions

the same as IP buffer minus detergents. Following centrifugation, sucrose gradients were fractioned into 0.5 mL volumes. Absorbance at 260 nm was measured by Nano-Drop spectrophotometry for each fraction and graphed in Excel. Half of each fraction was used to analyze protein and RNA. Proteins from each fraction was precipitated by the addition of 1/4th volume of 100% trichloroacetic acid (TCA) and incubated at 4^{o}C for 10 minutes. Precipitated proteins were pelleted at 15,000g for 5 minutes and pellets were washed two times with cold acetone. Proteins were subjected to SDS-PAGE and transferred to nitrocellulose membranes as described above. RNA was extracted from each fraction with TRIzol (Life Technologies) as per standard protocols. RNA was visualized by a 1% denaturing agarose-formaldehyde gel electrophoresis and stained with ethidium bromide.

Northern blot.

Cells were transfected with siRNA or FKBP25-FLAG vectors as described above. Cells were harvested 72 hours after transfection. Cells were treated for 6 hours with 100 nM rapamycin or ethanol control prior to harvesting. Total RNA was extracted with TRIzol. Northern blot analysis (adapted from Perkin Elmer protocols) was performed by separation on a 1% agarose-formaldehyde gel, run at 200V for 1.5hrs, and transferred overnight by capillary transfer to a Nylon membrane (Whatman, Inc. 10416230). The blot was rinsed in 2X SSPE and UV-crosslinked (auto crosslink setting, 254nm, Stratgene, Stratalinker). Membranes were pre-hybridized for 4-6hrs at 42^{o}C in prehybridization solution [5x SSPE, 50% deionized formamide, 5x Denhardt's Solution, 1% SDS, 10% dextran sulfate, and 100ug/ml sheared salmon sperm DNA]. Oligonucleotides were end-labeled with gamma ^{32}P (Perkin Elmer) and T4 polynucleotide kinase (NEB M0201) for 1 hour at 37°C and heat inactivated. Membranes were then incubated overnight with labeled probe. The blots were washed twice with 2x SSPE, 0.1% SDS for 10 minutes at room temperature, and then with 0.2XSSPE, 0.1% SDS until background signal was minimal. Blots were then exposed to a phosphor screen (Molecular Dynamics) and imaged using a Phosphorimager (STORM, GE Healthcare).

Chapter 4. Insight into FKBP25 as a ribosomal chaperone promoting RNA-protein interactions.

Contributions to this work: Experimentation (design and figures) was carried out by GG with the following exceptions: Meredith Jenkins and John Burke performed HDX experiments and analyzed data represented in Figure 26. Andrew Boyce collected immunofluorescence images in Figures 29 and 30.

4.1 Introduction.

Recruitment of structural ribosomal proteins and transient assembly factors is essential for the maturation of pre-ribosomes. In the previous chapter, I identified FKBP25 as a pre-ribosome associated factor, interacting with RNA-engaged nucleolin on the pre-60S subunit. Since FKBP25 has already been shown to promote YY1-DNA binding, a function for FKBP25 in ribosome biogenesis may occur through the regulation of protein-nucleic acid interactions. A number of PPIs have been demonstrated to promote or inhibit protein-nucleic acid interactions. For example, Cyp40 inhibits DNA binding of the transcription factor c-Myb *in vitro*, and this inhibition can be alleviated with CsA [224]. Additionally, both CypA and CypB are involved in hepatitis C viral replication, promoting RNA binding of NS5A and NS5B, respectively [40,225]. Similar to Cyp40, the action of CypA and CypB can be blocked by CsA. While there is evidence that a change in nucleic acid binding in these examples occurs through prolyl isomerization, demonstration of conformational changes to protein structure have yet to be shown and the regulatory mechanisms are unknown. The action of FKBP25 on YY1-DNA is distinct from the cyclophilins on the above-mentioned DNA binding proteins: its prolyl isomerase activity is not required to promote DNA binding. Instead, the N-terminal BTHB promotes this effect. In light of these examples, and the data presented in the previous Chapter, I hypothesize FKBP25 regulates protein-RNA interactions, but not rRNA processing in the assembly of the 60S ribosome.

Here, I demonstrate FKBP25 promotes nucleolin-RNA binding *in vitro*, independent of prolyl isomerase activity. My data supports a mechanism whereby

FKBP25 does not alter nucleolin structure, but likely involves an FKBP25-RNA interaction aiding RNA binding to nucleolin.

4.2 Results and Discussion.

4.2.1 FKBP25 promotes nucleolin RRM1-2-RNA interaction in vitro.

FKBP25 is known to regulate the protein-DNA interaction between YY1 and a 19 bp dsDNA *in vitro* [82]. To determine whether FKBP25 may also chaperone RNA binding events, I chose to examine its impact on nucleolin-RNA binding. The FKBP25-nucleolin interaction occurs after the A_2 cleavage event separating the 18S and 28S branches, therefore sourcing RNA in the ITS2 or 28S that nucleolin binds represents the ideal substrate to assay the effect of FKBP25. As described in the Introduction, nucleolin binds two motifs in the 5'ETS (ECM and NRE), however nucleolin's interaction surfaces throughout the 47S rRNA transcript have yet to be mapped. In the absence of an ITS2/28S sequence, I chose the well-defined NRE stem-loop RNA (referred to NRE hereafter) as the nucleolin substrate. The rationale for this substrate is as follows. First, nucleolin binds this RNA with high affinity and the structure of RRM1-2 bound to this RNA has been solved by NMR (Figure 23) [146-148]. Second, since FKBP25 interacts with RRM1-2, I reasoned that nucleolin-NRE complex provided a reasonable system to test if FKBP25 impacts RNA binding. Notably, the Cyp40-c-Myb, CypA-NS5A, CypB-NS5B and FKBP25-YY1 interactions all occur in the nucleic acid binding regions of the substrate proteins.

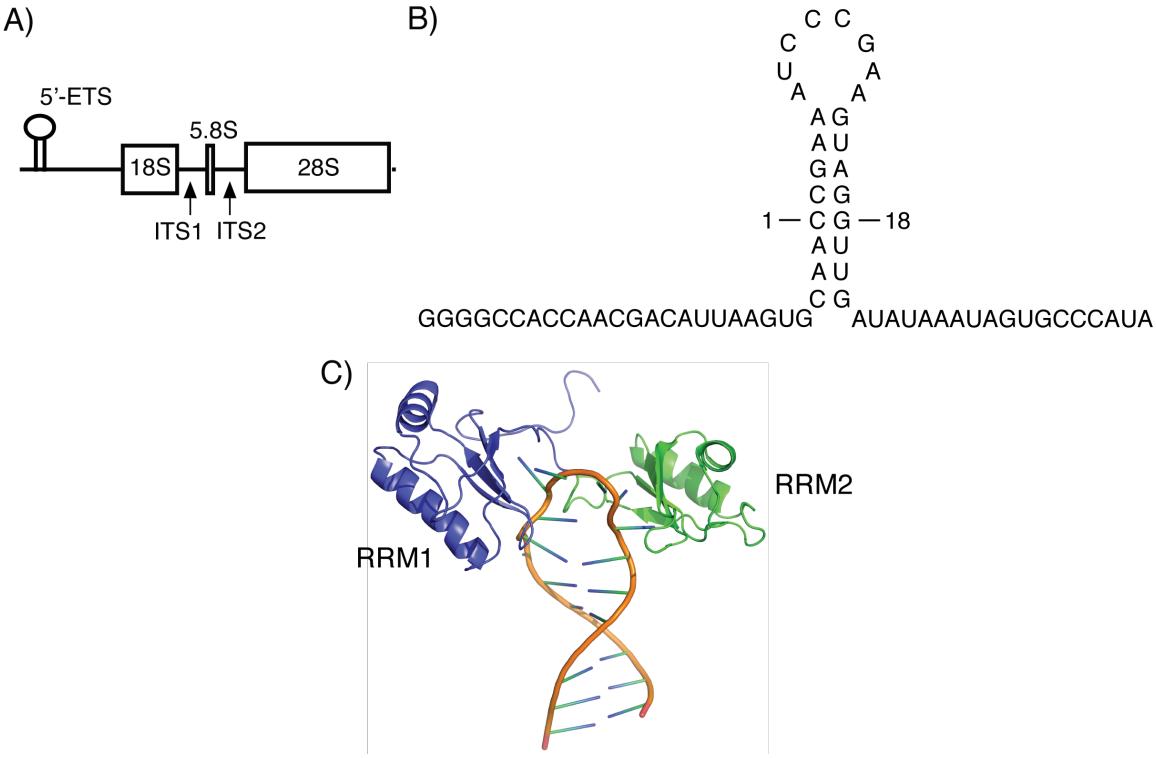

Figure 23. The NRE stem-loop is located in the 5'ETS and interacts with nucleolin RRM1-2.
A) The UCCCGA loop sequence corresponds to nt 159-164 of the human 47S rDNA transcript. B) RNA secondary structure of the NRE stem-loop used for nucleolin-RNA binding assays. Sequence noted from 1-18 represents the minimal sequence to bind nucleolin RRM1-2 determined by SELEX. C) Solution NMR structure of nucleolin RRM1-2 bound to the NRE RNA (PDB: 1RKJ). Structure rendered in PyMOL.

I first sought to recapitulate the high affinity nucleolin-NRE complex. Gel shift experiments titrating nucleolin RRM1-2 protein with ^{32}P-labeled NRE confirmed a strong interaction, whereas FKBP25 did not bind the RNA at the same protein concentrations (Figure 24a). To determine the effect of FKBP25 on nucleolin-NRE complex formation, I pre-incubated full-length FKBP25 with RRM1-2 prior to the addition of RNA. I found FKBP25 promoted nucleolin-NRE binding, increasing in a concentration dependent manner with FKBP25 (Figure 24b, left). Additionally, I performed experiments where FKBP25 was added after nucleolin-NRE incubation, which produced the same result (Data not shown).

Next, I asked if FKBP25 prolyl isomerase activity is involved in this effect, using an FKBP mutant from Chapter 2. I found that FKBP25 promoted nucleolin-RNA

interaction independent of the FKBP domain and its prolyl isomerase activity because the catalytically inactive F145A mutant, which I showed is unfolded *in vitro* (Chapter 2 Figure 11) promoted binding to a similar level as the wildtype (Figure 24b, right). Also, FKBP25 1-107 (which only contains the BTHB-Linker regions) enhanced nucleolin NRE binding better than the full length (Figure 24c). These data show that the BTHB-Linker of FKBP25 is necessary and sufficient to promote nucleolin-NRE interaction.

Surprisingly, I did not observe the formation of a super-shifted ternary complex containing FKBP25, RRM1-2 and the NRE in these assays. While this appears to contradict my previous result showing RNA is required to mediate an interaction between FKBP25 and nucleolin by immunoprecipitation and GST-pulldown, there are reasons for this discrepancy. First, the conditions in the EMSA may not be suitable to maintain complex formation and FKBP25 may dissociate when resolving the complex by electrophoresis. In this regard, it is noteworthy that FKBP25 does not form a trimeric complex with YY1 and DNA by gel shift assay, despite interacting with DNA, as well as YY1 in pulldown assays [82,83]. Therefore, in this case the ternary complex is likely disrupted during electrophoresis. Secondly, it is possible that the RNA does not confer the correct RRM1-2 structure/orientation to mediate FKBP25 binding that I observed in pulldown assays. In principle, this point could be addressed by using other nucleolin interacting RNAs to determine whether the lack of complex formation is due to the conditions or unknown structural features. Unfortunately this experiment is not yet feasible due to the lack of characterized nucleolin-RNA interactions.

Nucleolin is a highly abundant RNA binding protein, but its RNA interactome is only superficially understood. Nucleolin binds a number of mRNAs and ncRNAs, however they are often low affinity interactions and the minimal nucleolin domain requirements are not reported [118,226,227]. I have attempted to assay FKBP25's effect on nucleolin with different RNA substrates *in vitro*, however the interactions were non-specific, and any binding was of low affinity (Data not shown). Assaying nucleolin-RNA binding with an ITS2/28S RNA may yield different results, as alternative sequences may require different nucleolin domain features. Ultimately, different modes of nucleolin-RNA binding may be a mechanism by which FKBP25 confers specificity of nucleolin for specific RNA interaction motifs. Therefore, determining whether FKBP25 affects

nucleolin's binding of additional RNA substrates is limited by the lack of well-described nucleolin-RNA interactions.

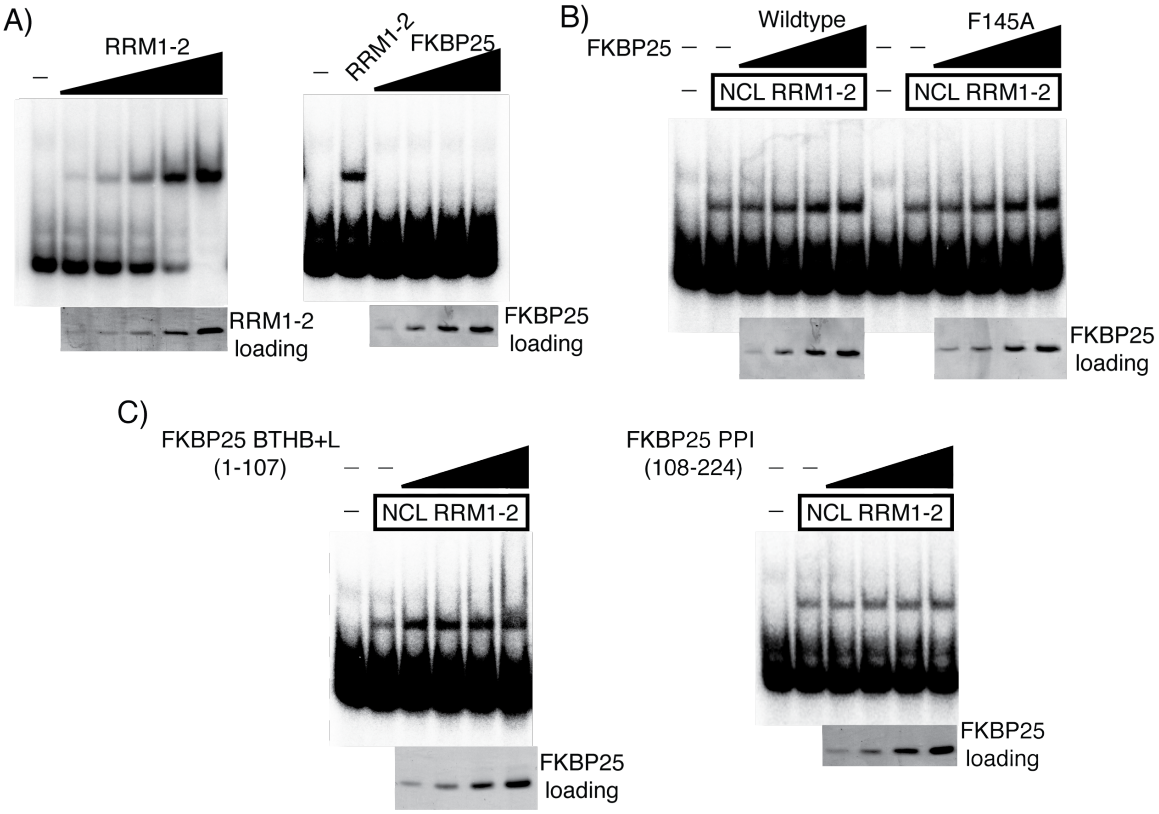

Figure 24. FKBP25's BTHB and linker promote nucleolin-RNA interaction in vitro. A) Gel shift experiments of nucleolin RRM1-2 and FKBP25. 25 (only RRM1-2), 50, 100, 200, 400 nM of proteins were used. The same RNA concentrations were used for both experiments. Increased exposure for FKBP25 titration was used to demonstrate no FKBP25-NRE binding. For the FKBP25 titration, 25 nM RRM1-2 was used as a control. B) Gel shift experiments assaying the effect of wildtype and F145A FKBP25 on RRM1-2-RNA complex formation. 25 nM RRM1-2 and 50-400 nM FKBP25 were used in each reaction with constant RNA concentration. C) Gel shift experiment assaying FKBP25 BTHB+Linker (aa 1-107) and PPI (aa 108-224) on RRM1-2-RNA binding. Proteins and RNA concentrations were the same as in B. All experiments were repeated with at least one different protein prep.

4.2.2 FKBP25 does not promote nucleolin-NRE binding through stabilizing nucleolin.

The data presented above, combined with FKBP25's effect on YY1-DNA binding suggests FKBP25 is a chaperone of protein-nucleic acid interactions. The effect of FKBP25 on nucleolin-RNA and YY1-DNA are strikingly similar: *in vitro*, FKBP25

interacts with both nucleolin and YY1 in pulldown assays and the BTHB augments protein-nucleic acid binding in both of these cases. While the mechanism of FKBP25 on YY1-DNA binding is unknown, two models have been proposed: 1. FKBP25 and YY1 interact forming a binary complex with increased affinity of YY1 for DNA or 2. FKBP25 and YY1 interact with DNA independently, which can then form a complex. Both models can be applied to FKBP25 and nucleolin, however the first model would be favoured as evidence for FKBP25 interacting with RNA is lacking from my experiments.

To determine if FKBP25 promotes a conformation of nucleolin that binds RNA, we utilized hydrogen-deuterium exchange mass spectrometry (HDX) in collaboration with John Burke's lab to probe for FKBP25-induced changes in nucleolin conformation. We reasoned any protection or conformational change caused by FKBP25 might impact nucleolin-RNA affinity. For this experiment, we used the same constructs and reagents as in the EMSAs. We incubated RRM1-2 and the NRE with a 5-fold excess of FKBP25 1-107 and measured deuterium incorporation of RRM1-2 at four time points. From this, we identified a single peptide in RRM1 of nucleolin that had decreased deuterium incorporation with the addition of FKBP25 (Figure 25). Although, the exchange on this peptide was small, results were reproducible. The peptide resides on the apical surface of RRM1 in an unstructured linker proximal to the RNA binding surfaces (Figure 26a). The location of this peptide coincides with my observations by EMSA, specifically that FKBP25 does not disrupt nucleolin-RNA binding. Therefore as this apical peptide is proximal to the RNA binding surface, stabilization of this region may poise the RRMs to bind the NRE.

I hypothesized that FKBP25 transiently interacts with the RRM1 apical peptide, stabilizing an RRM1-2 conformation that favours RNA binding and that mutagenizing charged residues in this surface would disrupt the FKBP25 interaction, rendering this nucleolin mutant immune to FKBP25 regulation.

A)

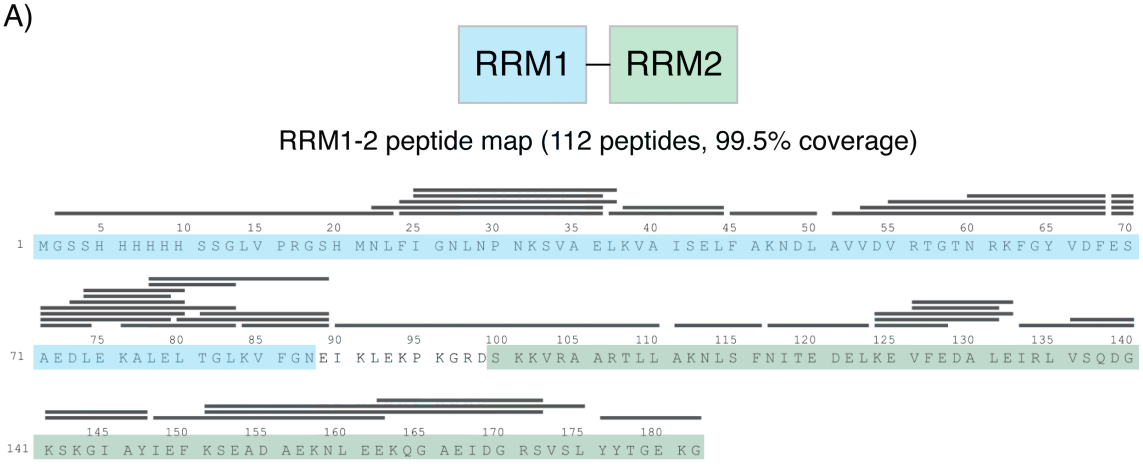

B)

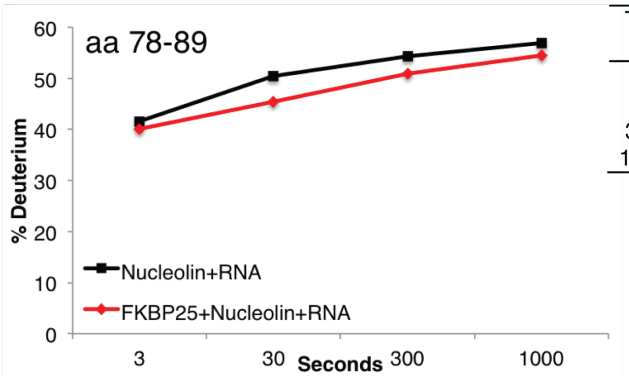

C)

Time	% Deuterium (- FKBP25)	% Deuterium (+ FKBP25)	% Difference
3s	41.6	40.1	1.5
30s	50.5	45.5	5
300s	54.3	51	3.3
1000s	57	54.5	2.5

Figure 25. Nucleolin RRM1 has reduced deuterium incorporation in the presence of FKBP25.
A) Peptide map of nucleolin RRM1-2. Black bars represent pepsin digested peptides over sequence coloured to RRM1 (blue) and RRM2 (green). B) HDX curve of RRM1 aa 78-89 for nucleolin-RNA complex with or without FKBP25. C) Percent change of deuterium incorporation at the various time points in B.

To test the above hypothesis I created mutations in the putative interaction site near the 78-89 peptide at the apical surface of RRM1. The unstructured peptide and surrounding sequence contains 7 charged residues extending from the surface. I expected that neutralizing the surface charge in this region would render nucleolin insensitive to FKBP25 by excluding FKBP25 from the surface and preventing augmented RNA binding to RRM1-2. Three RRM1 mutants that neutralize charged residues within the peptide and surrounding environment were used to assay FKBP25's effect when this apical region is altered (Figure 26a, b). I performed gel shift experiments with the wildtype and mutant RRM1-2 proteins to test their sensitivity to FKBP25 and found that

contrary to my hypothesis, FKBP25 maintains the ability to promote RNA binding of each nucleolin apical surface mutant (Figure 26c).

Together, this data suggests that any potential stabilization of nucleolin by FKBP25 is unlikely to be dependent on these residues. As the RRM1 peptide we identified was the only region that had a significant change in deuterium incorporation, I can rule out FKBP25 acting elsewhere in the RRM1-2 structure. As these binding assays are performed in a purified system, variables are kept to a minimum. The remaining possible mechanism of FKBP25 promoting nucleolin-RNA association is through FKBP25 targeting the RNA. Since I have never observed an FKBP25-RNA complex in dozens of NRE EMSAS, this interaction is either transient, or too weak to survive EMSA conditions. Alternatively, due to the conditions of these experiments and the high protein concentration, it is possible the gel shift assays are not sensitive enough to distinguish between subtle differences in RRM1-2-NRE binding upon mutation.

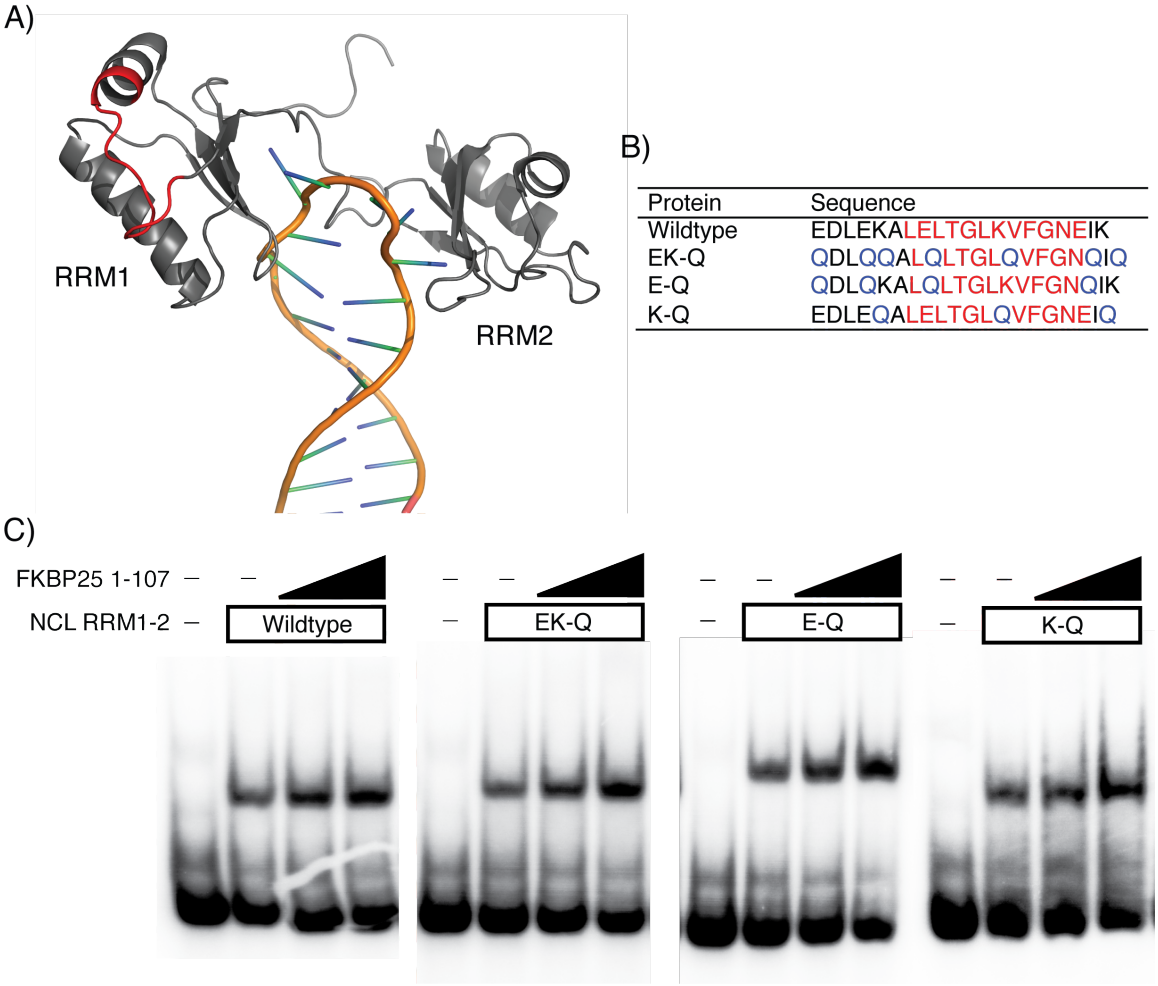

Figure 26. RRM1 mutants remain sensitive to FKBP25.
A) Structure of nucleolin RRM1-2 (PDB: 1RKJ) with peptide identified by HDX (aa 78-89) highlighted in red. Image rendered in PyMOL. B) Amino acid sequence surrounding aa 78-89, displaying charge neutralization mutants (blue) in the protein sequence. C) Gel shift experiments assaying FKBP25 action on wildtype and mutant nucleolin RRM1-2. Nucleolin wildtype and mutant proteins were normalized for protein loading prior to use. FKBP25 BTHB (1-107) lanes correspond to a two or four fold excess compared to RRM1-2.

While my data does not suggest FKBP25 is an RNA binding protein, there is recent evidence to the contrary. FKBP25 has recently been identified in a mass spectrometry screen cataloguing mRNA binding proteins [228]. Interestingly, the peptides identified in the screen were in the extreme N-terminus and linker region, however it is unclear at this point whether a significant portion of FKBP25 is bound to mRNA at any given time. Further, Cameron Mackereth's lab has also recently used NMR

to demonstrate FKBP25 binds RNA *in vitro*. FKBP25's BTHB binds with high affinity to dsRNA, whereas ssRNA and DNA bind at much lower affinity (C. Mackereth, personal communication). The regions responsible for binding identified by the Mackereth group lie in the central region of the BTHB (K22/K23, K48/K52) and do not correlate with the regions identified by the Hentze group. This discrepancy may be due to differences between ssRNA vs. dsRNA binding. In light of this, it is possible FKBP25 interacts with the double-stranded stem portion of the NRE and aids its placement with RRM1-2. However, as both Yang et al. and I did not observe interactions with FKBP25 and DNA or RNA, respectively, the EMSA conditions likely disrupted these interactions [82]. Utilizing mutagenesis in the RNA binding regions of FKBP25 could provide insight into whether this ability to promote nucleolin-RNA binding is through an interaction with the NRE. These experiments represent a future avenue to explore.

4.2.3 The addition of a FLAG epitope tag impairs nucleolin interactions.

I next asked whether FKBP25 alters nucleolin-rRNA interactions *in vivo*. Prior to performing these experiments, I sought to identify a suitable source of nucleolin protein to assay: endogenous or exogenous (FLAG-tagged). The use of exogenous nucleolin for these experiments was attractive: the epitope tag offers a simple and established method to purify nucleolin, I could generate stably expressing clones with ease and I could use the specific domain combinations used in my *in vitro* assays (ie. RRM1-2).

As the domain requirements for nucleolin to interact with pre-ribosomal subunits had not been addressed, I first sought to identify whether the RRMs and RGG exhibit a redundancy in their rRNA interactions. To carry this out, I constructed HEK293 cells stably expressing FLAG-tagged nucleolin domains and performed RNA immunoprecipitations to gauge the interactions with the ribosomal subunits (Figure 27a, b). As expected, I found the acidic domain of nucleolin does not enrich rRNA. Moreover, RRM1-2, RRM1-4-RGG and full-length interact with both the small and large subunits (based on 18S and 28S rRNAs) at approximately the same ratios. The ribosomal interactions with full-length nucleolin are consistent with my observations from sucrose gradient ultracentrifugation as there is no preference for the small or large subunit. Surprisingly, I found that RRM3-4 strongly favoured the large subunit (28S rRNA),

whereas RRM34-RGG and RRM1-4 favoured the small subunit (18S), but still enriched the 28S. This demonstrates that the domains of nucleolin are not redundant RNA binding domains and they each contribute differently to nucleolin's association with pre-ribosomes.

Since RNA immunoprecipitations do not measure direct RNA interactions, I then assayed RNA binding in a purified system. As full-length nucleolin could not be expressed recombinantly, I performed RIPs as above, and varied the protocol to strip the protein and RNA content interacting with nucleolin using stringent wash conditions and RNase T1 treatment. This resulted in a loss of interacting proteins (Figure 27c) and loss of rRNA signal as assayed by EtBr (Data not shown). I then used purified nucleolin protein to capture RNAs from purified total RNA. Interestingly, the eluted RNAs did not follow the same pattern as observed from the RIPs in panel B. I detected a weak interaction with RRM1-2 and the 28S, and no 18S rRNA (Figure 27d). Thus, RRM1-2 directly interacts with the 28S RNA and its interaction with the small subunit likely occurs through protein interactions. RRM3-4, RRM34-RGG and RRM1-4 exhibit similar interactions as observed in panel A, suggesting their ribosomal interactions are largely mediated by direct contacts with rRNA. Additionally, full-length nucleolin also has a slight preference for the 18S over the 28S. Despite FKBP25's enrichment with the large subunit in RIPs (Figure 27b), FKBP25 does not interact with either the 18S or 28S further confirming its association with the 60S requires additional contacts (Figure 27d), and that in this assay FKBP25 cannot stably bind to RNA.

These data suggest the RRMs and RGG of nucleolin are non-redundant RNA binding domains. Combinations of the domains confer specificity for RNA features in the 18S or 28S rRNAs, and this for the most part correlates with their ribosomal subunit interactions. However, RRM1-2 was an exception: it co-purifies with both the small and large subunit rRNAs, yet only the 28S rRNA is detected in a purified pulldown system that measures direct RRM-rRNA interactions. This data is consistent with my GST-pulldown experiments where GST-RRM1-2 interacts with the 28S rRNA in the absence of other proteins (Figure 18g). Together, this supports RRM1-2 as a potentially suitable source of nucleolin to assay the action of FKBP25 in cells.

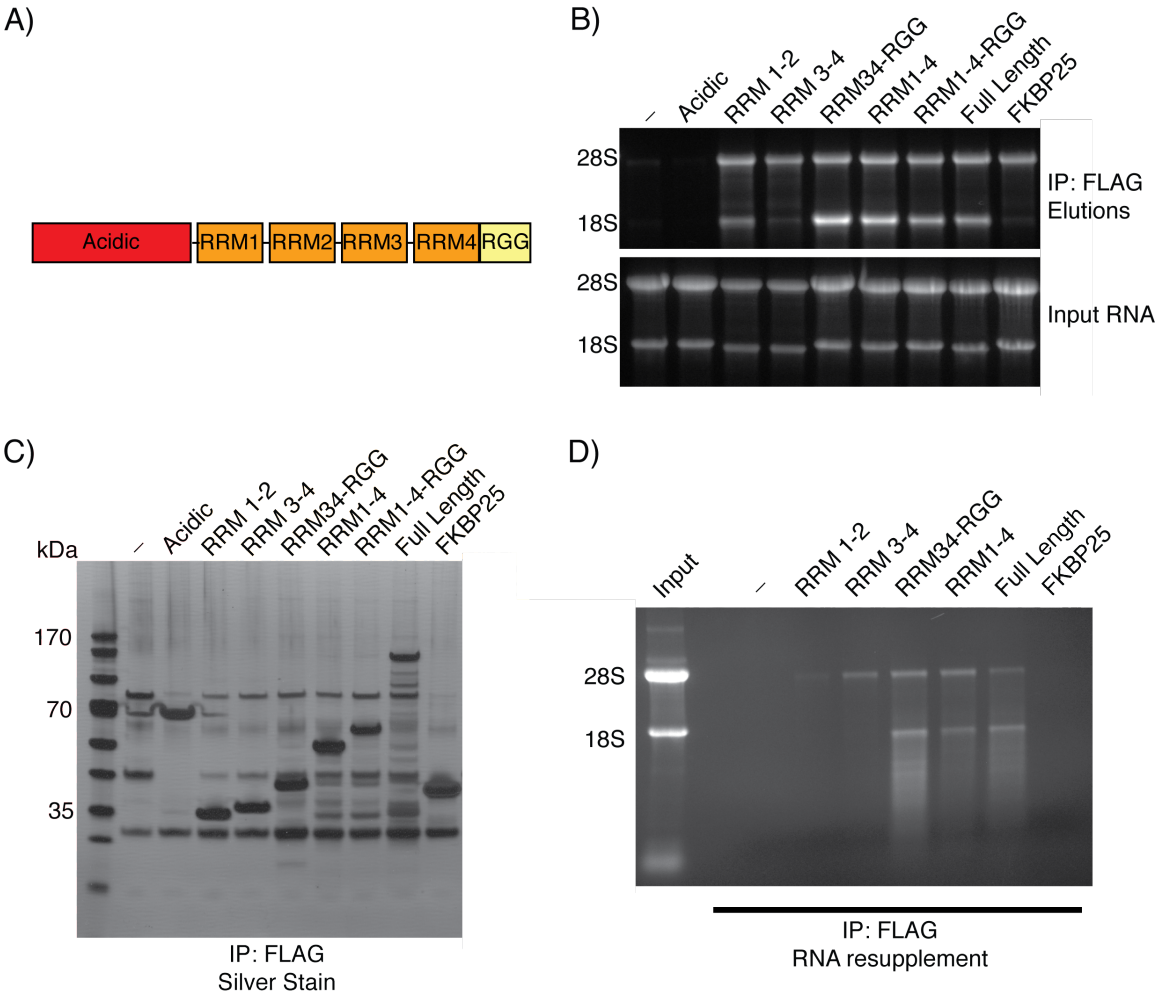

Figure 27. Nucleolin's RRMs and RGG are non-redundant RNA interaction domains.
A) Domain architecture of nucleolin. B) RNA immunoprecipitations of FLAG-nucleolin domain constructs and FKBP25. Proteins were immunoprecipitated and interacting RNA was extracted with Trizol. RNAs were resolved by formaldehyde-agarose gel electrophoresis. C) Silver stained SDS-PAGE of immunoprecipitated FLAG-nucleolin proteins treated with RNase T1 and extensively washed. D) RNA resupplementation experiments performed by first immunoprecipitating protein. Interacting protein and RNA was stripped by incubation with RNase T1. Purified nucleolin protein was used to capture RNAs from purified total RNA and extracted RNAs were separated by agarose gel. The identity of the RNA smears below the 18S in the RRM3-4RGG and full-length lanes are unknown.

I next sought to verify if full-length FLAG-nucleolin localized to the nucleolus, by performing immunofluorescence with the endogenous and tagged protein. As

expected, the endogenous nucleolin was abundant in the nucleolus, forming discrete foci (Figure 28a). FLAG-nucleolin, however, was evenly stained throughout the nucleus and nucleolar foci were not observed (Figure 28b). This difference could be explained by the over-expression of FLAG-nucleolin and an increased nuclear signal masking nucleolar foci.

To ensure the FLAG-nucleolin is forming stable nuclear interactions, I employed a cytoskeleton (CSK) stripping protocol. Under this treatment, a mild detergent wash prior to fixation is utilized to strip cytoplasmic and nucleosolic proteins that are not stably interacting with DNA or RNA. Consistent with other reports, endogenous nucleolin maintains nucleolar localization with CSK treatment [229]. FLAG-nucleolin however yields a complete loss of signal, suggesting the epitope tag affects nucleolin's interactions and potentially its functions (Figure 28c). This result is surprising given the fact the endogenous antibody is raised against the N-terminal acidic region of nucleolin (aa 1-100) and the FLAG tag is on the N-terminus as well. As the acidic domain of nucleolin is not a major protein/nucleic acid interaction surface as demonstrated above (Figure 27), it was expected that the addition of a FLAG tag would not largely impair its interactions or function, which is not the case from these data.

While there are a number of studies utilizing epitope tagged nucleolin, they have been used to identify or confirm protein interactions. The majority of studies assess nucleolin function by siRNA depletion, and the handful of studies over-expressing nucleolin accomplish this with untagged constructs. These results demonstrate that caution is required when assessing nucleolin functions using an exogenous tagged protein. Additionally, the application of CSK treatment may provide a general method to identify whether the addition of epitope tags affects the localization, interactions or function of nuclear proteins associated with DNA/RNA.

To determine if individual domains of nucleolin could be assayed for pre-ribosome binding in cells, I performed immunofluorescence experiments with and without CSK treatment for FLAG-tagged nucleolin RRM1-2. FLAG-RRM1-2 signal in the nucleolus is lost with CSK treatment (Figure 29a). This construct, much like the full-length protein does not represent an appropriate means to assay nucleolin's nucleolar

functions, such as pre-ribosome assembly *in vivo*. Furthermore, I performed the same experiments to compare the localization of endogenous and FLAG-tagged FKBP25. The addition of a FLAG-tag does not affect FKBP25: the cellular distribution is the same with no treatment or CSK (Figure 29b). This confirms that the addition of a FLAG-tag is not detrimental to all proteins.

Interestingly results from immunofluorescence experiments did not coincide with the nucleolin RNA immunoprecipitations above (Figure 27). Specifically, FLAG-nucleolin co-purifies pre-ribosomes by immunoprecipitation, whereas the same construct does not maintain stable nucleolar localization with CSK treatment. One possible explanation is the amount of FLAG-nucleolin in the nucleolus is far less than the endogenous protein. Therefore, the epitope tag may affect nucleolin's concentration and incorporation into rDNA chromatin and the maturing ribosomal subunits in the nucleolus. Additionally, since FLAG-nucleolin is nuclear localized, the interactions observed by immunoprecipitation may be a result of the high amount of nuclear nucleolin protein being exposed to the nucleolar content and interacting with rRNAs. Therefore, nuclear lysis may have created an artificial environment where FLAG-nucleolin is exposed to the pre-ribosomal subunits, yielding an interaction. Regardless, because these FLAG-nucleolin constructs do not behave as the endogenous protein, they cannot be used to assay if FKBP25 impacts rRNA interactions of nucleolin for my experiments.

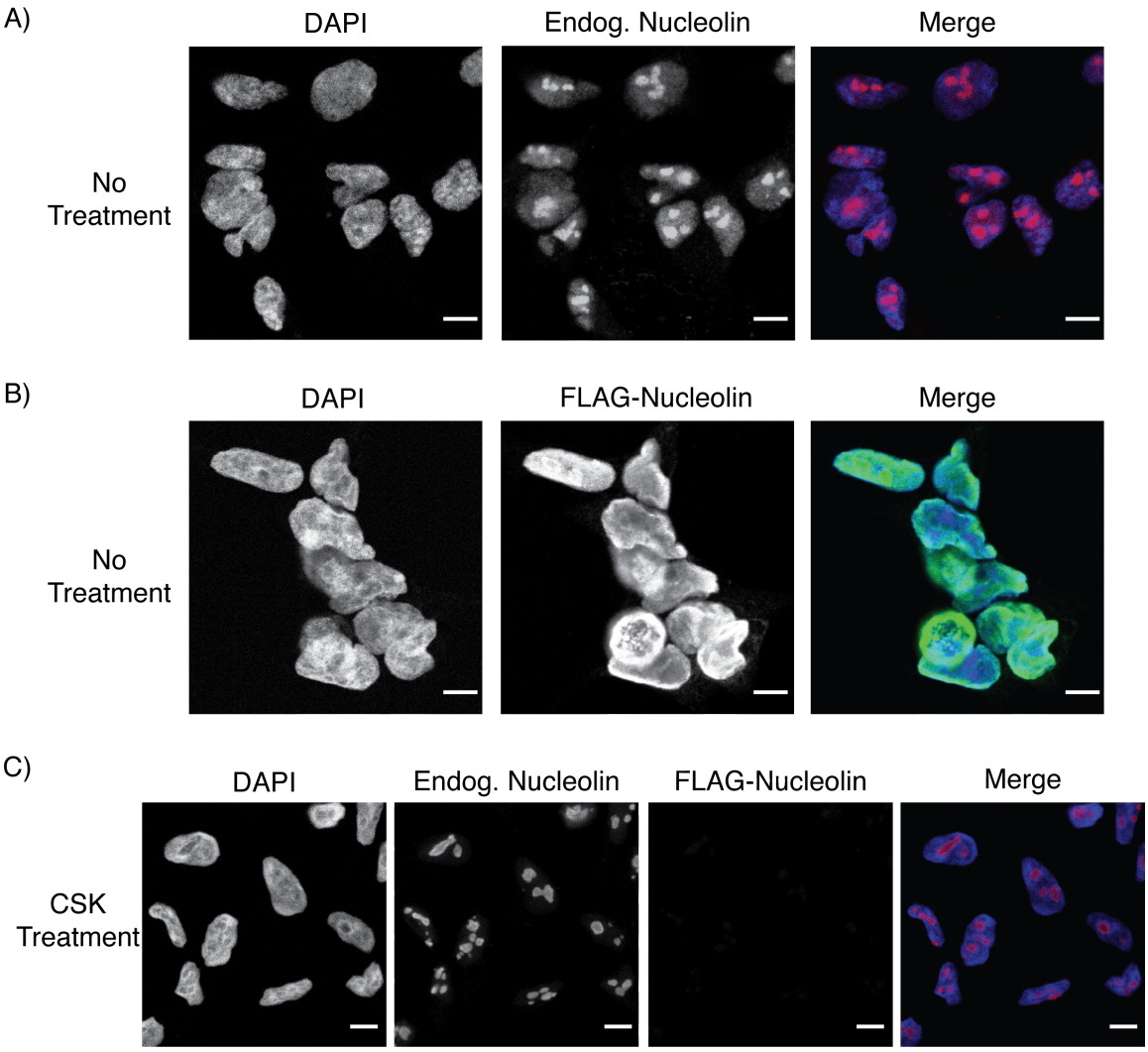

Figure 28. Comparison of endogenous and FLAG-tagged nucleolin localization. HEK293 cells expressing FLAG-nucleolin were fixed with paraformaldehyde and probed for endogenous nucleolin (A) or FLAG-nucleolin (B) and imaged by on a Leica SP8 confocal microscope. C) HEK293 cells expressing FLAG-nucleolin were treated with CSK buffer prior to fixation. Immunofluorescence was measured using endogenous nucleolin antibody or FLAG antibody. Bars – 10 μM.

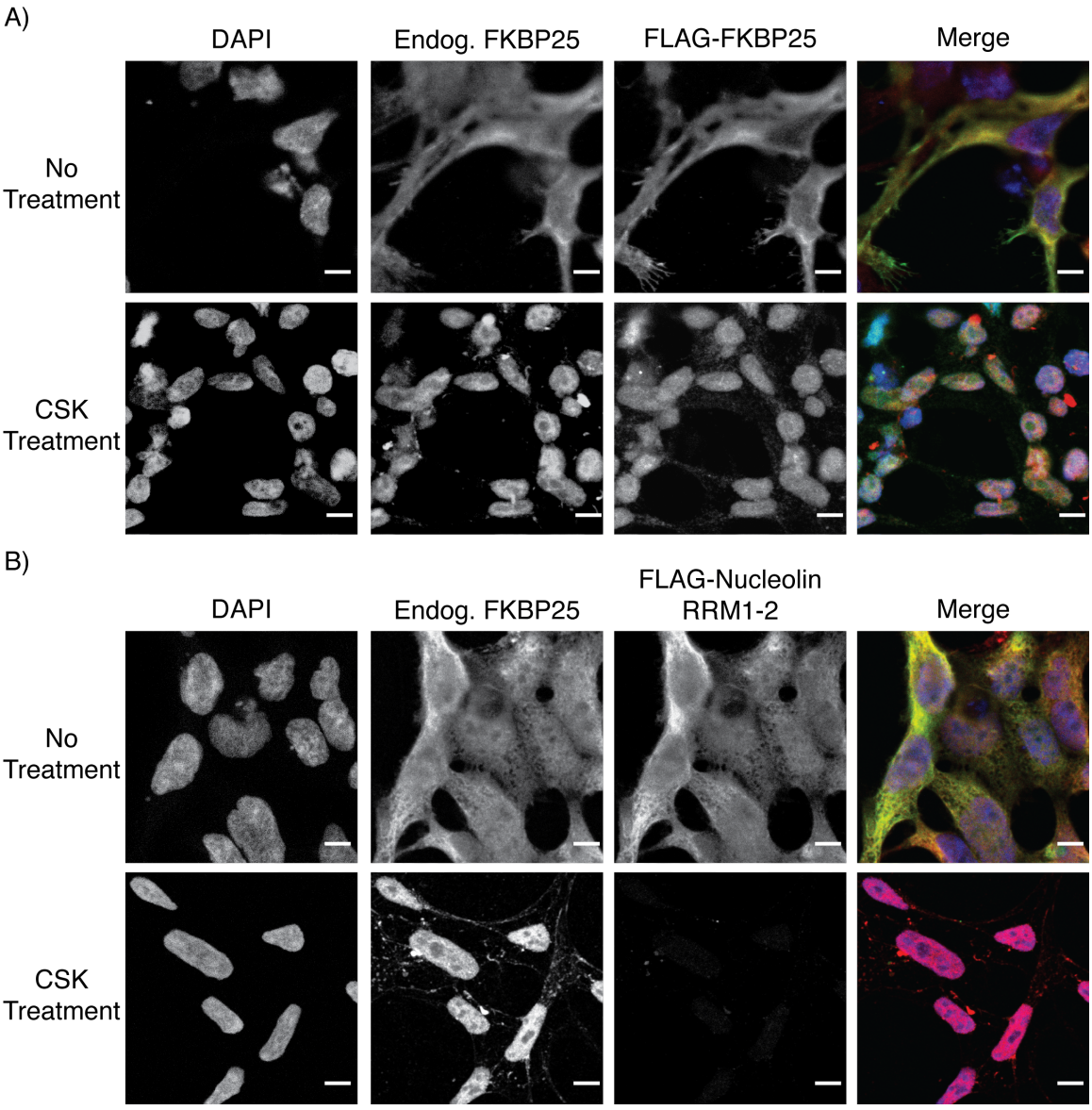

Figure 29. FKBP25 maintains nuclear localization with CSK treatment while nucleolin RRM1-2 signal is lost.
HEK293 cells expressing FLAG-FKBP25 (A) or FLAG-nucleolin RRM1-2 (B) were treated without (top) or with (bottom) CSK buffer prior to fixation. Cells were probed for endogenous FKBP25 and FLAG and imaged on a Leica SP8 confocal microscope. Bars – 10 μM.

4.2.4 FKBP25 does not alter nucleolin-rRNA interactions *in vivo*.

Since RNA immunoprecipitations with FLAG-nucleolin constructs were deemed an unsuitable means to determine if FKBP25 alters nucleolin-RNA binding in cells, I was forced to assay endogenous full-length nucleolin's rRNA association. Using cells

depleted of FKBP25 by shRNA, or over-expressing FLAG-FKBP25, I performed RNA immunoprecipitations of endogenous nucleolin. Interacting RNAs were reverse transcribed and quantified by qPCR analysis.

I found the knockdown of FKBP25 does not alter nucleolin association with 18S or 28S rRNAs (Figure 30a). Additionally, over-expression of FKBP25 yields no change in nucleolin-rRNA interaction (Figure 30b). These results suggest that FKBP25 does not alter the interaction between nucleolin and its most abundant interacting RNAs.

Based on the data in the preceding Chapter, the FKBP25 shRNA knockdown result is not necessarily a surprise. By sucrose density ultracentrifugation I demonstrated nucleolin to be an abundant component of pre-40S and pre-60S subunits in the nucleus (Figure 21). However, based on FKBP25-60S co-immunoprecipitation, I conclude that FKBP25 is a much less common component of pre-60S ribosomes. In other words, the number of nucleolin-pre-60S molecules in the cell is far greater than the number of FKBP25-nucleolin-pre-60S complexes.

Additionally, over-expression of FKBP25 is not adequate to promote or decrease nucleolin-RNA interactions. This may be due to the fact nucleolin engages rRNA in multiple places [142,148], and FKBP25's interaction with nucleolin only occurs on a small proportion of pre-60S molecules.

Because of this, FKBP25 altering nucleolin-RNA interactions cannot be completed ruled out; it may only affect a small proportion of nucleolin in the nucleus. The inability to enrich FKBP25 with a high proportion of pre-60S subunits limits our ability to study its function in this regard. Therefore, a more guided approach, focusing on the exact location of FKBP25 binding on the pre-60S subunit must be taken to understand the role of FKBP25 in ribosome assembly. This will be discussed in more detail in the following discussion chapter.

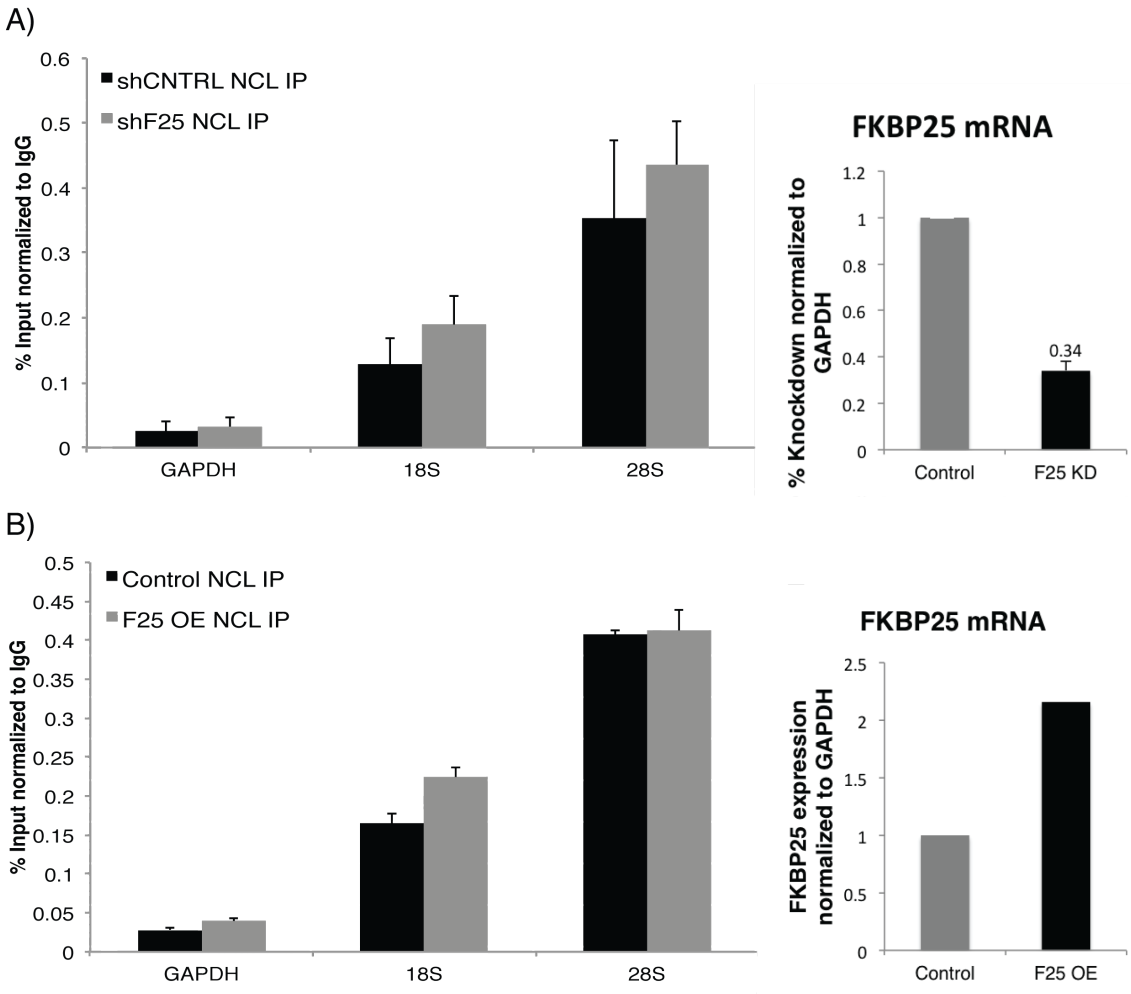

Figure 30. Depletion or over-expression of FKBP25 does not affect nucleolin-rRNA interaction.
RNA immunoprecipitations were performed from U2OS cells depleted of FKBP25 by shRNA (A) or over-expressing (OE) FKBP25-FLAG (B). Extracted RNA was reverse transcribed and subjected to qPCR. GAPDH serves as a negative control. FKBP25 mRNA levels for each experiment (right) were measured to confirm knockdown or over-expression.

4.3 Methods.

Cell lines and transfections.
HEK293 Flp-In T-Rex cells (Life Technologies) and U2OS cells were maintained in DMEM containing 10% BGS (HEK293) or FBS (U2OS) and Pen/Strep at 37^{o}C in 5% CO_2. For stable cells, nucleolin constructs were cloned into pcDNA5/FRT/TO and generated as per manufacturers recommendations. For transfections, HEK293 cells were transfected overnight using Lipofectamine 3000 (Life Technologies) in 24 well dishes as per manufacturers recommendations with pcDNA5/FRT/TO 3×-FLAG FKBP25 vector

constructs. Cells were split in the morning and incubated for 24 hours. For generation of U2OS cells, FKBP25 shRNA vectors (Origene) or FKBP25 cloned in pICE-HA-NLS-I-PpoI (Addgene) were transfected with Lipofectamine 2000. Clones were selected with puromycin and screened for knockdown/over-expression.

EMSA.

Nucleolin and FKBP25 proteins were expressed and purified as described previously. pET15b nucleolin RRM1-4 was a gift from P. Bouvet. A stop codon was added by site directed mutagenesis to create the RRM1-2 construct. pET15b RRM1-2 mutants were synthesized by BioBasic. RNA was prepared by *in vitro* T7 transcription using pSP72 355 NRE (A gift from P. Bouvet) as per manufacturers recommendations (Promega). RNA was purified by ethanol precipitation and resuspended in water prior to use. For gel retardation assays, proteins were pre-incubated for 30 minutes at room temperature in TMKC buffer (20 mM Tris-HCl, pH 7.4, 4 mM MgCl2, 200 mM KCl, 20% glycerol, 1 mM DTT, 0.5 mg/ml tRNA, 4 μg/ml BSA). RNA was added and incubated for a further 30 minutes. The mixture was loaded directly onto an 8% native polyacrylamide gel containing 5% glycerol in 0.5X TBE and electrophoresed at 150V at room temperature. Gels were dried and exposed to a Phosphorscreen (Molecular Dynamics) overnight and imaged with a Molecular Dynamics Storm 820 scanner.

RNA immunoprecipitation.

Nuclear extracts were prepared as described previously from U2OS controls or cells depleted of FKBP25 by shRNA or over-expressing FLAG-FKBP25. Extracts were normalized for protein by Bradford assay. Immunoprecipitation buffers and conditions were used as previously described. For each reaction, 2 μg antibody (IgG or anti-nucleolin (Abcam ab22758) was incubated for 1 hour with extracts prior to the addition of Protein A/G agarose beads (Pierce) and further incubation for 1 hour. Beads were washed five times and RNA was extracted with TRIzol reagent. cDNA was prepared by RT-PCR and qPCR was performed as described previously.

For RNA resupplement experiments, FLAG-nucleolin proteins were bound to beads and treated with RNase T1 for 1 hour at room temperature. Proteins were then extensively washed (5 times) with high salt IP buffer (500 mM NaCl). RNase T1 was inhibited with a

mixture of 2+ cations (Ca, Mg, Mn, Zn, Cu) added for 2 of the washes (1 mM final). Purified total RNA was then added, incubated for 1 hour, and washed 3 times with IP buffer. Interacting RNAs were extracted with Trizol and separated by formaldehyde-agarose gel electrophoresis.

Immunofluorescence.
Slides were pre-treated with poly-L-lysine for at least one hour, extensively washed and dried prior to use. Cells were seeded at approximately 50% density and incubated 24 hours. Cells were washed once with PBS (with 0.5 mM $MgCl_2$, 0.5 mM $CaCl_2$), followed by a wash with CSK buffer (100mM NaCl, 300mM sucrose, 3mM $MgCl_2$, 10mM PIPES pH 6.8). For CSK stripping, cells were incubated 2 minutes in CSK buffer with 1% Triton X100, followed by a wash with PBS. Cells were fixed with 4% paraformaldehyde for 10 minutes, washed once with PBS, permeabilized with PBS + 0.25% Triton X100 and washed three times with PBS. Cells were blocked in buffer containing 5% BSA, 0.1% Triton X100 in PBS for 30 minutes. Cells were incubated with primary antibody (Anti-FKBP25-C (epitope 201-224), anti-nucleolin, anti-FLAG-M2, anti-UBF (Santa Cruz sc13125) in blocking buffer for at least one hour or overnight. Cells were washed three times (5 minutes) with blocking buffer and incubated for 1-2 hours with secondary antibody (anti-rabbit, anti-mouse). Cells were washed three times and mounted with DAPI counterstain (Sigma). Imaging was performed using a Leica SP8 confocal microscope. Images were prepared using a combination of ImageJ and Adobe Photoshop CS5 software and adjusted for uniform brightness/contrast.

Hydrogen deuterium exchange mass spectrometry.
HDX experiments were conducted with 15pmol of Nucleolin RRM1-2 and 30pmol of NRE RNA, with or without a 5x molar excess of FKBP25 1-107. Proteins and RNA were expressed and purified as described above. Reactions were initiated by the addition of 44 µL of D2O Buffer Solution (10 mM HEPES pH 7.5, 50 mM NaCl, 97% D2O) to 6 µL of protein solution, to give a final concentration of 85% D2O. Exchange was carried out for 4 timepoints, (3s, 30s, 300s and 1000s at 23 °C). Exchange was terminated by the addition of an acidic quench buffer giving a final concentration 0.6 M guanidine-HCl, 0.8% formic acid. The project was carried out in triplicate. Samples were immediately

frozen in liquid nitrogen and stored at −80°C until mass analysis. Protein samples were rapidly thawed and injected onto a UPLC system kept in a cold box at 2°C. The protein was run over two immobilized pepsin columns (Applied Biosystems; porosyme, 2-3131-00) stored at 10°C and 2°C at 200 μL/min for 3 min and the peptides were collected onto a VanGuard precolumn trap (Waters). The trap was subsequently eluted in line with an Acquity 1.7 μm particle, 100 × 1 mm2 C18 UPLC column (Waters), using a gradient of 5-36% B (buffer A 0.1% formic acid, buffer B 100% acetonitrile) over 16 minutes. Mass spectrometry experiments were performed on an Impact II TOF (Bruker) acquiring over a mass range from 350 to 1500 m/z using an electrospray ionization source operated at a temperature of 200°C, and a spray voltage of 4.5 kV. Peptide identification was done by running tandem MS/MS experiments run in data dependent acquisition mode with a 0.5 s precursor scan from 200-2000 m/z, followed by 12 fragment scans from 150 to 2000 m/z of 0.25 s. The resulting MS/MS datasets were analyzed using PEAKS7 (PEAKS), and a false discovery rate was set at 1% using a database of known contaminants.

HD-Examiner Software (Sierra Analytics) was used to automatically calculate the level of deuterium incorporation into each peptide. All peptides were manually inspected for correct charge state and presence of overlapping peptides. Deuteration levels were calculated using the centroid of the experimental isotope clusters. Results for these proteins are presented as relative levels of deuterium incorporation and the only control for back exchange was the level of deuterium present in the buffer (85%). The real level of deuteration will be ~25–35% higher than shown, based on tests performed with fully deuterated standard peptides. The average error of all time points and conditions for each HDX project was less than 0.1Da.

Chapter 5: Discussion and Future Directions

5.1 Summary of research objectives.

Peptidyl-prolyl isomerases modulate protein structure and function. While PPIs are ubiquitous in prokaryotes and eukaryotes, the proline substrates for most of these enzymes are poorly resolved. Consequently there is a limited understanding of which biological processes employ these enzymes, and even less information on underlying mechanisms. In this thesis, I have biochemically characterized a nuclear FKBP prolyl isomerase, FKBP25. The data in the preceding three chapters provide significant advancement in the understanding of where this enzyme operates, which is a logical step towards novel therapeutic strategies targeting FKBP25 function.

In Chapter 2, I developed a necessary toolset of FKBP25 point mutants to dissect its catalytic and non-catalytic functions. These proteins represent the first FKBP catalytic point mutants to be structurally characterized. I uncovered a shortfall of using mutagenesis as an approach to study catalytic functions; where certain mutations can impact domain stability. While it appears we are not the first to observe this effect, we are surely the first to comment on the need for structural characterization when utilizing mutagenesis to study prolyl isomerases. The mutants presented provide the means to potentially distinguish between the catalytic and non-catalytic functions of FKBP25, which will serve as useful reagents for ongoing and future studies. I used these mutants later in my thesis research to decipher whether FKBP25's catalytic activity is required to promote nucleolin-RNA binding in Chapter 4. Additionally, these mutants have been used for David Dilworth's thesis work on FKBP25 and we now routinely rely on these two types of mutants in other FKBPs, such as yeast Fpr4.

The foundation of my thesis work was directed by a mass spectrometry screen to define FKBP25's protein-interactome. I predicted these experiments would guide this project towards chromatin and transcriptional regulation, and indeed a significant number of interacting proteins fall into this ontology. Additionally, I uncovered a novel association between FKBP25 and the maturing large ribosomal subunit in the nucleus. I

provided insight into the context of FKBP25 and nucleolin's interaction, which requires rRNA and occurs on the pre-60S ribosomal subunit. Moreover, I demonstrated FKBP25 is able to promote nucleolin-RNA binding *in vitro*, suggesting a potential role in ribosome assembly.

The picture of where and how FKBP25 functions is starting to become clearer (Figure 31). FKBP25 is recruited in close proximity to chromatin, where it augments YY1-DNA binding and may isomerize histone prolines. Additionally, through my work, we now know FKBP25 is a nucleolar protein and associates with nucleolin on the immature large subunit. My data suggests FKBP25 acts to stabilize nucleolin's interaction with the pre-60S subunit. Therefore, FKBP25 may function as a chaperone, regulating protein-RNA interactions, and aiding the recruitment or displacement of ribosomal proteins and transient processing factors to ensure proper structure/orientation of the pre-60S subunit.

While the work presented here sheds light on where FKBP25 is most likely to carry out prolyl isomerization events, there are clearly a number of outstanding questions. In this Chapter I discuss the future directions and avenues to explore to fully understand the implications of FKBP25 in the nuclear compartment.

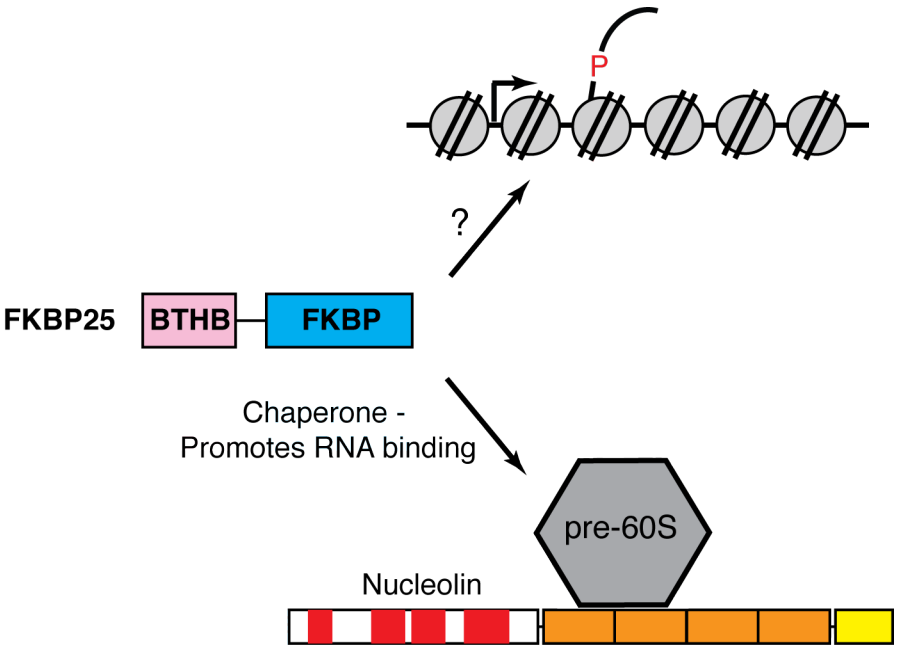

Figure 31. Model of FKBP25's nuclear function.

In this dissertation, I took an unbiased proteomics approach to identify the proteins interacting with FKBP25. This confirmed FKBP25 as a chromatin associated protein, however the direction of my research did not take this path. Questions remain as to whether FKBP25 regulates the chromatin landscape and its substrate(s) for prolyl isomerization. My research instead focused on FKBP25 in ribosome biogenesis. I identified an interaction between FKBP25 and nucleolin on the pre-60S ribosomal subunit in the nucleus, and suggest FKBP25 acts as a chaperone to promote RNA-protein binding.

5.2 FKBP25 and ribosome biogenesis.

Understanding the functions of FKBP25 in ribosome biogenesis has proven a significant challenge due to its low abundance within pre-ribosomes. I have been unable to detect a discernable difference in rRNA processing or ribosome assembly with standard methods used in the field. Whether this is due to an effect being masked by the sheer number of non-FKBP25 associated pre-ribosomes, or FKBP25's role occurs by alternative means requires further exploration. Alternatively, FKBP25 could be complemented by another FKBP, however this is unlikely, as no other human FKBP has been identified as pre-ribosome associated. Regardless, understanding where FKBP25 localizes on the pre-60S subunit is imperative to identifying its potential functions. As pre-ribosomal subunits are large complexes consist of rRNA, structural proteins and trans-acting factors, it is expected the bulk of the FKBP25 interacting proteins I identified are not direct interactions. Instead, there is likely just a small handful of closely associated proteins, therefore identifying the specific ribosomal surface(s) to which FKBP25 is recruited can provide insight into its potential substrates. For this, two complementary methods would define these protein or RNA surfaces: cross-linking mass spectrometry and proximity labeling, which I will describe below.

Crosslinking mass spectrometry provides probably the best approach to identify FKBP25's pre-60S interaction surface. This method utilizes chemical crosslinkers to covalently bridge interacting proteins, which are then digested and analyzed for crosslinked peptides by mass spectrometry. Crosslinking can be performed on purified complexes, thus FKBP25-60S complexes can be isolated by my established immunoprecipitation conditions (Chapter 3 Figure 15). These methods have been used to determine the architecture of the RNA polymerase II-TFIIF complex [230], thus it is amendable to large protein complexes such as pre-ribosomes. This technique can

therefore reveal FKBP25's direct protein-protein interactions, and would undoubtedly identify interactions with structural ribosomal proteins and/or closely associated ribosomal assembly and processing factors.

Proximity-dependent biotin identification (BioID) would serve as a complementary *in vivo* approach to crosslinking mass spectrometry [231]. This technique utilizes a promiscuous biotin ligase (BirA) fusion to the query protein (FKBP25) to biotinylate interacting and closely associated proteins. Labeled proteins can then be enriched with streptavidin and identified through mass spectrometry. The use of BirA alone as a control contributes to the exclusion of non-specific background labeling. Additionally, the use of N- and C-terminal BirA fusions can help resolve which end of the protein is proximal to a substrate protein.

BioID has several advantages over other interactome discovery methods, such as immunoprecipitation followed by mass spectrometry used in Chapter 3. First, BioID is performed in a native environment, which can reveal both stable and transient interactions in a complex cellular mixture. Therefore, the picture of the proteomic landscape surrounding the query protein provides insight into potential functions. Secondly, BioID is suitable for studying dynamic processes or events, as biotin is covalently attached and remains after processes are complete and interactions have ceased. Finally, labeled proteins can be purified under stringent wash conditions keeping background to a minimum with no sample loss. While BioID would provide insight into proteins proximal to FKBP25, combining this method with crosslinking-MS would serve to validate the results of each other.

Our lab has initiated these experiments. Francy Pesek-Jardim has performed preliminary experiments to identify FKBP25 interacting proteins with BioID. While this data represents only a single replicate, the top ontological hits relate to the ribosome and the majority of enriched ribosomal proteins are from the large subunit (Data not shown). This also serves as validation of my FKBP25 interactome dataset confirming FKBP25's association with the large subunit. Because of the enriched RPLs covering much of the 60S surface, assigning where FKBP25 localizes is difficult. Whether this is because FKBP25 interacts at multiple surfaces or the labeling needs optimization remains to be determined. This will be resolved with additional replicates, optimized conditions and

labeling times and the use of both N- and C-terminal BirA fusions. Nevertheless, this data reveals BioID is a feasible technique to identify FKBP25's ribosomal occupancy.

Interestingly, the second ranked hit in our FKBP25 BioID screen was the helicase DDX27. Depletion of DDX27 by siRNA results in RNA polymerase I read-through of the 3'ETS termination site in the 47S rRNA transcript [232]. Kellner et al. demonstrated this by northern blot, where they showed no detectable difference for normal 47S transcripts, however probes for the 3'ETS after the termination site yielded signal only in the DDX27 knockdown [232]. If FKBP25 and DDX27 cooperate in 3'ETS end formation, we may have narrowly missed detecting this, as our probes were for normal 47S transcripts. These experiments are in progress.

To identify the rRNA sequences of the pre-60S subunit that are proximal to FKBP25, an approach called TRIBE (Targets of RNA-binding proteins Identified By Editing), has recently been developed, which is effectively BioID for proximal RNA [233]. In place of a biotin-ligase, an RNA-modifying enzyme fusion marks nearby RNA by deaminating adenosine to inosine. Instead of using mass spectrometry to identify proximal proteins, high-throughput sequencing reveals proximal RNA sequences. Inosine is recognized as guanosine in sequencing, thus A→G mutations designate proximal RNA. As there is an exposed RNA content of ribosomes, TRIBE would provide additional information to identify interaction surfaces for FKBP25.

Together, the combination of BioID and TRIBE will provide much needed resolution to describe where FKBP25 localizes on the pre-60S complex. Additionally, these methods will also be informative for non-ribosomal interactions as well, such as proximal to chromatin. Both of these techniques are available to us with resources at UVic.

Cryo-EM has recently been used to study the role of assembly factors in the yeast pre-60S ribosome [116]. This structure has provided mechanistic details of three remodelling events of the pre-60S subunit prior to cytoplasmic export. Applying this same approach to FKBP25 may yield insight into the surface to which it is recruited and potential functions in ribosome maturation. This structural technique is advantageous, as it does not require high protein concentrations to determine structures, unlike NMR and

X-ray crystallography. Therefore, FKBP25-60S complexes could be enriched by immunoprecipitation. As the structure of FKBP25 has been solved, this could be used to dock FKBP25 on the pre-60S ribosome. Additionally, the use of wildtype and catalytic mutants of FKBP25 could also provide insight into dependency of its isomerase activity. Once we know where FKBP25 is localized, we can begin designing experiments to understand how it functions in pre-60S assembly.

5.3 FKBP25 and gene regulation.

FKBP25 was originally identified as a chromatin-associated prolyl isomerase [82]. This dissertation only addressed the chromatin aspect of FKBP25 peripherally; my data confirms the initial reports that FKBP25 is a nuclear enzyme [78,81], especially as the mass spectrometry screens in Chapter 3 identified novel FKBP25-associated chromatin factors.

David Dilworth has performed both ChIP-seq and RNA-seq experiments to identify regions of the genome occupied by FKBP25 and whether gene expression is altered upon depletion of FKBP25. Only subtle changes in global gene expression are observed with depletion of FKBP25 (data not shown) and in ChIP-seq, David could not detect FKBP25 enriched at specific genes or chromosomal loci. Given that some FKBP25 does fractionate with chromatin biochemically, the lack of ChIP-seq peaks could mean one of two things: First, that FKBP25 binds DNA in a non-specific manner. Alternatively, FKBP25 could interact with repetitive sequences that are challenging to align in reference genomes. Given nucleolar DNA sequences (ie. rDNA) are of this class, this is currently being pursued by the Nelson lab. Thus while several groups have published data implying FKBP25 is engaged with chromatin, precisely where remains unclear.

5.4 Chromatin, nucleolin and G-quadruplexes

There is a growing body of evidence that the *cis-trans* proline state in the histone H3 tail is important for gene regulation. In yeast, conformation at H3 P38 is important for methylation of K36 by Set2 [8]. Additionally, the acetylation of H3 K14 influences the isomeric state of H3 P16 [234]. While it has been demonstrated Fpr4 isomerizes H3 P38,

influencing the induction of transcription, H3 P16 is likely influenced by steric constraints rather than by a prolyl isomerase enzyme. These examples of histone prolyl isomerization both come from studies in yeast, and to date there is no evidence of *cis-trans* proline state in histones having a similar regulatory role in humans. However, that is not to say that histone prolyl isomerization is not important in humans. Importantly, I have demonstrated that FKBP25 exhibits isomerase activity towards histone H3 prolines *in vitro*. Additionally, Cyp33 also is active towards H3 P16 and P30 [44]. Studying histone prolyl isomerization is more amendable to yeast as there are only two genetic copies of each histone, thus mutating prolines comes with relative ease [235]. Humans, however, have 20 H3 genes comprised of replication dependent and independent variants [236], therefore mutagenizing H3 prolines in humans would be a formidable task. Instead, the use of isomer specific antibodies reactive against human histones proline states may shed light on the importance for gene expression.

As described in the Introduction, nucleolin is chromatin associated and regulates gene expression dependent on G-quadruplex binding. As we have demonstrated through ChIP of FKBP25 and nucleolin, they exhibit similar occupancy on rDNA. Thus, I have explored whether FKBP25's action is restricted to nucleolin-RNA binding or if it can also promote nucleolin-G-quadruplex binding.

My attempts to answer this have come with limited success due to inconsistencies between G-quadruplex preparations, yielding a variety of differently folded structures (Appendix Figure 33). Other groups have reported similar observations. Miller et al. used a combination of size exclusion chromatography and analytical ultracentrifugation to demonstrate ten commonly used G-quadruplex sequences form a variety of polymorphic structures [237]. A subsequent case study of the c-Myc G-quadruplex revealed at least 7 different structures, and the ratio of each species changed with the folding conditions [238]. Additionally, common techniques to study folded structures (ie. Circular dichroism spectroscopy, gel electrophoresis) are of too low resolution to resolve the variations. This represents a current limitation in studying G-quadruplexes *in vitro*, as the details of sample preparation and structural characterization are often not reported.

Despite these limitations, I have assayed the impact of FKBP25 on nucleolin-G-quadruplex binding with a variety of sequences. These correspond to the c-Myc

promoter, 5'ETS of rDNA (ETS-1) and a telomeric sequence (OX-1). Indeed I confirmed nucleolin interacts with these quadruplexes by gel shift assay (Appendix Figure 33b, c). Interestingly, I observed a slower migrating species upon the addition of FKBP25 to the nucleolin-c-Myc complex. Additionally, with the ETS-1 and OX-1 quadruplexes, I observed the opposite trend, where FKBP25 induced a faster migrating nucleolin-G-quadruplex species (Appendix Figure 33c). These effects are also distinct from the nucleolin-NRE results where I have only observed differences in binding and not changes in migration. While these results are encouraging and suggest a role for FKBP25 altering nucleolin-G-quadruplex structure, I have been unable to repeat these results with different G-quadruplex preparations. Ultimately, these experiments are limited by the *in vitro* folding of these structures and until uniform, repeatable preparations can be obtained, identifying whether FKBP25 affects nucleolin structure cannot be conclusively determined.

5.5 Identifying proline substrates of FKBP25.

Because of the non-covalent nature of *cis-trans* prolyl isomerization, demonstrating catalytic function is the crux of prolyl isomerase research. As such, the identification of novel proline substrates for these enzymes and implicating them in biological processes is a difficult feat to accomplish. Further complicating this are functions for PPIs that occur independent of catalytic activity [68,70,172].

Despite being originally identified over 25 years ago, FKBP25's catalytic functions have yet to be described. The reports on this enzyme have been few and far between, and during my thesis project, few manuscripts describing functions of FKBP25 were published. Thus, a major question left unanswered is: what are the substrates of FKBP25's isomerase activity?

The work presented in this dissertation took the direction of identifying substrates from a list of interacting proteins. This yielded over 100 associated proteins, where it is expected that the majority represent indirect interactions. Indeed, BioID with FKBP25 gives a smaller subset of ribosomal factors. As many PPIs interact with their substrates (ie. Fpr4 binds H3, FKBP12 binds h-Ras [8,169]), I inferred a strong interaction between FKBP25 and nucleolin suggested the possibility of it as a substrate. I demonstrated this

interaction is direct, however FKBP25 promoted nucleolin-RNA binding independent of catalytic activity.

In my opinion to pinpoint potential substrates a higher priority line of future investigation is to determine proteins proximal to the FKBP25's PPI domain using BioID. The BTHB of FKBP25 is the major protein interaction surface and the low interaction content of the PPI domain may be a result of transient or weak interactions. As described above, proximity labeling with BioID can help to resolve this and as protocols are optimized, novel insight into the placement or interactions of FKBP25's catalytic domain may reveal new avenues to explore. Utilizing N- and C-terminal BirA fusions for FKBP25 could provide insight for proteins proximal to the BTHB (ie. Protein interactions) and the PPI domain (ie. Potential substrates). Indeed, there are examples in the literature where N- and C-terminal BirA fusions provide resolution to the interactions mediated by opposite ends of the protein [239,240].

5.6 Utility of FKBP25 catalytic mutants.

As potential substrates for FKBP25 are identified, the toolset of mutants I have characterized in this dissertation will be of great use to determine catalytic mechanisms and serve as important reagents for rescue experiments. Importantly, these mutants will provide insight into the function of the PPI domain after recruitment. As described previously, recruitment can be mediated by: an accessory domain (ie. Pin1's WW domain binding pS/T-P motifs, placing PPI domain in proximity to substrates), through interactions of the PPI domain (ie. FKBP12 binding RyR) or prolyl isomerization by the PPI domain to create a binding surface (ie. Cyp33 isomerizing MLL1) [9,65,162]. The FKBP25 catalytic mutants can separate these mechanisms of recruitment and function. If catalytic activity is required to confer a phenotype by any of the three above mechanisms, the Y135/198F mutants should not rescue the effect. If however the Y-F mutants do rescue the phenotype, implementing the unfolded F145A mutant would identify whether non-catalytic features of the PPI domain are required.

As we now have a better understanding of where FKBP25 functions, the next step is to identify a role for its catalytic activity in these processes. While I have demonstrated that FKBP25's interactome does not largely change when comparing wildtype and the

catalytic inactive mutants, subtle differences may occur. Subjecting immunoprecipitated material from wildtype and mutant samples to more sensitive stable isotope labeling with amino acids in cell culture (SILAC) mass spectrometry may reveal differences in protein interactions. Additionally, parallel experiments can be performed with treating purified FKBP25 complexes with FK506 or rapamycin, attempting to disrupt interactions near the catalytic pocket.

Additionally, the impact of catalytic site mutations to cyclophilins and parvulins has yet to be structurally characterized. Thus, it will be interesting to determine whether domain stability is affected in a similar manner to my observations here. Extending these FKBP tools to the other two families of prolyl isomerases may contribute to the study of these enzymes as well and shed light on their catalytic dependent and independent functions.

5.7 Therapeutic strategies of the FKBP inhibitors tacrolimus and sirolimus.

Tacrolimus (FK506) was first isolated in 1987 and was noted for its immunosuppressive properties [57]. The FDA subsequently approved tacrolimus in 1994 as a treatment to prevent rejection for liver transplantation patients. While tacrolimus is still in use today, its usage has extended beyond preventing transplant rejection. These include inflammatory diseases such as eczema and ulcerative colitis.

Much like tacrolimus, sirolimus (rapamycin) followed a similar path, first being approved by the FDA as a drug to prevent transplant rejection. Sirolimus' mechanistic properties inhibiting mTOR has directed therapeutic strategies separate from tacrolimus. Sirolimus has been shown to increase the lifespan of mice [241], and inhibit cellular proliferation in cancer cells [242]. Owing to the importance of tacrolimus and sirolimus, thousands of clinical studies involving these compounds have been completed or are currently underway (clinicaltrials.gov).

While tacrolimus and sirolimus do target FKBP12 and inhibit calcineurin and mTOR, respectively, we are currently blind to how these molecules impact the function of the other 17 human FKBPs. FKBP12 and FKBP25 have similar affinities for sirolimus (0.2 vs. 0.9 nM, respectively [80,180]) and clinical doses will inhibit both FKBPs.

Therefore, knowing the processes linked to FKBPs can help address the information gap and provide novel uses for these approved drugs.

My thesis work has provided a link between FKBP25 and nucleolar function: we can place FKBP25 at rDNA chromatin and with maturing ribosomal subunits. As ribosome biogenesis is misregulated in cancers [109,110], FKBP25 may be poised as a novel target in this process. Since rDNA is epigenetically regulated, pharmaceutical intervention could rewrite epigenetic markers and alter the chromatin landscape, decreasing rDNA transcriptional output. As the underlying mechanisms of how FKBP25 functions in ribosome biogenesis are determined, the opportunity for inhibition in combination with other therapies will be determined.

Bibliography

[1] Luger, K., Mader, A.W., Richmond, R.K., Sargent, D.F. and Richmond, T.J. (1997). Crystal structure of the nucleosome core particle at 2.8 A resolution. Nature 389, 251-60.

[2] Bannister, A.J. and Kouzarides, T. (2011). Regulation of chromatin by histone modifications. Cell Res 21, 381-95.

[3] Allahverdi, A., Yang, R., Korolev, N., Fan, Y., Davey, C.A., Liu, C.F. and Nordenskiold, L. (2011). The effects of histone H4 tail acetylations on cation-induced chromatin folding and self-association. Nucleic Acids Res 39, 1680-91.

[4] Tessarz, P. and Kouzarides, T. (2014). Histone core modifications regulating nucleosome structure and dynamics. Nat Rev Mol Cell Biol 15, 703-8.

[5] Smallwood, A., Esteve, P.O., Pradhan, S. and Carey, M. (2007). Functional cooperation between HP1 and DNMT1 mediates gene silencing. Genes Dev 21, 1169-78.

[6] Murzina, N., Verreault, A., Laue, E. and Stillman, B. (1999). Heterochromatin dynamics in mouse cells: interaction between chromatin assembly factor 1 and HP1 proteins. Mol Cell 4, 529-40.

[7] Park, I.Y. et al. (2016). Dual Chromatin and Cytoskeletal Remodeling by SETD2. Cell 166, 950-62.

[8] Nelson, C.J., Santos-Rosa, H. and Kouzarides, T. (2006). Proline isomerization of histone H3 regulates lysine methylation and gene expression. Cell 126, 905-16.

[9] Wang, Z., Song, J., Milne, T.A., Wang, G.G., Li, H., Allis, C.D. and Patel, D.J. (2010). Pro isomerization in MLL1 PHD3-bromo cassette connects H3K4me readout to CyP33 and HDAC-mediated repression. Cell 141, 1183-94.

[10] Wulf, G.M., Ryo, A., Wulf, G.G., Lee, S.W., Niu, T., Petkova, V. and Lu, K.P. (2001). Pin1 is overexpressed in breast cancer and cooperates with Ras signaling in increasing the transcriptional activity of c-Jun towards cyclin D1. EMBO J 20, 3459-72.

[11] Stewart, D.E., Sarkar, A. and Wampler, J.E. (1990). Occurrence and role of cis peptide bonds in protein structures. J Mol Biol 214, 253-60.

[12] Weiss, M.S., Jabs, A. and Hilgenfeld, R. (1998). Peptide bonds revisited. Nat Struct Biol 5, 676.

[13] Joseph, R.E., Ginder, N.D., Hoy, J.A., Nix, J.C., Fulton, D.B., Honzatko, R.B. and Andreotti, A.H. (2012). Structure of the interleukin-2 tyrosine kinase Src homology 2 domain; comparison between X-ray and NMR-derived structures. Acta Crystallogr Sect F Struct Biol Cryst Commun 68, 145-53.

[14] Maigret, B., Perahia, D. and Pullman, B. (1970). Molecular orbital calculations on the conformation of polypeptides and proteins. IV. The conformation of the prolyl and hydroxyprolyl residues. J Theor Biol 29, 275-91.

[15] Ramachandran, G.N. and Mitra, A.K. (1976). An explanation for the rare occurrence of cis peptide units in proteins and polypeptides. J Mol Biol 107, 85-92.

[16] Reimer, U., Scherer, G., Drewello, M., Kruber, S., Schutkowski, M. and Fischer, G. (1998). Side-chain effects on peptidyl-prolyl cis/trans isomerisation. J Mol Biol 279, 449-60.

[17] Grathwohl, C.W., K. (1981). NMR studies of the rates of proline cis-trans isomerization in oligopeptides. Biopolymers 20, 2623-2633.

[18] Brandts, J.F., Halvorson, H.R. and Brennan, M. (1975). Consideration of the Possibility that the slow step in protein denaturation reactions is due to cis-trans isomerism of proline residues. Biochemistry 14, 4953-63.

[19] Schmid, F.X. and Baldwin, R.L. (1978). Acid catalysis of the formation of the slow-folding species of RNase A: evidence that the reaction is proline isomerization. Proc Natl Acad Sci U S A 75, 4764-8.

[20] Kelley, R.F. and Stellwagen, E. (1984). Conformational transitions of thioredoxin in guanidine hydrochloride. Biochemistry 23, 5095-102.

[21] Kiefhaber, T., Quaas, R., Hahn, U. and Schmid, F.X. (1990). Folding of ribonuclease T1. 2. Kinetic models for the folding and unfolding reactions. Biochemistry 29, 3061-70.

[22] Fischer, G., Bang, H. and Mech, C. (1984). [Determination of enzymatic catalysis for the cis-trans-isomerization of peptide binding in proline-containing peptides]. Biomed Biochim Acta 43, 1101-11.

[23] Fischer, G. and Bang, H. (1985). The refolding of urea-denatured ribonuclease A is catalyzed by peptidyl-prolyl cis-trans isomerase. Biochim Biophys Acta 828, 39-42.

[24] Kofron, J.L., Kuzmic, P., Kishore, V., Colon-Bonilla, E. and Rich, D.H. (1991). Determination of kinetic constants for peptidyl prolyl cis-trans isomerases by an improved spectrophotometric assay. Biochemistry 30, 6127-34.

[25] Stoller, G., Rucknagel, K.P., Nierhaus, K.H., Schmid, F.X., Fischer, G. and Rahfeld, J.U. (1995). A ribosome-associated peptidyl-prolyl cis/trans isomerase identified as the trigger factor. EMBO J 14, 4939-48.

[26] Deuerling, E., Schulze-Specking, A., Tomoyasu, T., Mogk, A. and Bukau, B. (1999). Trigger factor and DnaK cooperate in folding of newly synthesized proteins. Nature 400, 693-6.

[27] Ferbitz, L., Maier, T., Patzelt, H., Bukau, B., Deuerling, E. and Ban, N. (2004). Trigger factor in complex with the ribosome forms a molecular cradle for nascent proteins. Nature 431, 590-6.

[28] Kang, C.B., Feng, L., Chia, J. and Yoon, H.S. (2005). Molecular characterization of FK-506 binding protein 38 and its potential regulatory role on the anti-apoptotic protein Bcl-2. Biochem Biophys Res Commun 337, 30-8.

[29] Pirkl, F. and Buchner, J. (2001). Functional analysis of the Hsp90-associated human peptidyl prolyl cis/trans isomerases FKBP51, FKBP52 and Cyp40. J Mol Biol 308, 795-806.

[30] Park, S.T., Aldape, R.A., Futer, O., DeCenzo, M.T. and Livingston, D.J. (1992). PPIase catalysis by human FK506-binding protein proceeds through a conformational twist mechanism. J Biol Chem 267, 3316-24.

[31] Fischer, S., Michnick, S. and Karplus, M. (1993). A mechanism for rotamase catalysis by the FK506 binding protein (FKBP). Biochemistry 32, 13830-7.

[32] Lu, K.P., Finn, G., Lee, T.H. and Nicholson, L.K. (2007). Prolyl cis-trans isomerization as a molecular timer. Nat Chem Biol 3, 619-29.

[33] Pemberton, T.J. and Kay, J.E. (2005). Identification and comparative analysis of the peptidyl-prolyl cis/trans isomerase repertoires of H. sapiens, D. melanogaster, C. elegans, S. cerevisiae and Sz. pombe. Comp Funct Genomics 6, 277-300.

[34] Borel, J.F., Feurer, C., Gubler, H.U. and Stahelin, H. (1994). Biological effects of cyclosporin A: a new antilymphocytic agent. 1976. Agents Actions 43, 179-86.

[35] Bunjes, D., Hardt, C., Rollinghoff, M. and Wagner, H. (1981). Cyclosporin A mediates immunosuppression of primary cytotoxic T cell responses by impairing the release of interleukin 1 and interleukin 2. Eur J Immunol 11, 657-61.

[36] Handschumacher, R.E., Harding, M.W., Rice, J., Drugge, R.J. and Speicher, D.W. (1984). Cyclophilin: a specific cytosolic binding protein for cyclosporin A. Science 226, 544-7.

[37] Liu, J., Farmer, J.D., Jr., Lane, W.S., Friedman, J., Weissman, I. and Schreiber, S.L. (1991). Calcineurin is a common target of cyclophilin-cyclosporin A and FKBP-FK506 complexes. Cell 66, 807-15.

[38] Clipstone, N.A. and Crabtree, G.R. (1992). Identification of calcineurin as a key signalling enzyme in T-lymphocyte activation. Nature 357, 695-7.

[39] Colgan, J. et al. (2004). Cyclophilin A regulates TCR signal strength in CD4+ T cells via a proline-directed conformational switch in Itk. Immunity 21, 189-201.

[40] Watashi, K., Ishii, N., Hijikata, M., Inoue, D., Murata, T., Miyanari, Y. and Shimotohno, K. (2005). Cyclophilin B is a functional regulator of hepatitis C virus RNA polymerase. Mol Cell 19, 111-22.

[41] Chatterji, U. et al. (2009). The isomerase active site of cyclophilin A is critical for hepatitis C virus replication. J Biol Chem 284, 16998-7005.

[42] Mesa, A., Somarelli, J.A. and Herrera, R.J. (2008). Spliceosomal immunophilins. FEBS Lett 582, 2345-51.

[43] Li, H., He, Z., Lu, G., Lee, S.C., Alonso, J., Ecker, J.R. and Luan, S. (2007). A WD40 domain cyclophilin interacts with histone H3 and functions in gene repression and organogenesis in Arabidopsis. Plant Cell 19, 2403-16.

[44] Park, S., Osmers, U., Raman, G., Schwantes, R.H., Diaz, M.O. and Bushweller, J.H. (2010). The PHD3 domain of MLL acts as a CYP33-regulated switch between MLL-mediated activation and repression. Biochemistry 49, 6576-86.

[45] Rahfeld, J.U., Rucknagel, K.P., Schelbert, B., Ludwig, B., Hacker, J., Mann, K. and Fischer, G. (1994). Confirmation of the existence of a third family among peptidyl-prolyl cis/trans isomerases. Amino acid sequence and recombinant production of parvulin. FEBS Lett 352, 180-4.

[46] Yaffe, M.B. et al. (1997). Sequence-specific and phosphorylation-dependent proline isomerization: a potential mitotic regulatory mechanism. Science 278, 1957-60.

[47] Uchida, T., Fujimori, F., Tradler, T., Fischer, G. and Rahfeld, J.U. (1999). Identification and characterization of a 14 kDa human protein as a novel parvulin-like peptidyl prolyl cis/trans isomerase. FEBS Lett 446, 278-82.

[48] Lu, K.P., Hanes, S.D. and Hunter, T. (1996). A human peptidyl-prolyl isomerase essential for regulation of mitosis. Nature 380, 544-7.

[49] You, H., Zheng, H., Murray, S.A., Yu, Q., Uchida, T., Fan, D. and Xiao, Z.X. (2002). IGF-1 induces Pin1 expression in promoting cell cycle S-phase entry. J Cell Biochem 84, 211-6.

[50] Pulikkan, J.A. et al. (2010). Elevated PIN1 expression by C/EBPalpha-p30 blocks C/EBPalpha-induced granulocytic differentiation through c-Jun in AML. Leukemia 24, 914-23.

[51] Liou, Y.C. et al. (2002). Loss of Pin1 function in the mouse causes phenotypes resembling cyclin D1-null phenotypes. Proc Natl Acad Sci U S A 99, 1335-40.

[52] Steger, M. et al. (2013). Prolyl isomerase PIN1 regulates DNA double-strand break repair by counteracting DNA end resection. Mol Cell 50, 333-43.

[53] Dilworth, D., Gudavicius, G., Leung, A. and Nelson, C.J. (2012). The roles of peptidyl-proline isomerases in gene regulation. Biochem Cell Biol 90, 55-69.

[54] Lin, C.H., Li, H.Y., Lee, Y.C., Calkins, M.J., Lee, K.H., Yang, C.N. and Lu, P.J. (2015). Landscape of Pin1 in the cell cycle. Exp Biol Med (Maywood) 240, 403-8.

[55] Lu, Z. and Hunter, T. (2014). Prolyl isomerase Pin1 in cancer. Cell Res 24, 1033-49.

[56] Liou, Y.C., Zhou, X.Z. and Lu, K.P. (2011). Prolyl isomerase Pin1 as a molecular switch to determine the fate of phosphoproteins. Trends Biochem Sci 36, 501-14.

[57] Kino, T. et al. (1987). FK-506, a novel immunosuppressant isolated from a Streptomyces. I. Fermentation, isolation, and physico-chemical and biological characteristics. J Antibiot (Tokyo) 40, 1249-55.

[58] Bierer, B.E., Schreiber, S.L. and Burakoff, S.J. (1990). Mechanisms of immunosuppression by FK506. Preservation of T cell transmembrane signal transduction. Transplantation 49, 1168-70.

[59] Harding, M.W., Galat, A., Uehling, D.E. and Schreiber, S.L. (1989). A receptor for the immunosuppressant FK506 is a cis-trans peptidyl-prolyl isomerase. Nature 341, 758-60.

[60] Siekierka, J.J., Hung, S.H., Poe, M., Lin, C.S. and Sigal, N.H. (1989). A cytosolic binding protein for the immunosuppressant FK506 has peptidyl-prolyl isomerase activity but is distinct from cyclophilin. Nature 341, 755-7.

[61] Chiu, M.I., Katz, H. and Berlin, V. (1994). RAPT1, a mammalian homolog of yeast Tor, interacts with the FKBP12/rapamycin complex. Proc Natl Acad Sci U S A 91, 12574-8.

[62] Brown, E.J., Albers, M.W., Shin, T.B., Ichikawa, K., Keith, C.T., Lane, W.S. and Schreiber, S.L. (1994). A mammalian protein targeted by G1-arresting rapamycin-receptor complex. Nature 369, 756-8.

[63] Laplante, M. and Sabatini, D.M. (2009). mTOR signaling at a glance. J Cell Sci 122, 3589-94.

[64] Terada, N., Takase, K., Papst, P., Nairn, A.C. and Gelfand, E.W. (1995). Rapamycin inhibits ribosomal protein synthesis and induces G1 prolongation in mitogen-activated T lymphocytes. J Immunol 155, 3418-26.

[65] Jayaraman, T., Brillantes, A.M., Timerman, A.P., Fleischer, S., Erdjument-Bromage, H., Tempst, P. and Marks, A.R. (1992). FK506 binding protein associated with the calcium release channel (ryanodine receptor). J Biol Chem 267, 9474-7.

[66] Yan, Z. et al. (2015). Structure of the rabbit ryanodine receptor RyR1 at near-atomic resolution. Nature 517, 50-5.

[67] Timerman, A.P., Ogunbumni, E., Freund, E., Wiederrecht, G., Marks, A.R. and Fleischer, S. (1993). The calcium release channel of sarcoplasmic reticulum is modulated by FK-506-binding protein. Dissociation and reconstitution of FKBP-12 to the calcium release channel of skeletal muscle sarcoplasmic reticulum. J Biol Chem 268, 22992-9.

[68] Timerman, A.P., Wiederrecht, G., Marcy, A. and Fleischer, S. (1995). Characterization of an exchange reaction between soluble FKBP-12 and the FKBP.ryanodine receptor complex. Modulation by FKBP mutants deficient in peptidyl-prolyl isomerase activity. J Biol Chem 270, 2451-9.

[69] Erlejman, A.G. et al. (2014). NF-kappaB transcriptional activity is modulated by FK506-binding proteins FKBP51 and FKBP52: a role for peptidyl-prolyl isomerase activity. J Biol Chem 289, 26263-76.

[70] Ochocka, A.M. et al. (2009). FKBP25, a novel regulator of the p53 pathway, induces the degradation of MDM2 and activation of p53. FEBS Lett 583, 621-6.

[71] Edlich-Muth, C. et al. (2015). The pentameric nucleoplasmin fold is present in Drosophila FKBP39 and a large number of chromatin-related proteins. J Mol Biol 427, 1949-63.

[72] Kuzuhara, T. and Horikoshi, M. (2004). A nuclear FK506-binding protein is a histone chaperone regulating rDNA silencing. Nat Struct Mol Biol 11, 275-83.

[73] Xiao, H., Jackson, V. and Lei, M. (2006). The FK506-binding protein, Fpr4, is an acidic histone chaperone. FEBS Lett 580, 4357-64.

[74] Ho, Y. et al. (2002). Systematic identification of protein complexes in Saccharomyces cerevisiae by mass spectrometry. Nature 415, 180-3.

[75] Saveanu, C. et al. (2003). Sequential protein association with nascent 60S ribosomal particles. Mol Cell Biol 23, 4449-60.

[76] Krogan, N.J. et al. (2006). Global landscape of protein complexes in the yeast Saccharomyces cerevisiae. Nature 440, 637-43.

[77] Helander, S. et al. (2014). Basic Tilted Helix Bundle - a new protein fold in human FKBP25/FKBP3 and HectD1. Biochem Biophys Res Commun 447, 26-31.

[78] Jin, Y.J. and Burakoff, S.J. (1993). The 25-kDa FK506-binding protein is localized in the nucleus and associates with casein kinase II and nucleolin. Proc Natl Acad Sci U S A 90, 7769-73.

[79] Angelov, D. et al. (2006). Nucleolin is a histone chaperone with FACT-like activity and assists remodeling of nucleosomes. EMBO J 25, 1669-79.

[80] Galat, A., Lane, W.S., Standaert, R.F. and Schreiber, S.L. (1992). A rapamycin-selective 25-kDa immunophilin. Biochemistry 31, 2427-34.

[81] Riviere, S., Menez, A. and Galat, A. (1993). On the localization of FKBP25 in T-lymphocytes. FEBS Lett 315, 247-51.

[82] Yang, W.M., Yao, Y.L. and Seto, E. (2001). The FK506-binding protein 25 functionally associates with histone deacetylases and with transcription factor YY1. EMBO J 20, 4814-25.

[83] Prakash, A., Shin, J., Rajan, S. and Yoon, H.S. (2016). Structural basis of nucleic acid recognition by FK506-binding protein 25 (FKBP25), a nuclear immunophilin. Nucleic Acids Res 44, 2909-25.

[84] Galat, A. and Thai, R. (2014). Rapamycin-binding FKBP25 associates with diverse proteins that form large intracellular entities. Biochem Biophys Res Commun 450, 1255-60.

[85] Barak, Y., Juven, T., Haffner, R. and Oren, M. (1993). mdm2 expression is induced by wild type p53 activity. EMBO J 12, 461-8.

[86] Haupt, Y., Maya, R., Kazaz, A. and Oren, M. (1997). Mdm2 promotes the rapid degradation of p53. Nature 387, 296-9.

[87] Itahana, K. et al. (2007). Targeted inactivation of Mdm2 RING finger E3 ubiquitin ligase activity in the mouse reveals mechanistic insights into p53 regulation. Cancer Cell 12, 355-66.

[88] Ahn, J., Murphy, M., Kratowicz, S., Wang, A., Levine, A.J. and George, D.L. (1999). Down-regulation of the stathmin/Op18 and FKBP25 genes following p53 induction. Oncogene 18, 5954-8.

[89] Anderson, P. and Kedersha, N. (2006). RNA granules. J Cell Biol 172, 803-8.

[90] Elvira, G. et al. (2006). Characterization of an RNA granule from developing brain. Mol Cell Proteomics 5, 635-51.

[91] Galat, A., Thai, R. and Stura, E.A. (2014). Diversified targets of FKBP25 and its complex with rapamycin. Int J Biol Macromol 69, 344-52.

[92] Recher, L., Whitescarver, J. and Briggs, L. (1969). The fine structure of a nucleolar constituent. J Ultrastruct Res 29, 1-14.

[93] Puvion-Dutilleul, F., Bachellerie, J.P. and Puvion, E. (1991). Nucleolar organization of HeLa cells as studied by in situ hybridization. Chromosoma 100, 395-409.

[94] Tafforeau, L., Zorbas, C., Langhendries, J.L., Mullineux, S.T., Stamatopoulou, V., Mullier, R., Wacheul, L. and Lafontaine, D.L. (2013). The complexity of human ribosome biogenesis revealed by systematic nucleolar screening of Pre-rRNA processing factors. Mol Cell 51, 539-51.

[95] Olson, M.O. (2011). The Nucleolus. Springer Protein Reviews

[96] Nerurkar, P., Altvater, M., Gerhardy, S., Schutz, S., Fischer, U., Weirich, C. and Panse, V.G. (2015). Eukaryotic Ribosome Assembly and Nuclear Export. Int Rev Cell Mol Biol 319, 107-40.

[97] Henras, A.K., Soudet, J., Gerus, M., Lebaron, S., Caizergues-Ferrer, M., Mougin, A. and Henry, Y. (2008). The post-transcriptional steps of eukaryotic ribosome biogenesis. Cell Mol Life Sci 65, 2334-59.

[98] Conconi, A., Widmer, R.M., Koller, T. and Sogo, J.M. (1989). Two different chromatin structures coexist in ribosomal RNA genes throughout the cell cycle. Cell 57, 753-61.

[99] Learned, R.M., Learned, T.K., Haltiner, M.M. and Tjian, R.T. (1986). Human rRNA transcription is modulated by the coordinate binding of two factors to an upstream control element. Cell 45, 847-57.

[100] Miller, G., Panov, K.I., Friedrich, J.K., Trinkle-Mulcahy, L., Lamond, A.I. and Zomerdijk, J.C. (2001). hRRN3 is essential in the SL1-mediated recruitment of RNA Polymerase I to rRNA gene promoters. EMBO J 20, 1373-82.

[101] Tuan, J.C., Zhai, W. and Comai, L. (1999). Recruitment of TATA-binding protein-TAFI complex SL1 to the human ribosomal DNA promoter is mediated by the carboxy-terminal activation domain of upstream binding factor (UBF) and is regulated by UBF phosphorylation. Mol Cell Biol 19, 2872-9.

[102] Grummt, I. and Langst, G. (2013). Epigenetic control of RNA polymerase I transcription in mammalian cells. Biochim Biophys Acta 1829, 393-404.

[103] Pich, A., Chiusa, L. and Margaria, E. (2000). Prognostic relevance of AgNORs in tumor pathology. Micron 31, 133-41.

[104] Zhao, J., Yuan, X., Frodin, M. and Grummt, I. (2003). ERK-dependent phosphorylation of the transcription initiation factor TIF-IA is required for RNA polymerase I transcription and cell growth. Mol Cell 11, 405-13.

[105] Mayer, C., Zhao, J., Yuan, X. and Grummt, I. (2004). mTOR-dependent activation of the transcription factor TIF-IA links rRNA synthesis to nutrient availability. Genes Dev 18, 423-34.

[106] Arabi, A. et al. (2005). c-Myc associates with ribosomal DNA and activates RNA polymerase I transcription. Nat Cell Biol 7, 303-10.

[107] Voit, R., Schafer, K. and Grummt, I. (1997). Mechanism of repression of RNA polymerase I transcription by the retinoblastoma protein. Mol Cell Biol 17, 4230-7.

[108] Budde, A. and Grummt, I. (1999). p53 represses ribosomal gene transcription. Oncogene 18, 1119-24.

[109] Trere, D., Ceccarelli, C., Montanaro, L., Tosti, E. and Derenzini, M. (2004). Nucleolar size and activity are related to pRb and p53 status in human breast cancer. J Histochem Cytochem 52, 1601-7.

[110] Williamson, D., Lu, Y.J., Fang, C., Pritchard-Jones, K. and Shipley, J. (2006). Nascent pre-rRNA overexpression correlates with an adverse prognosis in alveolar rhabdomyosarcoma. Genes Chromosomes Cancer 45, 839-45.

[111] Ferreira-Cerca, S., Poll, G., Kuhn, H., Neueder, A., Jakob, S., Tschochner, H. and Milkereit, P. (2007). Analysis of the in vivo assembly pathway of eukaryotic 40S ribosomal proteins. Mol Cell 28, 446-57.

[112] Gamalinda, M., Ohmayer, U., Jakovljevic, J., Kumcuoglu, B., Woolford, J., Mbom, B., Lin, L. and Woolford, J.L., Jr. (2014). A hierarchical model for assembly of eukaryotic 60S ribosomal subunit domains. Genes Dev 28, 198-210.

[113] Bernstein, K.A., Gallagher, J.E., Mitchell, B.M., Granneman, S. and Baserga, S.J. (2004). The small-subunit processome is a ribosome assembly intermediate. Eukaryot Cell 3, 1619-26.

[114] Grandi, P. et al. (2002). 90S pre-ribosomes include the 35S pre-rRNA, the U3 snoRNP, and 40S subunit processing factors but predominantly lack 60S synthesis factors. Mol Cell 10, 105-15.

[115] Kornprobst, M. et al. (2016). Architecture of the 90S Pre-ribosome: A Structural View on the Birth of the Eukaryotic Ribosome. Cell 166, 380-93.

[116] Wu, S. et al. (2016). Diverse roles of assembly factors revealed by structures of late nuclear pre-60S ribosomes. Nature 534, 133-7.

[117] Bugler, B., Caizergues-Ferrer, M., Bouche, G., Bourbon, H. and Amalric, F. (1982). Detection and localization of a class of proteins immunologically related to a 100-kDa nucleolar protein. Eur J Biochem 128, 475-80.

[118] Sengupta, T.K., Bandyopadhyay, S., Fernandes, D.J. and Spicer, E.K. (2004). Identification of nucleolin as an AU-rich element binding protein involved in bcl-2 mRNA stabilization. J Biol Chem 279, 10855-63.

[119] Takagi, M., Absalon, M.J., McLure, K.G. and Kastan, M.B. (2005). Regulation of p53 translation and induction after DNA damage by ribosomal protein L26 and nucleolin. Cell 123, 49-63.

[120] Nisole, S. et al. (2002). The anti-HIV pentameric pseudopeptide HB-19 binds the C-terminal end of nucleolin and prevents anchorage of virus particles in the plasma membrane of target cells. J Biol Chem 277, 20877-86.

[121] Hirano, M. et al. (2003). Direct interaction between nucleolin and hepatitis C virus NS5B. J Biol Chem 278, 5109-15.

[122] Goldstein, M., Derheimer, F.A., Tait-Mulder, J. and Kastan, M.B. (2013). Nucleolin mediates nucleosome disruption critical for DNA double-strand break repair. Proc Natl Acad Sci U S A 110, 16874-9.

[123] Reyes-Reyes, E.M., Salipur, F.R., Shams, M., Forsthoefel, M.K. and Bates, P.J. (2015). Mechanistic studies of anticancer aptamer AS1411 reveal a novel role for nucleolin in regulating Rac1 activation. Mol Oncol 9, 1392-405.

[124] Soundararajan, S., Chen, W., Spicer, E.K., Courtenay-Luck, N. and Fernandes, D.J. (2008). The nucleolin targeting aptamer AS1411 destabilizes Bcl-2 messenger RNA in human breast cancer cells. Cancer Res 68, 2358-65.

[125] Christian, S., Pilch, J., Akerman, M.E., Porkka, K., Laakkonen, P. and Ruoslahti, E. (2003). Nucleolin expressed at the cell surface is a marker of endothelial cells in angiogenic blood vessels. J Cell Biol 163, 871-8.

[126] Abdelmohsen, K. and Gorospe, M. (2012). RNA-binding protein nucleolin in disease. RNA Biol 9, 799-808.

[127] Koutsioumpa, M. and Papadimitriou, E. (2014). Cell surface nucleolin as a target for anti-cancer therapies. Recent Pat Anticancer Drug Discov 9, 137-52.

[128] Scott, D.D. and Oeffinger, M. (2016). Nucleolin and nucleophosmin: nucleolar proteins with multiple functions in DNA repair. Biochem Cell Biol, 1-14.

[129] Egyhazi, E., Pigon, A., Chang, J.H., Ghaffari, S.H., Dreesen, T.D., Wellman, S.E., Case, S.T. and Olson, M.O. (1988). Effects of anti-C23 (nucleolin) antibody on transcription of ribosomal DNA in Chironomus salivary gland cells. Exp Cell Res 178, 264-72.

[130] Roger, B., Moisand, A., Amalric, F. and Bouvet, P. (2002). Repression of RNA polymerase I transcription by nucleolin is independent of the RNA sequence that is transcribed. J Biol Chem 277, 10209-19.

[131] Rickards, B., Flint, S.J., Cole, M.D. and LeRoy, G. (2007). Nucleolin is required for RNA polymerase I transcription in vivo. Mol Cell Biol 27, 937-48.

[132] Storck, S., Thiry, M. and Bouvet, P. (2009). Conditional knockout of nucleolin in DT40 cells reveals the functional redundancy of its RNA-binding domains. Biol Cell 101, 153-67.

[133] Ugrinova, I., Monier, K., Ivaldi, C., Thiry, M., Storck, S., Mongelard, F. and Bouvet, P. (2007). Inactivation of nucleolin leads to nucleolar disruption, cell cycle arrest and defects in centrosome duplication. BMC Mol Biol 8, 66.

[134] Cong, R., Das, S., Ugrinova, I., Kumar, S., Mongelard, F., Wong, J. and Bouvet, P. (2012). Interaction of nucleolin with ribosomal RNA genes and its role in RNA polymerase I transcription. Nucleic Acids Res 40, 9441-54.

[135] Elsasser, S.J. and D'Arcy, S. (2013). Towards a mechanism for histone chaperones. Biochim Biophys Acta 1819, 211-21.

[136] Birch, J.L. et al. (2009). FACT facilitates chromatin transcription by RNA polymerases I and III. EMBO J 28, 854-65.

[137] Cong, R., Das, S., Douet, J., Wong, J., Buschbeck, M., Mongelard, F. and Bouvet, P. (2014). macroH2A1 histone variant represses rDNA transcription. Nucleic Acids Res 42, 181-92.

[138] Mamrack, M.D., Olson, M.O. and Busch, H. (1979). Amino acid sequence and sites of phosphorylation in a highly acidic region of nucleolar nonhistone protein C23. Biochemistry 18, 3381-6.

[139] Orrick, L.R., Olson, M.O. and Busch, H. (1973). Comparison of nucleolar proteins of normal rat liver and Novikoff hepatoma ascites cells by two-dimensional polyacrylamide gel electrophoresis. Proc Natl Acad Sci U S A 70, 1316-20.

[140] Herrera, A.H. and Olson, M.O. (1986). Association of protein C23 with rapidly labeled nucleolar RNA. Biochemistry 25, 6258-64.

[141] Ginisty, H., Amalric, F. and Bouvet, P. (1998). Nucleolin functions in the first step of ribosomal RNA processing. EMBO J 17, 1476-86.

[142] Ginisty, H., Serin, G., Ghisolfi-Nieto, L., Roger, B., Libante, V., Amalric, F. and Bouvet, P. (2000). Interaction of nucleolin with an evolutionarily conserved pre-ribosomal RNA sequence is required for the assembly of the primary processing complex. J Biol Chem 275, 18845-50.

[143] Ginisty, H., Amalric, F. and Bouvet, P. (2001). Two different combinations of RNA-binding domains determine the RNA binding specificity of nucleolin. J Biol Chem 276, 14338-43.

[144] Ghisolfi, L., Kharrat, A., Joseph, G., Amalric, F. and Erard, M. (1992). Concerted activities of the RNA recognition and the glycine-rich C-terminal domains of nucleolin are required for efficient complex formation with pre-ribosomal RNA. Eur J Biochem 209, 541-8.

[145] Bouvet, P., Jain, C., Belasco, J.G., Amalric, F. and Erard, M. (1997). RNA recognition by the joint action of two nucleolin RNA-binding domains: genetic analysis and structural modeling. EMBO J 16, 5235-46.

[146] Serin, G., Joseph, G., Ghisolfi, L., Bauzan, M., Erard, M., Amalric, F. and Bouvet, P. (1997). Two RNA-binding domains determine the RNA-binding specificity of nucleolin. J Biol Chem 272, 13109-16.

[147] Allain, F.H., Gilbert, D.E., Bouvet, P. and Feigon, J. (2000). Solution structure of the two N-terminal RNA-binding domains of nucleolin and NMR study of the interaction with its RNA target. J Mol Biol 303, 227-41.

[148] Serin, G., Joseph, G., Faucher, C., Ghisolfi, L., Bouche, G., Amalric, F. and Bouvet, P. (1996). Localization of nucleolin binding sites on human and mouse pre-ribosomal RNA. Biochimie 78, 530-8.

[149] Bouvet, P., Diaz, J.J., Kindbeiter, K., Madjar, J.J. and Amalric, F. (1998). Nucleolin interacts with several ribosomal proteins through its RGG domain. J Biol Chem 273, 19025-9.

[150] Borer, R.A., Lehner, C.F., Eppenberger, H.M. and Nigg, E.A. (1989). Major nucleolar proteins shuttle between nucleus and cytoplasm. Cell 56, 379-90.

[151] Daniely, Y., Dimitrova, D.D. and Borowiec, J.A. (2002). Stress-dependent nucleolin mobilization mediated by p53-nucleolin complex formation. Mol Cell Biol 22, 6014-22.

[152] Daniely, Y. and Borowiec, J.A. (2000). Formation of a complex between nucleolin and replication protein A after cell stress prevents initiation of DNA replication. J Cell Biol 149, 799-810.

[153] Huppert, J.L. and Balasubramanian, S. (2005). Prevalence of quadruplexes in the human genome. Nucleic Acids Res 33, 2908-16.

[154] Hansel-Hertsch, R. et al. (2016). G-quadruplex structures mark human regulatory chromatin. Nat Genet

[155] Dempsey, L.A., Sun, H., Hanakahi, L.A. and Maizels, N. (1999). G4 DNA binding by LR1 and its subunits, nucleolin and hnRNP D, A role for G-G pairing in immunoglobulin switch recombination. J Biol Chem 274, 1066-71.

[156] Hanakahi, L.A., Sun, H. and Maizels, N. (1999). High affinity interactions of nucleolin with G-G-paired rDNA. J Biol Chem 274, 15908-12.

[157] Hay, N., Bishop, J.M. and Levens, D. (1987). Regulatory elements that modulate expression of human c-myc. Genes Dev 1, 659-71.

[158] Siddiqui-Jain, A., Grand, C.L., Bearss, D.J. and Hurley, L.H. (2002). Direct evidence for a G-quadruplex in a promoter region and its targeting with a small molecule to repress c-MYC transcription. Proc Natl Acad Sci U S A 99, 11593-8.

[159] Gonzalez, V., Guo, K., Hurley, L. and Sun, D. (2009). Identification and characterization of nucleolin as a c-myc G-quadruplex-binding protein. J Biol Chem 284, 23622-35.

[160] Gonzalez, V. and Hurley, L.H. (2010). The C-terminus of nucleolin promotes the formation of the c-MYC G-quadruplex and inhibits c-MYC promoter activity. Biochemistry 49, 9706-14.

[161] Drygin, D. et al. (2009). Anticancer activity of CX-3543: a direct inhibitor of rRNA biogenesis. Cancer Res 69, 7653-61.

[162] Lu, P.J., Wulf, G., Zhou, X.Z., Davies, P. and Lu, K.P. (1999). The prolyl isomerase Pin1 restores the function of Alzheimer-associated phosphorylated tau protein. Nature 399, 784-8.

[163] Lu, P.J., Zhou, X.Z., Shen, M. and Lu, K.P. (1999). Function of WW domains as phosphoserine- or phosphothreonine-binding modules. Science 283, 1325-8.

[164] Mamane, Y., Sharma, S., Petropoulos, L., Lin, R. and Hiscott, J. (2000). Posttranslational regulation of IRF-4 activity by the immunophilin FKBP52. Immunity 12, 129-40.

[165] Xia, Z.B., Anderson, M., Diaz, M.O. and Zeleznik-Le, N.J. (2003). MLL repression domain interacts with histone deacetylases, the polycomb group proteins HPC2 and BMI-1, and the corepressor C-terminal-binding protein. Proc Natl Acad Sci U S A 100, 8342-7.

[166] Wang, Y., Han, R., Zhang, W., Yuan, Y., Zhang, X., Long, Y. and Mi, H. (2008). Human CyP33 binds specifically to mRNA and binding stimulates PPIase activity of hCyP33. FEBS Lett 582, 835-9.

[167] Costanzo, M. et al. (2010). The genetic landscape of a cell. Science 327, 425-31.

[168] Davis, T.L. et al. (2010). Structural and biochemical characterization of the human cyclophilin family of peptidyl-prolyl isomerases. PLoS Biol 8, e1000439.

[169] Ahearn, I.M. et al. (2011). FKBP12 binds to acylated H-ras and promotes depalmitoylation. Mol Cell 41, 173-85.

[170] Czar, M.J., Lyons, R.H., Welsh, M.J., Renoir, J.M. and Pratt, W.B. (1995). Evidence that the FK506-binding immunophilin heat shock protein 56 is required for trafficking of the glucocorticoid receptor from the cytoplasm to the nucleus. Mol Endocrinol 9, 1549-60.

[171] Riggs, D.L. et al. (2003). The Hsp90-binding peptidylprolyl isomerase FKBP52 potentiates glucocorticoid signaling in vivo. EMBO J 22, 1158-67.

[172] Riggs, D.L., Cox, M.B., Tardif, H.L., Hessling, M., Buchner, J. and Smith, D.F. (2007). Noncatalytic role of the FKBP52 peptidyl-prolyl isomerase domain in the regulation of steroid hormone signaling. Mol Cell Biol 27, 8658-69.

[173] Fischer, G., Bang, H., Berger, E. and Schellenberger, A. (1984). Conformational specificity of chymotrypsin toward proline-containing substrates. Biochim Biophys Acta 791, 87-97.

[174] Harrison, R.K. and Stein, R.L. (1990). Substrate specificities of the peptidyl prolyl cis-trans isomerase activities of cyclophilin and FK-506 binding protein: evidence for the existence of a family of distinct enzymes. Biochemistry 29, 3813-6.

[175] Edvarddson, A. (2007). PEPTIDYL-PROLYL CIS-TRANS ISOMERASES IN THE CHLOROPLAST THYLAKOID LUMEN. Linköping University Medical Dissertations No. 983

[176] Monneau, Y.R., Soufari, H., Nelson, C.J. and Mackereth, C.D. (2013). Structure and activity of the peptidyl-prolyl isomerase domain from the histone chaperone Fpr4 toward histone H3 proline isomerization. J Biol Chem 288, 25826-37.

[177] Dolinski, K., Scholz, C., Muir, R.S., Rospert, S., Schmid, F.X., Cardenas, M.E. and Heitman, J. (1997). Functions of FKBP12 and mitochondrial cyclophilin active site residues in vitro and in vivo in Saccharomyces cerevisiae. Mol Biol Cell 8, 2267-80.

[178] Kern, D., Kern, G., Scherer, G., Fischer, G. and Drakenberg, T. (1995). Kinetic analysis of cyclophilin-catalyzed prolyl cis/trans isomerization by dynamic NMR spectroscopy. Biochemistry 34, 13594-602.

[179] Nakamura, K., Greenwood, A., Binder, L., Bigio, E.H., Denial, S., Nicholson, L., Zhou, X.Z. and Lu, K.P. (2012). Proline isomer-specific antibodies reveal the early pathogenic tau conformation in Alzheimer's disease. Cell 149, 232-44.

[180] Bierer, B.E., Mattila, P.S., Standaert, R.F., Herzenberg, L.A., Burakoff, S.J., Crabtree, G. and Schreiber, S.L. (1990). Two distinct signal transmission pathways in T lymphocytes are inhibited by complexes formed between an immunophilin and either FK506 or rapamycin. Proc Natl Acad Sci U S A 87, 9231-5.

[181] DeCenzo, M.T., Park, S.T., Jarrett, B.P., Aldape, R.A., Futer, O., Murcko, M.A. and Livingston, D.J. (1996). FK506-binding protein mutational analysis: defining the active-site residue contributions to catalysis and the stability of ligand complexes. Protein Eng 9, 173-80.

[182] Tradler, T., Stoller, G., Rucknagel, K.P., Schierhorn, A., Rahfeld, J.U. and Fischer, G. (1997). Comparative mutational analysis of peptidyl prolyl cis/trans isomerases: active sites of Escherichia coli trigger factor and human FKBP12. FEBS Lett 407, 184-90.

[183] Olsen, J.V. et al. (2010). Quantitative phosphoproteomics reveals widespread full phosphorylation site occupancy during mitosis. Sci Signal 3, ra3.

[184] Rollins, C.T. et al. (2000). A ligand-reversible dimerization system for controlling protein-protein interactions. Proc Natl Acad Sci U S A 97, 7096-101.

[185] Goudarzi, K.M., Nister, M. and Lindstrom, M.S. (2014). mTOR inhibitors blunt the p53 response to nucleolar stress by regulating RPL11 and MDM2 levels. Cancer Biol Ther 15, 1499-514.

[186] Du, W., Yi, Y., Zhang, H., Bergholz, J., Wu, J., Ying, H., Zhang, Y. and Xiao, Z.X. (2013). Rapamycin inhibits IGF-1-mediated up-regulation of MDM2 and sensitizes cancer cells to chemotherapy. PLoS One 8, e63179.

[187] Banaszynski, L.A., Chen, L.C., Maynard-Smith, L.A., Ooi, A.G. and Wandless, T.J. (2006). A rapid, reversible, and tunable method to regulate protein function in living cells using synthetic small molecules. Cell 126, 995-1004.

[188] Fair, K., Anderson, M., Bulanova, E., Mi, H., Tropschug, M. and Diaz, M.O. (2001). Protein interactions of the MLL PHD fingers modulate MLL target gene regulation in human cells. Mol Cell Biol 21, 3589-97.

[189] Fujiyama, S., Yanagida, M., Hayano, T., Miura, Y., Isobe, T., Fujimori, F., Uchida, T. and Takahashi, N. (2002). Isolation and proteomic characterization of human Parvulin-associating preribosomal ribonucleoprotein complexes. J Biol Chem 277, 23773-80.

[190] Fujiyama-Nakamura, S. et al. (2009). Parvulin (Par14), a peptidyl-prolyl cis-trans isomerase, is a novel rRNA processing factor that evolved in the metazoan lineage. Mol Cell Proteomics 8, 1552-65.

[191] Huang da, W., Sherman, B.T. and Lempicki, R.A. (2009). Systematic and integrative analysis of large gene lists using DAVID bioinformatics resources. Nat Protoc 4, 44-57.

[192] Huang da, W., Sherman, B.T. and Lempicki, R.A. (2009). Bioinformatics enrichment tools: paths toward the comprehensive functional analysis of large gene lists. Nucleic Acids Res 37, 1-13.

[193] Ray, S., Panova, T., Miller, G., Volkov, A., Porter, A.C., Russell, J., Panov, K.I. and Zomerdijk, J.C. (2013). Topoisomerase IIalpha promotes activation of RNA polymerase I transcription by facilitating pre-initiation complex formation. Nat Commun 4, 1598.

[194] Tan, B.C., Yang, C.C., Hsieh, C.L., Chou, Y.H., Zhong, C.Z., Yung, B.Y. and Liu, H. (2012). Epigeneitc silencing of ribosomal RNA genes by Mybbp1a. J Biomed Sci 19, 57.

[195] Murano, K., Okuwaki, M., Hisaoka, M. and Nagata, K. (2008). Transcription regulation of the rRNA gene by a multifunctional nucleolar protein, B23/nucleophosmin, through its histone chaperone activity. Mol Cell Biol 28, 3114-26.

[196] Zhang, Y. et al. (2013). The SWI/SNF chromatin remodeling complex influences transcription by RNA polymerase I in Saccharomyces cerevisiae. PLoS One 8, e56793.

[197] Henning, D., So, R.B., Jin, R., Lau, L.F. and Valdez, B.C. (2003). Silencing of RNA helicase II/Gualpha inhibits mammalian ribosomal RNA production. J Biol Chem 278, 52307-14.

[198] Gautier, T., Berges, T., Tollervey, D. and Hurt, E. (1997). Nucleolar KKE/D repeat proteins Nop56p and Nop58p interact with Nop1p and are required for ribosome biogenesis. Mol Cell Biol 17, 7088-98.

[199] Ziv, Y. et al. (2006). Chromatin relaxation in response to DNA double-strand breaks is modulated by a novel ATM- and KAP-1 dependent pathway. Nat Cell Biol 8, 870-6.

[200] Gagne, J.P., Isabelle, M., Lo, K.S., Bourassa, S., Hendzel, M.J., Dawson, V.L., Dawson, T.M. and Poirier, G.G. (2008). Proteome-wide identification of poly(ADP-ribose) binding proteins and poly(ADP-ribose)-associated protein complexes. Nucleic Acids Res 36, 6959-76.

[201] Zou, Y., Liu, Y., Wu, X. and Shell, S.M. (2006). Functions of human replication protein A (RPA): from DNA replication to DNA damage and stress responses. J Cell Physiol 208, 267-73.

[202] Yang, T.H., Tsai, W.H., Lee, Y.M., Lei, H.Y., Lai, M.Y., Chen, D.S., Yeh, N.H. and Lee, S.C. (1994). Purification and characterization of nucleolin and its identification as a transcription repressor. Mol Cell Biol 14, 6068-74.

[203] Haluska, P., Jr., Saleem, A., Edwards, T.K. and Rubin, E.H. (1998). Interaction between the N-terminus of human topoisomerase I and SV40 large T antigen. Nucleic Acids Res 26, 1841-7.

[204] Becherel, O.J., Gueven, N., Birrell, G.W., Schreiber, V., Suraweera, A., Jakob, B., Taucher-Scholz, G. and Lavin, M.F. (2006). Nucleolar localization of aprataxin is dependent on interaction with nucleolin and on active ribosomal DNA transcription. Hum Mol Genet 15, 2239-49.

[205] Iadevaia, V., Zhang, Z., Jan, E. and Proud, C.G. (2012). mTOR signaling regulates the processing of pre-rRNA in human cells. Nucleic Acids Res 40, 2527-39.

[206] Itahana, K., Bhat, K.P., Jin, A., Itahana, Y., Hawke, D., Kobayashi, R. and Zhang, Y. (2003). Tumor suppressor ARF degrades B23, a nucleolar protein involved in ribosome biogenesis and cell proliferation. Mol Cell 12, 1151-64.

[207] Maggi, L.B., Jr., Kuchenruether, M., Dadey, D.Y., Schwope, R.M., Grisendi, S., Townsend, R.R., Pandolfi, P.P. and Weber, J.D. (2008). Nucleophosmin serves as a rate-limiting nuclear export chaperone for the Mammalian ribosome. Mol Cell Biol 28, 7050-65.

[208] Yu, Y., Maggi, L.B., Jr., Brady, S.N., Apicelli, A.J., Dai, M.S., Lu, H. and Weber, J.D. (2006). Nucleophosmin is essential for ribosomal protein L5 nuclear export. Mol Cell Biol 26, 3798-809.

[209] Schilders, G., van Dijk, E. and Pruijn, G.J. (2007). C1D and hMtr4p associate with the human exosome subunit PM/Scl-100 and are involved in pre-rRNA processing. Nucleic Acids Res 35, 2564-72.

[210] Schilders, G., Raijmakers, R., Raats, J.M. and Pruijn, G.J. (2005). MPP6 is an exosome-associated RNA-binding protein involved in 5.8S rRNA maturation. Nucleic Acids Res 33, 6795-804.

[211] Mitchell, P., Petfalski, E., Shevchenko, A., Mann, M. and Tollervey, D. (1997). The exosome: a conserved eukaryotic RNA processing complex containing multiple 3'-->5' exoribonucleases. Cell 91, 457-66.

[212] Sun, C. and Woolford, J.L., Jr. (1994). The yeast NOP4 gene product is an essential nucleolar protein required for pre-rRNA processing and accumulation of 60S ribosomal subunits. EMBO J 13, 3127-35.

[213] Jalal, C., Uhlmann-Schiffler, H. and Stahl, H. (2007). Redundant role of DEAD box proteins p68 (Ddx5) and p72/p82 (Ddx17) in ribosome biogenesis and cell proliferation. Nucleic Acids Res 35, 3590-601.

[214] Phipps, K.R., Charette, J. and Baserga, S.J. (2011). The small subunit processome in ribosome biogenesis-progress and prospects. Wiley Interdiscip Rev RNA 2, 1-21.

[215] Hayano, T., Yanagida, M., Yamauchi, Y., Shinkawa, T., Isobe, T. and Takahashi, N. (2003). Proteomic analysis of human Nop56p-associated pre-ribosomal ribonucleoprotein complexes. Possible link between Nop56p and the nucleolar protein treacle responsible for Treacher Collins syndrome. J Biol Chem 278, 34309-19.

[216] Xue, S. and Barna, M. (2012). Specialized ribosomes: a new frontier in gene regulation and organismal biology. Nat Rev Mol Cell Biol 13, 355-69.

[217] Baudin-Baillieu, A., Fabret, C., Liang, X.H., Piekna-Przybylska, D., Fournier, M.J., Rousset, J.P. (2009). Nucleotide modifications in three functionally important regions of the Saccharomyces cerevisiae ribosome affect translation accuracy. Nucleic Acids Res 37, 7665-77.

[218] Marcel, V. et al. (2013). p53 acts as a safeguard of translational control by regulating fibrillarin and rRNA methylation in cancer. Cancer Cell 24, 318-30.

[219] Decatur, W.A. and Fournier, M.J. (2002). rRNA modifications and ribosome function. Trends Biochem Sci 27, 344-51.

[220] Lafontaine, D.L. (2015). Noncoding RNAs in eukaryotic ribosome biogenesis and function. Nat Struct Mol Biol 22, 11-9.

[221] Supek, F., Bosnjak, M., Skunca, N. and Smuc, T. (2011). REVIGO summarizes and visualizes long lists of gene ontology terms. PLoS One 6, e21800.

[222] Andersen, J.S., Lam, Y.W., Leung, A.K., Ong, S.E., Lyon, C.E., Lamond, A.I. and Mann, M. (2005). Nucleolar proteome dynamics. Nature 433, 77-83.

[223] Yoshikawa, H. et al. (2011). Splicing factor 2-associated protein p32 participates in ribosome biogenesis by regulating the binding of Nop52 and fibrillarin to preribosome particles. Mol Cell Proteomics 10, M110 006148.

[224] Leverson, J.D. and Ness, S.A. (1998). Point mutations in v-Myb disrupt a cyclophilin-catalyzed negative regulatory mechanism. Mol Cell 1, 203-11.

[225] Foster, T.L., Gallay, P., Stonehouse, N.J. and Harris, M. (2011). Cyclophilin A interacts with domain II of hepatitis C virus NS5A and stimulates RNA binding in an isomerase-dependent manner. J Virol 85, 7460-4.

[226] Bunimov, N., Smith, J.E., Gosselin, D. and Laneuville, O. (2007). Translational regulation of PGHS-1 mRNA: 5' untranslated region and first two exons conferring negative regulation. Biochim Biophys Acta 1769, 92-105.

[227] Miniard, A.C., Middleton, L.M., Budiman, M.E., Gerber, C.A. and Driscoll, D.M. (2010). Nucleolin binds to a subset of selenoprotein mRNAs and regulates their expression. Nucleic Acids Res 38, 4807-20.

[228] Castello, A. et al. (2016). Comprehensive Identification of RNA-Binding Domains in Human Cells. Mol Cell 63, 696-710.

[229] Britton, S., Coates, J. and Jackson, S.P. (2013). A new method for high-resolution imaging of Ku foci to decipher mechanisms of DNA double-strand break repair. J Cell Biol 202, 579-95.

[230] Chen, Z.A. et al. (2010). Architecture of the RNA polymerase II-TFIIF complex revealed by cross-linking and mass spectrometry. EMBO J 29, 717-26.

[231] Roux, K.J., Kim, D.I., Raida, M. and Burke, B. (2012). A promiscuous biotin ligase fusion protein identifies proximal and interacting proteins in mammalian cells. J Cell Biol 196, 801-10.

[232] Kellner, M. et al. (2015). DEAD-box helicase DDX27 regulates 3' end formation of ribosomal 47S RNA and stably associates with the PeBoW-complex. Exp Cell Res 334, 146-59.

[233] McMahon, A.C., Rahman, R., Jin, H., Shen, J.L., Fieldsend, A., Luo, W. and Rosbash, M. (2016). TRIBE: Hijacking an RNA-Editing Enzyme to Identify Cell-Specific Targets of RNA-Binding Proteins. Cell 165, 742-53.

[234] Howe, F.S. et al. (2014). Lysine acetylation controls local protein conformation by influencing proline isomerization. Mol Cell 55, 733-44.

[235] Smith, M.M. and Murray, K. (1983). Yeast H3 and H4 histone messenger RNAs are transcribed from two non-allelic gene sets. J Mol Biol 169, 641-61.

[236] Sadakierska-Chudy, A., Kostrzewa, R.M. and Filip, M. (2015). A comprehensive view of the epigenetic landscape part I: DNA methylation, passive and active DNA demethylation pathways and histone variants. Neurotox Res 27, 84-97.

[237] Miller, M.C., Le, H.T., Dean, W.L., Holt, P.A., Chaires, J.B. and Trent, J.O. (2011). Polymorphism and resolution of oncogene promoter quadruplex-forming sequences. Org Biomol Chem 9, 7633-7.

[238] Le, H.T., Miller, M.C., Buscaglia, R., Dean, W.L., Holt, P.A., Chaires, J.B. and Trent, J.O. (2012). Not all G-quadruplexes are created equally: an investigation of the structural polymorphism of the c-Myc G-quadruplex-forming sequence and its interaction with the porphyrin TMPyP4. Org Biomol Chem 10, 9393-404.

[239] Van Itallie, C.M., Aponte, A., Tietgens, A.J., Gucek, M., Fredriksson, K. and Anderson, J.M. (2013). The N and C termini of ZO-1 are surrounded by distinct proteins and functional protein networks. J Biol Chem 288, 13775-88.

[240] Fredriksson, K., Van Itallie, C.M., Aponte, A., Gucek, M., Tietgens, A.J. and Anderson, J.M. (2015). Proteomic analysis of proteins surrounding occludin and claudin-4 reveals their proximity to signaling and trafficking networks. PLoS One 10, e0117074.

[241] Harrison, D.E. et al. (2009). Rapamycin fed late in life extends lifespan in genetically heterogeneous mice. Nature 460, 392-5.

[242] Easton, J.B. and Houghton, P.J. (2006). mTOR and cancer therapy. Oncogene 25, 6436-46.

Appendix

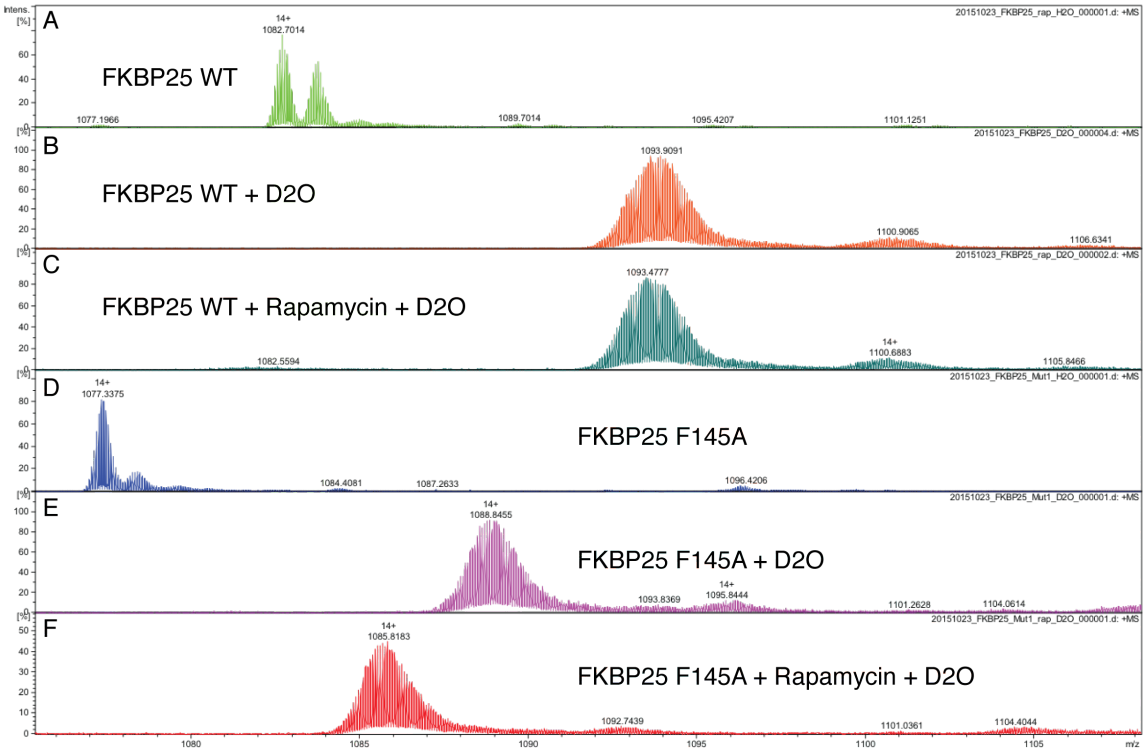

Figure 32. The addition of rapamycin promotes FKBP25 F145A folding. Mass spectra of control (A, D), D2O (B, E) and D2O + Rapamycin (C, F) treated wildtype (A-C) or F145A (D-F) FKBP25. Wildtype protein alone has 73 residues protected, and the additon of rapamycin shifts this to 76 protected. F145A protein alone has 57 residues protected, indicating increased D2O accessibility. The addition of rapamycin to F145A results in 108 residues protected. Experiment performed by Nick Brodie.

Table 4. DAVID functional annotation and enrichment analysis of all FKBP25 interacting proteins (MALDI + Orbitrap).

Term	Count	%	PValue	List Total	Pop Hits	Pop Total	Fold Enrichment	Bonferroni	Benjamini	FDR
GO:0006414~translational elongation	34	30.0884956	8.42E-47	103	101	13528	44.2134	5.37E-44	5.37E-44	1.25E-43
GO:0006412~translation	38	33.6283186	6.25E-34	103	331	13528	15.0782859	3.99E-31	1.99E-31	9.31E-31
GO:0022613~ribonucleoprotein complex biogenesis	16	14.159292	5.14E-12	103	180	13528	11.6746494	3.28E-09	1.09E-09	7.65E-09
GO:0042254~ribosome biogenesis	13	11.5044248	1.14E-10	103	122	13528	13.9952252	7.27E-08	1.82E-08	1.70E-07
GO:0006364~rRNA processing	11	9.73451327	1.64E-09	103	92	13528	15.7036724	1.04E-06	2.09E-07	2.44E-06
GO:0016072~rRNA metabolic process	11	9.73451327	2.50E-09	103	96	13528	15.0493528	1.59E-06	2.66E-07	3.72E-06
GO:0006333~chromatin assembly or disassembly	12	10.619469	2.79E-09	103	127	13528	12.4100604	1.78E-06	2.54E-07	4.15E-06
GO:0006396~RNA processing	21	18.5840708	3.64E-09	103	547	13528	5.04229602	2.32E-06	2.90E-07	5.42E-06
GO:0006334~nucleosome assembly	10	8.84955752	1.27E-08	103	84	13528	15.6356912	8.10E-06	9.00E-07	1.89E-05
GO:0034622~cellular macromolecular complex assembly	16	14.159292	1.47E-08	103	318	13528	6.60829212	9.36E-06	9.36E-07	2.18E-05
GO:0006323~DNA packaging	11	9.73451327	1.73E-08	103	117	13528	12.3481869	1.11E-05	1.01E-06	2.58E-05
GO:0031497~chromatin assembly	10	8.84955752	1.74E-08	103	87	13528	15.0965294	1.11E-05	9.23E-07	2.58E-05
GO:0065004~protein-DNA complex assembly	10	8.84955752	2.59E-08	103	91	13528	14.4329457	1.65E-05	1.27E-06	3.85E-05
GO:0034728~nucleosome organization	10	8.84955752	3.14E-08	103	93	13528	14.1225598	2.00E-05	1.43E-06	4.67E-05
GO:0034621~cellular macromolecular complex subunit organization	16	14.159292	6.79E-08	103	357	13528	5.88637785	4.33E-05	2.89E-06	1.01E-04
GO:0042273~ribosomal large subunit biogenesis	5	4.42477876	6.18E-07	103	10	13528	65.6699029	3.94E-04	2.46E-05	9.20E-04
GO:0051276~chromosome organization	17	15.0442478	6.43E-07	103	485	13528	4.6036633	4.10E-04	2.41E-05	9.57E-04
GO:0034470~ncRNA processing	11	9.73451327	1.42E-06	103	187	13528	7.72587093	9.05E-04	5.03E-05	0.00211341
GO:0065003~macromolecular complex assembly	18	15.9292035	8.91E-06	103	665	13528	3.55506241	0.00566986	2.99E-04	0.01327238
GO:0034660~ncRNA metabolic process	11	9.73451327	9.01E-06	103	230	13528	6.28146897	0.00573411	2.87E-04	0.01342321
GO:0043933~macromolecular complex subunit organization	18	15.9292035	2.08E-05	103	710	13528	3.32974156	0.01320983	6.33E-04	0.0310374
GO:0006325~chromatin organization	13	11.5044248	2.67E-05	103	378	13528	4.51697745	0.01688398	7.74E-04	0.03974222
GO:0016071~mRNA metabolic process	12	10.619469	1.06E-04	103	370	13528	4.25966938	0.06543489	0.00293802	0.15785195
GO:0022618~ribonucleoprotein complex assembly	6	5.30973451	1.69E-04	103	69	13528	11.4208527	0.10238058	0.00449027	0.25181652
GO:0008380~RNA splicing	10	8.84955752	2.90E-04	103	284	13528	4.62464105	0.16907799	0.0073814	0.4314386
GO:0006413~translational initiation	5	4.42477876	3.58E-04	103	45	13528	14.5933118	0.20421585	0.00874718	0.53181654
GO:0043488~regulation of mRNA stability	4	3.53982301	5.77E-04	103	22	13528	23.8799647	0.30825795	0.01355697	0.85662662
GO:0043487~regulation of RNA stability	4	3.53982301	7.51E-04	103	24	13528	21.8899676	0.38068421	0.01696656	1.11226202
GO:0010608~posttranscriptional regulation of gene expression	8	7.07964602	0.00107329	103	211	13528	4.97970828	0.4959721	0.02334807	1.58661623
GO:0006265~DNA topological change	3	2.65486726	0.00115342	103	7	13528	56.2884882	0.52112171	0.02424488	1.70413571
GO:0019047~provirus integration	3	2.65486726	0.00153034	103	8	13528	49.2524272	0.62360053	0.03102793	2.25511433
GO:0030069~lysogeny	3	2.65486726	0.00153034	103	8	13528	49.2524272	0.62360053	0.03102793	2.25511433
GO:0042255~ribosome assembly	3	2.65486726	0.00243538	103	10	13528	39.4019417	0.78895126	0.0474518	3.56636472
GO:0006397~mRNA processing	9	7.96460177	0.00292535	103	321	13528	3.68242446	0.84573935	0.05506558	4.26939464
GO:0042274~ribosomal small subunit biogenesis	3	2.65486726	0.00296197	103	11	13528	35.819947	0.84931145	0.05414211	4.32173644
GO:0043489~RNA stabilization	3	2.65486726	0.00554466	103	15	13528	26.2679612	0.97119877	0.09638554	7.94723721
GO:0048255~mRNA stabilization	3	2.65486726	0.00554466	103	15	13528	26.2679612	0.97119877	0.09638554	7.94723721
GO:0006913~nucleocytoplasmic transport	6	5.30973451	0.00649681	103	156	13528	5.05153099	0.98436883	0.10909151	9.25119112
GO:0051169~nuclear transport	6	5.30973451	0.00684883	103	158	13528	4.98758756	0.98753195	0.11175025	9.72889998
GO:0015074~DNA integration	3	2.65486726	0.00979043	103	20	13528	19.7009709	0.99812111	0.15226415	13.630076
GO:0019059~initiation of viral infection	3	2.65486726	0.01178729	103	22	13528	17.9099735	0.99948171	0.17632026	16.188078
GO:0000723~telomere maintenance	3	2.65486726	0.01873204	103	28	13528	14.0721221	0.99999424	0.26037338	24.5446065
GO:0032200~telomere organization	3	2.65486726	0.02002191	103	29	13528	13.5868765	0.99999751	0.27000801	26.0083994
GO:0042257~ribosomal subunit assembly	2	1.7699115	0.02245128	103	3	13528	87.5598706	0.99999949	0.29173171	28.693667
GO:0000245~spliceosome assembly	3	2.65486726	0.02410612	103	32	13528	12.3131068	0.99999983	0.30375184	30.4704695
GO:0006606~protein import into nucleus	4	3.53982301	0.0271376	103	86	13528	6.10882818	0.99999998	0.32896441	33.6186948
GO:0000398~nuclear mRNA splicing, via spliceosome	5	4.42477876	0.02848264	103	153	13528	4.29215052	0.99999999	0.33613938	34.9724943
GO:0000375~RNA splicing, via transesterification reactions	5	4.42477876	0.02848264	103	153	13528	4.29215052	0.99999999	0.33613938	34.9724943
GO:0000377~RNA splicing, via transesterification reactions with bulged adenosine as	5	4.42477876	0.02848264	103	153	13528	4.29215052	0.99999999	0.33613938	34.9724943
GO:0051170~nuclear import	4	3.53982301	0.028789	103	88	13528	5.96999117	0.99999999	0.33312405	35.2772255
GO:0034504~protein localization in nucleus	4	3.53982301	0.03405645	103	94	13528	5.58892791	1	0.37521881	40.3127821
GO:0019058~viral infectious cycle	3	2.65486726	0.04161088	103	43	13528	9.16324227	1	0.43159128	46.8997003
GO:0006310~DNA recombination	4	3.53982301	0.04491708	103	105	13528	5.00342117	1	0.45029881	49.5634797

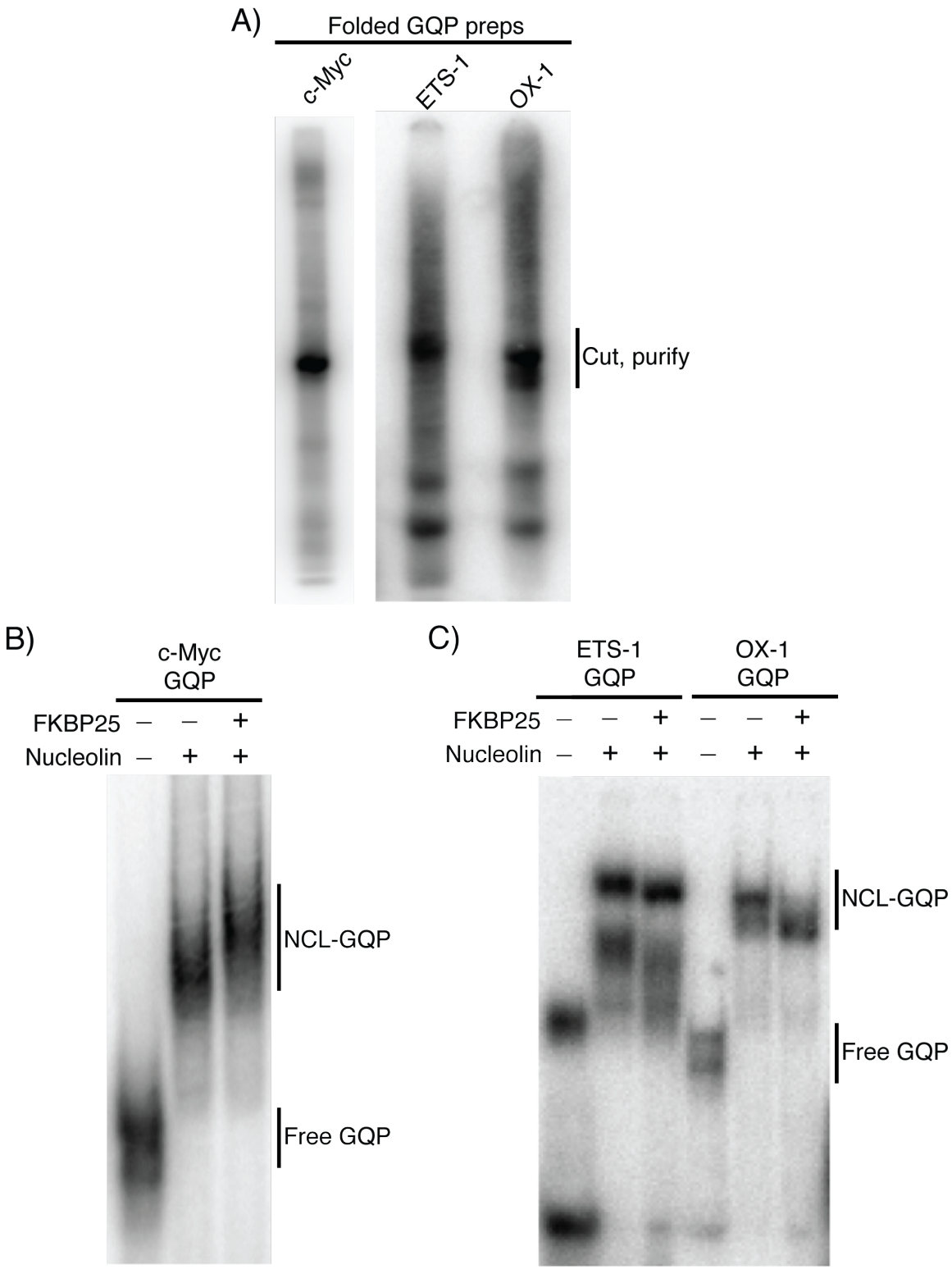

Figure 33. Assaying the effect of FKBP25 on nucleolin-G-quadruplexes.
A) Heterogeneity in G-quadruplex structures from c-Myc, ETS-1 and OX-1 sequences. Oligos were first labeled with ^{32}P by polynucleotide kinase. Folded samples were prepared by heating oligos to 95^{o}C for 5 minutes followed by a slow cool to room

temperature. The major bands were purified by a ‘cut and soak’ protocol to obtain a single migrating species. B) Gel shift assays with the c-Myc G-quadruplex, showing binding to nucleolin and the effect of FKBP25 addition. C) Gel shift assays with ETS-1 and OX-1 G-quadruplexes showing binding to nucleolin and the effect of FKBP25 addition. Gel shift assays were performed by incubating FKBP25 and nucleolin prior to the addition of G-quadruplex. Samples were resolved on native polyacrylamide gels, dried and exposed to screens.

Table 5. Oligonucleotide sequences used for qPCR and northern blot.

Transcript	Sequence	Application
GAPDH	F – 5′-TGCACCACCAACTGCTTAGC-3′ R – 5′-GGCATGGACTGTGGTCATGAG-3	RIP/qPCR
5’ETS	F – 5′-CCTCGGTGAGAAAAGCCTTC-3′ R –5′-GCTACCATAACGGAGGCAGA-3′	ChIP/RIP/qPCR
18S	F – 5′ -CGACGACCCATTCGAACGTC-3′ R – 5′-CTCTCCGGAATCGAACCCTG-3′	RIP/qPCR
ITS1	F – 5′ -CCCGTGGTGTGAAACCTTC-3′ R – 5′-AAGAGGAGAGGGGGTTGC-3′	ChIP/RIP/qPCR
ITS2	F – 5′ -GTCCCCCTAAGCGCAGAC-3′ R – 5′-CCGGCTCTCTCTTTCCCTCT-3′	RIP/qPCR
28S	F – 5′ -AGTCGGGTTGCTTGGGAATGC-3′ R – 5′-CCCTTACGGTACTTGTTGACT-3′	ChIP/RIP/qPCR
ITS1	5′ -CCTCGCCCTCCGGGCTCCGTTAATTGATC-3′	Northern
ITS2	5′ -CGCACCCCGAGGAGCCCGGAGGCACCCCCGG-3′	Northern
1 kb upstream	F – 5′-CCGTGGGTTGTCTTCTGAC-3′ R – 5′-AAGCGAAACCGTGAGTCG-3′	ChIP/qPCR
shGFP	5’-CACAAGCTGGAGTACAACTACAACAGCCA-3’	RIP/qPCR
shFKBP25	5’-CAGGAACACGGTTCAGATTCGTTTCTTGC-3’	RIP/qPCR
siGFP	5’-GGCUACGUCCAGGAGCGCACCtt-3’	Northern
siFKBP25	5’- CCACUUGGUUACAGCCUAtt-3’	Northern